Spatiotemporal Kinetics of AMPAR Trafficking in Single Spines

by

Michael Andrew Patterson

Department of Neurobiology
Duke University

Date: April 2, 2010
Approved:

_____

Ryohei Yasuda, Supervisor

_____

Michael Ehlers

_____

Sri Raghavachari

_____

Scott Soderling

Dissertation submitted in partial fulfillment of
the requirements for the degree of Doctorate of Philosophy in the Department of Neurobiology in the Graduate School
of Duke University
2010

ABSTRACT

Spatiotemporal Kinetics of AMPAR Trafficking in Single Spines

by

Michael Andrew Patterson

Department of Neurobiology
Duke University

Date: April 2, 2010
Approved:

_____

Ryohei Yasuda, Supervisor

_____

Michael Ehlers

_____

Sri Raghavachari

_____

Scott Soderling

An abstract of a dissertation submitted in partial fulfillment of
the requirements for the degree of Doctorate of Philosophy in the Department of
Neurobiology in the Graduate School
of Duke University
2010

Abstract

Learning and memory is one of the critical components of the human experience. In one model of memory, hippocampal LTP, it is believed that the trafficking of AMPA receptors to the synapse is a fundamental process, yet the spatiotemporal kinetics of the process remain under dispute. In this work, we imaged the trafficking of AMPA receptors by combining two-photon glutamate uncaging on single spines with a fluorescent reporter for surface AMPA receptors. We found that AMPA receptors are trafficked to the spine at the same time as the spine size is increasing. Using a bleaching protocol, we found that the receptors that reach the spine come from a combination of the surface and endosomal pools. Imaging exocytosis in real time, we found that the exocytosis rate increases briefly (~1 min.), both in the spine and neighbouring dendrite. Finally, we performed pharmacological and genetic manipulations of signaling pathways, and found that the Ras-ERK signaling pathway is necessary for AMPAR exocytosis.

In a set of related experiments, we also investigated the capacity of single spines to undergo potentiation multiple times. By stimulating spines twice using glutamate uncaging, we found that there is a refractory period for synaptic plasticity in spines during which they cannot further be potentiated. We furthermore found that inducing plasticity in a given spine inhibits plasticity at nearby spines.

Contents

List of Tables

List of Figures

Chapter I: Introduction

1.1 Preface

When Susumu Tonegawa visited Duke, he indelibly reminded me how important memory is, “Memory is important not only for mice but for us. For people who are not studying memory, memory may be recalling your childhood, like learning how to ride a bicycle, or a missing bunch of keys. But it’s more profound than our day to day life. You could say that memory is what connects you to the outside world, including all other people.… Alzheimer’s patients often ask their relatives, ‘Remind me who I am.’ That is how important memory is” (Tonegawa, 2008).

Philosophers and psychologists have studied memory since the ability was named. They have enumerated how many numbers a person can remember, and have formulated schema of memory ranging from working memory that lasts only a few seconds to long term memory which can last a lifetime (Unsworth and Engle, 2007). Yet all of these studies are descriptive, characterizing what people can remember, without yielding insight into how memory works.

Neuroscience can offer the insight into how memory works, albeit on a reduced level. Rather than study memory at the level of whole organisms, it is simpler to study memory in reduced preparations. One of the most commonly studied systems is the hippocampus, which is the part of the mammalian brain that stores spatial and declarative memory.

In humans, the hippocampal formation lies in the temporal lobe. Information (or synaptic activity) in the hippocampus flows unidirectionally, entering the hippocampus

from entorhinal cortex into the dentate gyrus (DG; Fig. 1A). It then flows to Cornu Ammonis 3 (CA3), then to CA1, and finally out through the septum. The synapses between these areas are named the perforant path (entorhinal cortex-DG), mossy fibre (DG-CA3), and Schaffer collateral (CA3-CA1) synapses; together they are called the trisynaptic circuit. Each of these synapses is able to be potentiated, or strengthened, a primitive form of memory. Potentiation means that following strong stimulation, these synapses become more efficacious, and continue to stay strong for some time. Long-term potentiation (LTP) of Schaffer collateral synapses will be the focus of this thesis.

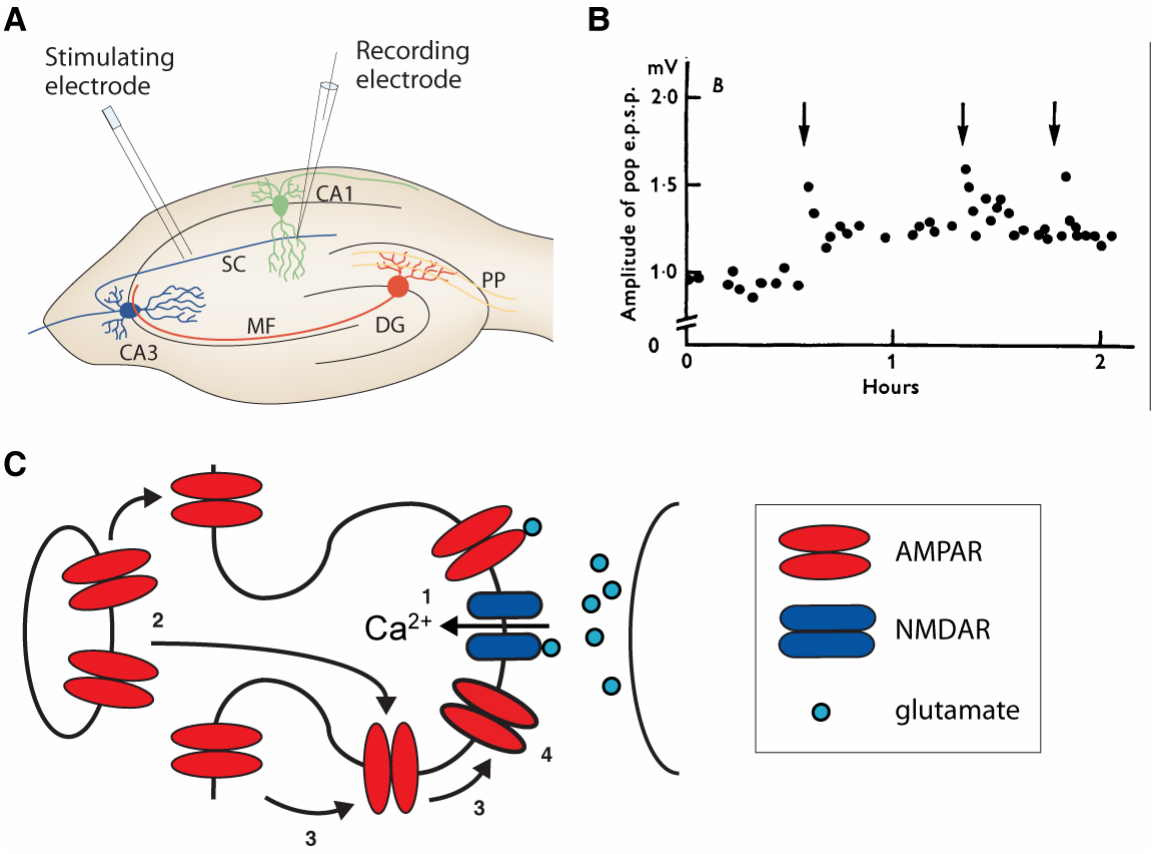

Figure 1: Schematic of hippocampus, LTP, and the synapse
A. Diagram of hippocampus. Information enters the hippocampus through the perforant path (PP) into the dentate gyrus (DG). It then moves along the mossy fibres (MF) into CA3. Activity then traverses the Schaffer Collateral (SC) to CA1. The most commonly studied form of LTP is that of the SC from CA3 to CA1. To observe this LTP, one records from neurons in CA1 while stimulating the SC. Modified with permission from (Collingridge et al., 2004). **B.** One of the earliest examples of LTP of the PP in rabbits. The field EPSP was recorded for two hours while the PP was stimulated at 100 Hz. This elicited an increase in EPSP amplitude. Reproduced, with permission, from (Bliss and Lomo, 1973). **C.** Diagram of synapse during LTP. Glutamate is released from the presynaptic terminal (right side), and bind both AMPA and NMDA receptors. Ca^{2+} flows into the spine through NMDAR, and activates a signaling cascade (1). AMPAR move into the synapse in a multi-step process, starting with the exocytosis of AMPAR (2). Receptors at the surface diffuse into the spine, and then the synapse (3), where they are anchored (4).

LTP was first discovered in the 1960s, and over the past four decades the NMDA receptor hypothesis of LTP has emerged (Bliss and Lomo, 1973; Derkach et al., 2007). LTP at Schaffer collaterals begins with activation of NMDA-type glutamate receptors (NMDAR), which allows Ca^{2+} to flow into the synapse. The elevated Ca^{2+} activates a variety of signaling cascades, which in the end causes an increase in the number of AMPA-type glutamate receptors (AMPAR) in the stimulated synapse. These AMPAR exist in two functional pools in neurons, at the cell surface, and in endosomes, and it is believed that the exocytosis of AMPAR is essential for LTP.

Given this limn of LTP, there remain many unanswered questions. These include: What fraction of AMPAR come from portions already at the surface, versus those from internal endosomes? When do AMPAR reach the synapse during LTP, and more specifically, when does exocytosis occur? Where does AMPAR exocytosis occur? What signaling pathways lead to AMPAR exocytosis? And finally, what are the characteristics of stimulated spines? Can they be potentiated multiple times, and on what time scale? The goal of this thesis will be to perform experiments to address these questions.

For the remainder of this introduction, I will present a brief history of LTP, then an overview of AMPAR structure, function, and trafficking. Next I will review AMPAR's role in LTP, and the signaling pathways regulating LTP. At the end of the introduction is a more in-depth consideration of the goals of this dissertation.

1.2 History of LTP

The study of synaptic strength in the hippocampus began to take form in the 1960s in Oslo, Norway (Bliss and Lomo, 1973). A trio, Andersen, Lomo, and Bliss, stuck electrodes into the DG of rabbits, and measured the field potential following stimulation of the perforant path (Fig. 1B). They noticed that if they stimulated infrequently (<1Hz), the recorded fEPSP strength was constant. However, if they increased the stimulation frequency to 5-10 Hz, the fEPSP increased over time. In 1973, they published their seminal work showing that 100Hz stimulation for ~3s caused a rapid increase in fEPSP strength that could be sustained for over twelve hours. They furthermore established that this was pathway specific by placing stimulating electrodes in two parts of the perforant path, and recording from separate locations. Strong stimulation of one pathway did not increase the strength of the unstimulated pathway. They termed this phenomena “long-lasting potentiation.”

Over the next decade, the characteristics of the phenomena were further specified and refined. The basic result was repeated in acute slices (Andersen et al., 1977), and the phenomena was extended to more synapses, including the mossy fibre, and Schaffer collateral synapses (Schwartzkroin and Wester, 1975). Some looked for the duration of potentiation, and found it could last for months (Abraham et al., 2002). The stimulus parameters that lead to LTP were explored, including a variety of more physiologically relevant stimuli like theta burst stimulation (Douglas and Goddard, 1975), and spike timing dependent plasticity (Bi and Poo, 1998; Markram et al., 1997). These investigations into the stimulus parameters helped establish the idea of cooperativity, namely that there is a threshold for stimulation which must be exceeded to potentiate a

synapse (McNaughton et al., 1978). Stimuli below the threshold are ineffective. In 1986, three labs furthered the cooperativity finding by showing that weak stimuli, when paired with depolarization, could still cause potentiation (Kelso et al., 1986; Sastry et al., 1986). LTP was also discovered to be associative, in that weak stimuli which do not normally cause potentiation can do so if they are applied simultaneously with strong stimuli to a different pathway (McNaughton et al., 1978).

While many were elucidating the properties of LTP, others began to explore the pharmacology. In 1981 it was discovered that bath application of an NMDAR antagonist, APV, blocked LTP (Davies et al., 1981). Furthermore, in living rats, ventricular injection of APV caused memory deficits while performing the Morris Water Maze task, which requires hippocampal memory (Morris et al., 1986). It was also found that application of the Ca^{2+} chelator EGTA blocked LTP (Lynch et al., 1983). In the mid-1980s, biophysicists discovered two key properties of NMDARs. First, NMDARs are blocked by Mg^{2+} at hyperpolarized voltages, preventing them from passing current; at depolarized voltages, however, NMDARs conduct current (Mayer et al., 1984; Nowak et al., 1984). Second, NMDARs were discovered to be Ca^{2+}-permeable, in contrast to most AMPAR (MacDermott et al., 1986).

Combining these findings, the NMDAR hypothesis of LTP began to coalesce, which explained the principal properties of cooperativity, associativity, and input specificity. The NMDAR hypothesis is that strong stimuli can depolarize a postsynaptic cell, relieving the NMDAR of its Mg^{2+} blockade. Subsequent stimuli through the pathway will result in the influx of Ca^{2+}, and initiate a signaling cascade that eventually causes LTP. This hypothesis explains that the cooperativity of LTP comes from the Mg^{2+} block

of NMDAR, which must be relieved by sufficiently strong stimuli that depolarizes the dendrite. The input specificity is determined because NMDAR act as a coincidence detector for post-synaptic depolarization and presynaptic input. Only the stimulated pathway will meet these two requirements; the unstimulated pathway will have only presynaptic input. Finally, associativity is explained because when a strong stimulus opens NMDAR, it will allow weak stimuli to also potentiate. Experiments have now confirmed that this is the induction mechanism for LTP at the Schaffer collateral synapse.

Having described the basics of how LTP is induced, scientists next turned to its mechanism. First, scientists had to determine the site of potentiation, whether it was pre- or post-synaptic. We now know that potentiation is possible at both sites depending on the form of LTP, so let us concentrate on mechanism of LTP at the Schaffer collateral.

On the presynaptic side, possible sources of potentiation include increasing the number of vesicles released, increasing the probability of release, or developing new active zones for release. To investigate changes in the release probability, many experimenters used paired pulse facilitation (PPF), the ratio of the magnitude of two stimuli into a given cell in rapid succession (second pulse magnitude over first, paired pulse ratio or PPR). If the release probability of the presynaptic site increases, more vesicles will fuse during the first stimuli, leaving fewer vesicles for subsequent stimuli, thus causing the second pulse to have a lower current which can be measured as a decrease in the paired pulse ratio. Many scientists measured this ratio in both individual cells and populations of cells, but found no consistent result (Kleschevnikov et al., 1996;

Manabe et al., 1993; Schulz et al., 1994). More recently, however, the Choquet lab has reported that the PPR decreases following stimulation (Heine et al., 2008). Their explanation for this phenomena, however, was that postsynaptic AMPAR are desensitized during paired pulse protocols, and that the diffusion rate of AMPAR changes during plasticity. Others investigated the presynaptic locus by looking at the failure rate of synaptic transmission, and found that it went down following LTP induction (Bekkers and Stevens, 1990; Malinow and Tsien, 1990).

On the postsynaptic side, there are many possible mechanisms by which to increase synaptic currents. LTP could cause an increase in the strength of individual channels, for example by increase the open probability or single channel conductance. LTP could also increase in the number of channels at the PSD, yielding more response to each stimuli. On a larger scale, LTP could induce the formation of new synapses. There had been some indirect evidence that non-NMDAR glutamate receptors were inserted into the post-synaptic density following LTP (Kauer et al., 1988; Muller and Lynch, 1988). In 1995, two labs showed conclusively that there is a post-synaptic locus for LTP. In these experiments they recorded intracellularly from neurons and found that many synapses had large (NMDAR) currents when depolarized, but passed no currents when hyperpolarized. These synapses would then be “silent” at the hyperpolarized potentials the cell normally rests at. Then, when they stimulated these cells to induce LTP, they found that these silent synapses potentiated, and were able to pass current at all potentials, showing that AMPAR had been inserted (Isaac et al., 1995; Liao et al., 1995). Silent synapses were later verified using EM (Baude et al., 1995; Nusser et al., 1998). The identification of silent synapses also helped explain the decrease in failure

rate that otherwise would have been evidence for a presynaptic locus. It was later proposed that the trafficking of one subtype of AMPAR, GluR1, was responsible for LTP, delineating separate roles for different AMPAR subtypes (Hayashi et al., 2000; Shi et al., 2001; Shi et al., 1999).

The basic hypothesis for synaptic plasticity at the Schaffer Collateral now stands that the influx of Ca^{2+} through NMDAR initiates a signaling cascade with the end result that AMPAR are inserted into the post-synaptic density. This finding is specific to Schaffer Collateral synapses, as at other synapses plasticity can be induced by other pathways, like metabotropic glutamate receptors, or have different expression mechanisms like an increase in presynaptic release probability (e.g. the mossy fibre synapse). While the NMDAR hypothesis is the standard model for plasticity, occasional papers continue to advocate for different forms of plasticity at this synapse (Enoki et al., 2009). The rest of the introduction will concern the structure and function of AMPAR, how AMPAR are trafficked, and the signaling pathways important in AMPAR trafficking.

1.3 AMPAR structure and function

AMPAR are one of the most common neurotransmitter receptor in the brain (Hollmann and Heinemann, 1994) , and are responsible for the majority of fast excitatory transmission. They have been studied extensively, including their expression, structure, function, modification, and trafficking. This part of the introduction will explore all of those areas.

AMPAR subtypes

Functional AMPAR are formed by tetramers composed of one or two of the four AMPAR subtypes, GluR1-4. GluR1 and 4 have long carboxy-terminal tails, while GluR2 and 3 have short tails (Kohler et al., 1994). GluR4 is expressed early in development, while the others are expressed as adults (Zhu et al., 2000). The tetrameric structure is composed of either homomers of the same subtype; or heteromers of two differing subtypes, typically either GluR1/2 or GluR2/3 (Boulter et al., 1990; Nakanishi et al., 1990; Sakimura et al., 1990; Wenthold et al., 1996). The subunit composition of receptors determines their ionic conductances and trafficking.

AMPAR are expressed throughout the adult brain in pyramidal and granule cells (Sato et al., 1993), with expression peaking in adolescence (Pellegrini-Giampietro et al., 1991). Within the CA1 region of the hippocampus, AMPAR density increases with distance from the soma in both the synapse and dendrite, which leads to a normalization of somatic EPSPs (Andrasfalvy and Magee, 2001; Magee and Cook, 2000; Smith et al., 2003)

AMPAR general structure

AMPAR are ionotropic glutamate receptors, and as such have the canonical structure including an extracellular N-terminus, four membrane domains (M1-4), including a membrane loop (M2), and an intracellular C-terminus (Fig. 2A).

The extracellular amino terminus contains over half the amino acids of the receptor. The initial N-terminus of AMPAR contains an ER start transfer sequence

common to all transmembrane proteins. Downstream of this motif is the LIVBP domain, which is involved in the initiation of dimerization of receptors. Next is the S1 segment which in combination with the S2 domain (see below) forms the ligand binding domain (LBD). M2 forms the pore loop. Between transmembrane domains M3 and M4 is an extracellular loop, S2, that combines with S1 to form the LBD (Greger et al., 2007). Finally, the C-terminal of the protein is involved in intracellular signaling and trafficking of receptors. (Fig. 2A)

M2 contains the pore loop, and has a site for post-translational editing at a Q/R site. In the unedited form, the uncharged amino acid glutamine (Q) is in the pore, which allows Ca^{2+} to pass through. However, in the GluR2 subunit this residue is modified to arginine (R) which has a positive charge, preventing Ca^{2+} from passing through (Hume et al., 1991). Since this editing is specific to GluR2, GluR2 containing AMPAR cannot conduct Ca2+. The positive charge from arginine has the secondary effect of preventing positively charged polyamines from blocking the channel at depolarized voltages (Hume et al., 1991). Thus, GluR2-containing AMPAR are non-rectifying channels at depolarized voltages. In contrast, GluR2-lacking receptors are inwardly rectifying.

The extracellular loop has two sites of potential variation, R/G editing and the flip/flop domain. The R/G editing modifies an arginine to a glycine, which prevents the formation of salt bridges with nearby negative charges as seen in kainate receptors, and can speed recovery from desensitization (Lomeli et al., 1994). The flip/flop site are two alternative splice variants, which in combination with TARPs (see below) determine channel conductance and desensitization (Dingledine et al., 1999; Kott et al., 2007; Partin et al., 1993).

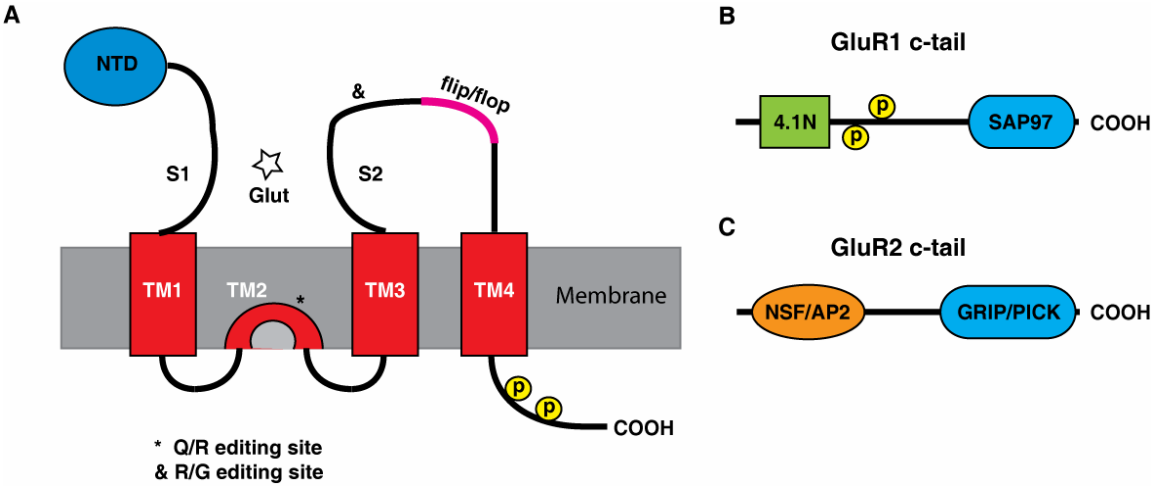

Figure 2: Schematics of AMPAR structure
A. Overall structure of AMPAR. Definitions are as follows: NTD, n-terminal domain; S1/S2, parts of ligand binding domain; TM, transmembrane domain; p, phosphorylation sites **B.** Layout of GluR1 c-tail, with c-terminus to right. p represent phosphorylation sites S831, T840, and S845. **C.** Layout of GluR2 c-tail.

AMPAR channel function

AMPAR are activated by ligand binding to the LBD formed by S1 and S2. The most common ligand is glutamate, although AMPAR also preferentially bind AMPA, giving the receptor its name. The LBD can alternatively be split into D1 (upper) and D2 (lower) domains, where D1 is the N-terminal part of S1, and D2 is a combination of the c-terminal portion of S1 and all of S2. At rest, D2 is thought to lie closed at the end of the ion pore, preventing current flow. When glutamate binds to D1, it causes D2 to tilt upwards, opening the channel (Hansen et al., 2007). A minimum of two glutamate molecules must bind before the channel will open, and the channel widens as more LBDs are occupied, increasing channel conductance from 5-12 pS (Raghavachari and Lisman, 2004; Robert and Howe, 2003; Rosenmund et al., 1998; Smith and Howe, 2000). After 5-10ms, however, the channel desensitizes when the D1 segment changes

conformation, allowing D2 to fall down and close the channel (Armstrong et al., 2006; Lisman et al., 2007). This desensitization can be blocked by the drug cyclothiazide, which interacts with the LBD (Partin et al., 1993). The rapid desensitization of AMPAR is unique among iGluRs. Channel conductances can be further modified by phosphorylation (see below).

AMPAR auxiliary subunits

Beyond the core subunits, auxiliary subunits can regulate AMPAR function, including transmembrane AMPA Receptor regulatory proteins (TARP), cornichons, and CKAMP44. TARPs (γ2, γ3, γ4, and γ8) are four-transmembrane domain proteins that interact with AMPAR's LBD, and can control surface expression of AMPAR, as well as channel conductances and desensitization (Kott et al., 2007; Tomita et al., 2007; Tomita et al., 2003). They contain an intracellular PDZ domain that can interact with PSD-95, a synaptic anchoring protein (Dakoji et al., 2003; Schnell et al., 2002), which may be involved in regulating the surface levels of GluR1 (Shi et al., 2001) and the mobility of AMPAR in the synapse (Bats et al., 2007). Knock-in of a truncated form of PSD-95 does not change basal synaptic transmission (Migaud et al., 1998), probably due to compensation by other MAGUKs (Elias et al., 2006). In contrast, acute knockdown of PSD-95 impairs the late phase of LTP, but not the early phases, indicating a selective interference with late-phase retainment (Ehrlich et al., 2007).

The cornichon (CNIH-2 and -3) family competes with TARPs for AMPAR binding, and similarly regulate AMPAR surface expression, slow deactivation, and reduce desensitization (Schwenk et al., 2009). In contrast to TARPS and cornichons, which

increase AMPAR conductances, CKAMP44 decreases AMPAR currents, and slows recovery from desensitization (von Engelhardt et al., 2010).

AMPAR carboxy terminus

The C-tail of AMPAR contains a large number of domains that can control AMPAR function; generally, proteins either interact with short- or long-tail subunits. Starting from the N-tail of long-tail subunits, the first interaction domain is for 4.1N (Fig. 2B) (Shen et al., 2000). The 4.1 family of proteins is involved in the organization of the spectrin-actin cytoskeleton, and disruption of 4.1 binding reduces AMPAR surface expression (Coleman et al., 2003; Shen et al., 2000). The binding of 4.1 to AMPAR is enhanced by phosphorylation of S816 and S818, depalmitoylation of S811, and is involved in the exocytosis of AMPAR in a PKC dependent manner (Lin et al., 2009).

The next important sites on long-tail subunits are a trio of phosphorylation sites, S831, T840, and S845. S831 is phosphorylated by CaMKII and PKC (Barria et al., 1997a; Roche et al., 1996), specifically during LTP (Barria et al., 1997b). Phosphorylation of S831 increases the open channel conductance (Derkach et al., 1999), and is sufficient to drive AMPAR to synapses (Hayashi et al., 2000). Mutant mice deficient in S831 phosphorylation learn normally, but have impaired memory (Lee et al., 2003). T840 has only recently been discovered, is phosphorylated by p70S6 kinase, and is dephosphorylated by NMDAR activation via PP1 or PP2A (Delgado et al., 2007; Lee et al., 2007). S845 is phosphorylated by PKA, and increases the peak open probability of receptors (Banke et al., 2000). S845 phosphorylation is required for synaptic retention of AMPAR (Esteban et al., 2003; Lee et al., 2003). More recently, it was discovered that

cGKII also phosphorylates S845, but the role of this phosphorylation is still unclear (Serulle et al., 2007).

The last 3-4 amino acids of the C-tail form a PDZ binding site, and are common to both long- and short-tail AMPAR. PDZ domains consist of a repeated GLGF motif, and are common to many proteins in the PSD (Feng and Zhang, 2009; Garner et al., 2000). There are three classes (1-3) of PDZ binding domains, which selectively bind to different PDZ domains to determine binding specificity (Doyle et al., 1996; Hung and Sheng, 2002). For AMPAR, long-tail subunits have a class I PDZ binding domain, which binds the protein SAP97 (Cai et al., 2002; Leonard et al., 1998). SAP97 is a member of the MAGUK family of proteins, and is involved in trafficking AMPAR from the ER to the membrane (Sans et al., 2001; Waites et al., 2009), and may regulate the interaction of AMPAR with PKA (Colledge et al., 2000). SAP97 can also interact with myosin VI, which plays a role in endocytosis (Osterweil et al., 2005; Wu et al., 2002). Overexpression of SAP97 causes an increase in spine size and mEPSC frequency (Rumbaugh et al., 2003).

Short-tail AMPAR contain a consensus SVKI, class II PDZ binding domain which interacts with the proteins GRIP1, PICK1, and ABP/GRIP2, all of which compete for binding (Fig. 2C). The GRIP family of proteins contains seven PDZ domains, and is thought to be involved in connecting AMPAR to a variety of other proteins (Dong et al., 1997), including kinesin 5 (Setou et al., 2002), and liprin (Wyszynski et al., 2002). The consensus from the literature is that GRIP is involved in bringing AMPAR to the membrane and retaining them there, in a phosphorylation dependent manner (Kulangara

et al., 2007; Osten et al., 1998). GRIP1 binding is inhibited by phosphorylation of S880 (Chung et al., 2003; Chung et al., 2000).

In competition with GRIP1, PICK1 appears to prevent AMPAR from reaching the membrane. It does this by directing PKC to AMPAR, which phosphorylates S880 of GluR2, which in turn prevents GRIP1 binding (Perez et al., 2001). Furthermore, PICK1's BAR domain is able to directly interact with GRIP/ABP, preventing it from interacting with GluR2 (Lu and Ziff, 2005). Without GRIP1 binding, GluR2-containing AMPAR remain bound to PICK1, and retained in intracellular stores (Lin and Huganir, 2007). Overexpression of PICK1 causes an increase in basal AMPAR current in an NMDAR-dependent manner, occluding LTP, and preventing LTD (Terashima et al., 2004; Terashima et al., 2008). However, shRNA and KO of PICK1 also prevents LTP and LTD (Terashima et al., 2008). How this works remains unclear.

NSF is an exocytosis associated protein that is involved in disassembling SNARE complexes following membrane fusion, and binds to GluR2 near the membrane. Intracellular infusion of peptides preventing NSF-GluR2 association leads to a decrease in surface expression of AMPAR and a run-down of synaptic strength (Luscher et al., 1999; Nishimune et al., 1998; Noel et al., 1999; Osten et al., 1998; Song et al., 1998). Given NSF's putative role in exocytosis, it was hypothesized that NSF was involved in delivering AMPAR to the surface, although others thought it may be play a role in keeping AMPAR at the surface, preventing endocytosis. One lab measured endocytosis rates, and found that by excising the NSF binding domain from GluR2, the activity-dependent exocytosis rate was decreased (Braithwaite et al., 2002). Later research from Morgan Sheng's lab showed that there is an AP2 binding site that overlaps with NSF

(Lee et al., 2002). AP2 is a clathrin adaptor complex, and helps mediate endocytosis, and interference with AP2 binding prevents activity dependent endocytosis (Lee et al., 2002). Thus, the previous results may be explained by effecting AP-2. In the same paper, the Sheng lab used more specific peptide inhibitors, and showed that interference of NSF binding causes a decrease in evoked EPSCs, but not surface expression, while interfering with AP-2 prevented LTD. Thus, the current hypotheses are that NSF regulates GluR2 anchoring in the synapse, while AP-2 is involved in activity-dependent endocytosis. NSF may also play a role in preventing GluR2-contatining AMPAR from being sorted to lysosomes (Lee et al., 2004).

1.4 AMPAR Trafficking

Like all membrane bound proteins, AMPAR are synthesized in the ER, then trafficked through the Golgi network and endosomes before reaching the plasma membrane (Kennedy and Ehlers, 2006). As the focus of this thesis is the role of AMPAR in plasticity, I will concentrate on trafficking from endosomes to the plasma membrane (exocytosis), diffusion within the plasma membrane, and endocytosis back to endosomes.

AMPAR exocytosis

To reach to the plasma membrane, receptors must be exocytosed from endosomes. Before considering the specifics of AMPAR exocytosis, it may be useful to briefly describe general vesicular trafficking and membrane proteins. Once synthesized

in the ER, membrane and secretory proteins move into vesicles that bud off the ER and are transported to the Golgi for sorting. From there, proteins bound for the plasma membrane (i.e. AMPAR) are sorted into secretory vesicles, or endosomes, which are directed along microtubules to their destination. Once there, the multi-step process of fusion is facilitated by the SNARE complex. The SNARE complex is formed by complementary sets of vesicle and target SNAREs, the specific identity of which will determine that vesicles bind with their correct target. Both types of SNAREs contain alpha helices that intermingle, and may create leverage to bring the two membranes together. Once the two membranes are directly apposed, first one half of the lipid bilayer fuses (called hemifusion), and then the second layer also fuses. Once fusion has begun, the hole can either close again quickly (called kiss-and-run exocytosis), or expand, uniting the vesicle and plasma membranes. Following full fusion, the SNARE complex disassociates.

AMPAR-containing endosomes can be found in endosomes in the dendrite, in the spine shaft, and even within spines themselves (Park et al., 2006). AMPAR are exocytosed in the classical SNARE-dependent manner. The exocyst protein sec8 is involved in bringing endosomes to their destination while exo70 is involved in the exocytosis fusion event (Gerges et al., 2006). Both GluR1 and GluR2 have specific binding sites which modulate exocytosis. For GluR1 it is the 4.1N binding site, which if disrupted downregulates exocytosis (Lin et al., 2009). For GluR2, its NSF binding site mediates exocytosis, and disruption of this interaction cause a rundown of synaptic currents (Luscher et al., 1999; Nishimune et al., 1998). Three groups have estimated the basal turnover rate: one group used immunofluorescence, removed all surface

fluorescence, and saw recovery of 10-40% after thirty minutes; a second used an irreversible AMPAR antagonist for surface receptors, and found that it took hours for surface currents to recover, although the rate is faster in the soma (Adesnik et al., 2005); and a last group performed biotinylation assays and saw AMPAR are internalized within tens of minutes (Ehlers, 2000)

The exocytosis of AMPAR, and specifically GluR1, is an essential part of LTP. Blockade of SNARE mediated exocytosis by tetanus toxin (TeTX) or Botulinum toxin completely blocks LTP (Lu et al., 2001; Park et al., 2004; Yang et al., 2008b). Myosins Va and Vb have been implicated in bringing endosomes to the spine, as disruption of their function prevents activity dependent exocytosis (Correia et al., 2008; Wang et al., 2008).

The specific site of activity dependent exocytosis is under debate. Under basal conditions, dendritic exocytosis has been almost exclusively observed (Leonoudakis et al., 2008; Lin et al., 2009; Yudowski et al., 2007). Furthermore, following glycine application Yudowski and colleagues saw an increase in exocytosis rate exclusively in the dendrite. Outside-out patches taken from dendrites before and after LTP show that the dendritic AMPAR current increases following LTP (Andrasfalvy and Magee, 2004). However, imaging of non-specific exocytosis using phluorin-tagged transferrin receptor has shown that spine exocytosis can occur (Park et al., 2006; Wang et al., 2008). One possible resolution to these discrepancies is that there are multiple exocytosis pathways and payloads, and the transferrin receptor exocytosis is separate from AMPAR exocytosis. To identify the sites of AMPAR exocytosis, in Chapter II we perform real

time imaging of AMPAR exocytosis while we stimulate single spines using glutamate uncaging.

Surface diffusion and endocytosis

Once exocytosed, AMPAR are localized to different surface compartments depending on their subtype. GluR2/3 heteromers are anchored in spines at synaptic sites, while GluR1 containing receptors diffuse along the extrasynaptic membrane, including the dendrite (Passafaro et al., 2001). (While GluR2-containing receptors on the surface are found at the synapse, most GluR2-containing endosomes are in the dendrite (Ashby et al., 2004).) Once exocytosed, GluR2-containing receptors quickly cluster in spines (Passafaro et al., 2001).

When not anchored, AMPAR diffuse along the plasma membrane. Single particle tracking studies give an estimated diffusion constant of ~0.1$\mu m^2/s$ (Borgdorff and Choquet, 2002; Tardin et al., 2003). AMPAR are able to diffuse freely in the dendrite, but have their movement inside spines either constrained or completely immobilized (Bats et al., 2007; Ehlers et al., 2007). AMPAR immobilization inside spines is probably due to interaction with PSD proteins like PSD-95; disruption of TARP-PSD-95 interaction decreases the number of immobilized receptors (Bats et al., 2007). Others have investigated AMPAR diffusion by using phluorin-tagged AMPAR, and performed FRAP. Initial experiments indicated that the half-time of recovery was on the order of 2-3 minutes, which implies a diffusion constant of ~0.01 um^2/s, much slower than the single particle diffusion value (Table 1) (Ashby et al., 2006; Axelrod et al., 1976; Sharma et al., 2006). They interpreted this data as showing that the spine neck acts as a diffusion

barrier for AMPAR, similar to how the spine neck compartmentalizes Ca^{2+} (Bloodgood and Sabatini, 2005; Grunditz et al., 2008; Koch and Zador, 1993; Muller and Connor, 1991). However, more recent experiments have yielded time constants of 60-90 seconds, which is more harmonious with the single particle tracking data (Makino and Malinow, 2009; Waites et al., 2009). Of note, the GluR2 time constants are all significantly longer than the GluR1 time constants, reflecting that GluR2 is more strongly anchored in the synapse.

	GluR1			GluR2	
	Mobile fraction (%)	Time constant (s)		Mobile fraction (%)	Time constant (s)
Sharma[a]			Ashby[b]		
Dendrite	78±8	48±3	Dendrite	84±4	11±3
Spine	56±4	198±42	Mushroom spine	54±4	223±25
Soma	78±8	26±5	Stubby	47±4	101±30
Makino[c]			Makino[c]		
Spines (naïve)	103±6	72±18	Spines (naïve)	81±3	108±36
Spines (cLTP)	70±4	NA	Spines (cLTP)	77±5	NA
Spines (uncaged)	79±6	NA	Spines (uncaged)	79±6	NA
Waites[d]			Arendt[e]		
Spines (αSAP97)	35±6	90±24	Spines (naïve)	26	342
Spines (βSAP97)	54±6	84±24	Spines (LY290042)	52	354
Spines (ΔSAP97)	70±6	72±24			
Me (Fig. 5)					
Spines (naïve)	81±7	60±18			
Spines (uncaged)	74±4	78±20			

Table 1: FRAP data from literature

[a](Sharma et al., 2006); [b](Ashby et al., 2006); [c](Makino and Malinow, 2009); [d](Waites et al., 2009); [e] (Arendt et al., 2009)

AMPAR are returned to recycling endosomes by endocytosis (Ehlers, 2000; Luscher et al., 1999). There are endocytic zones in the dendrite and inside spines nearby the PSD, as shown by EM (Petralia et al., 2003; Racz et al., 2004) and clathrin fluorescence microscopy (Blanpied et al., 2002). These zones can trap AMPAR for endocytosis, and interference with endocytosis decreases both the mobile pool of AMPAR and AMPAR increase following exocytosis (Lu et al., 2007; Petrini et al., 2009). The time constant of exocytosis is approximately 10 minutes, similar to that of exocytosis (Ehlers, 2000; Passafaro et al., 2001). Application of endocytosis antagonists cause a gradual increase in EPSC size (Luscher et al., 1999). Endocytosis of AMPAR can also be activity dependent (Ehlers, 2000). Two proteins have been identified as signalers of endocytosis: hippocalcin is a Ca^{2+} sensor which mediates AP2 binding to GluR2 (Palmer et al., 2005); PICK1 is a Ca^{2+} sensor which competes for GluR2's PDZ domain, and regulates NMDAR-dependent endocytosis (Hanley and Henley, 2005; Lu and Ziff, 2005).

1.5 AMPAR role in LTP

It is currently believed that the trafficking of AMPARs containing GluR1 is responsible for the increase of synaptic strength following LTP. This is based on the initial finding that following tetanic stimulation of CA1 pyramidal neurons, GFP-GluR1 translocates into spines (Shi et al., 1999). Reports from the same lab further showed that interference with GluR1's PDZ binding domain also prevented LTP (Hayashi et al., 2000). Finally, studies using chimeras of GluR1 and GluR2's carboxy terminus showed that GluR1 is trafficked to the spine following LTP while GluR2 is responsible for basal transmission (Shi et al., 2001). Besides increasing the synaptic strength, it has also

been proposed that AMPAR have a role in stabilizing spines (Kopec et al., 2007), although triple knockout mice lacking GluR1-3 have normal spines (Lu et al., 2009).

One way to measure the subtype composition of AMPAR in the synapse is to measure the rectification index. GluR2-containing receptors do not suffer polyamine block, so they do not rectify (see section 1.4 AMPAR channel function); GluR2-lacking receptors (i.e. GluR1 homomers) are blocked by polyamines, and do not pass currents at depolarized voltages. Thus one can measure the GluR1/2 ratio by comparing the current at depolarized versus hyperpolarized voltages, called the rectification index. When GluR1 is overexpressed, initiation of LTP by tetanic stimulation or CaMKII expression causes an increase in rectification (Arendt et al., 2009; Hayashi et al., 2000). Furthermore, two labs have reported an increase in rectification following LTP with no overexpressed proteins (McCormack et al., 2006; Plant et al., 2006). Given that GluR2 is nominally responsible for basal synaptic transmission, these labs also recorded the return to basal rectification as 20 minutes (Plant et al., 2006) or 15-18 hours (McCormack et al., 2006). Other labs, however, have reported no change in rectification or polyamine block following LTP (Adesnik and Nicoll, 2007; Andrasfalvy and Magee, 2004).

Further support for the GluR1 hypothesis comes from knockout studies which show that GluR1 null mice have no Schaffer Collateral LTP (but do have theta burst Schaffer Collateral LTP and perforant path LTP) (Hoffman et al., 2002; Zamanillo et al., 1999). Surprisingly, after being run through a gamut of memory tests, GluR1 mice had no deficits to spatial memory as measured by the Morris Water maze, and impaired memory on only one test, an alternating Y-maze task (Reisel et al., 2002; Zamanillo et

al., 1999). This result was followed up recently showing that the GluR1 KO mice had specific deficiencies in short term memory after acquisition, and not days later (Sanderson et al., 2009).

One niggling problem with the GluR1 dogma is that the subunit composition of endogenous receptors in CA1 is still under debate. The current hypothesis is that the two most prevalent dimers in the hippocampus are GluR1/2 and GluR2/3. As both of these dimers contain GluR2, neither would be inwardly rectifying. This explains why systems in which GluR1 is overexpressed and is able to form functional homomers more readily show rectification. Furthermore, it was presumed that GluR2/3 dimers are responsible for basal synaptic transmission. However a recent paper using single-cell genetic techniques has shown that a majority of receptors may in fact be GluR1/2 heteromers, and that they are incorporated into synapses (Lu et al., 2009). It will take further experiments to sort out the subunit composition of AMPAR in the hippocampus, and specifically in CA1 pyramidal cells.

1.6 Signaling pathways in LTP

Many signaling pathways have been identified as necessary for long term potentiation, but the organization and function of these signaling pathways is still being disentangled. The signaling cascade is initiated by calcium influx through NMDAR, which then binds to calmodulin (Davies et al., 1981; Lynch et al., 1983; Malenka et al., 1989). Two calmodulin kinases, calcium-calmodulin kinases I and II (CaMKI and CaMKII) are activated by calmodulin. Inhibition of CaMKI, the lesser studied kinase, by pharmacological inhibitors (STO-609) or dominant negative expression reduces LTP

magnitude, and also causes a decrease of phosphorylation of ERK (see below) (Schmitt et al., 2005). Similarly, peptide inhibitors of CaMKII block induction (Otmakhov et al., 1997), and the maintenance of LTP (Sanhueza et al., 2007). Furthermore, as mentioned in section 1.5 (AMPAR role in LTP), expression of a constitutively active form of CaMKII is sufficient to drive GluR1 into synapses, and increase synaptic currents (Hayashi et al., 2000). Later, it was discovered that CaMKII can associate directly with the NR2B subunit, which can mechanistically explain the link between NMDAR Ca^{2+} currents and LTP (Barria and Malinow, 2005). A recent study using a CaMKII FRET sensor showed that CaMKII is activated only briefly in the spine, with highly restricted localization (Lee et al., 2009).

One of the best described signaling pathways in LTP is the Ras-MEK-ERK pathway. Uncaging experiments using a FRET sensor for Ras activity have shown that Ras is activated in stimulated spines, as well as the neighbouring dendrite (Harvey et al., 2008). Dominant negative forms of the small GTPase Ras impair LTP, and appear to be upstream of the MAP kinase ERK (Qin et al., 2005; Zhu et al., 2002). Part of Ras's role in LTP is likely due to its regulation of MAP kinases, which are also necessary for LTP (English and Sweatt, 1997). Interestingly, a related Ras-family GTPase, Rap, may play the opposite functional role, and be involved in LTD (Qin et al., 2005; Zhu et al., 2002). One side component of the Ras pathway are the phosphoinositol-3 kinases (PI3K), which form a feedback loop with Ras. Pharmacological inhibition of PI3K has been shown to block LTP, although labs differ as to whether PI3K is involved in the induction or maintenance of LTP (Man et al., 2003; Sanna et al., 2002).

The Ras signaling pathway is particularly interesting given the role of other small GTPases in membrane trafficking. Many small GTPases can transition between the cytosol and membranes depending on lipid modification like palmitoylation or prenylation. Typically, these proteins are cytosolic when GDP-bound and membrane associated when GTP-bound. The Rab family of GTPases is especially well known for their involvement in membrane dynamics, and each member of the family is associated with different, specific organelles. Their membrane specificity is thought to enhance the specificity of SNAREs. In theme with their membrane specificity, each Rab also has unique effectors. Given that Ras is also a small GTPase, it may similarly play a role in membrane trafficking.

Beside the well described Ras-MEK-ERK pathway are a variety of less well known pathways. Many proteins which regulate AMPAR trafficking also influence LTP, and will not be covered here (see sections 1.3 and 1.4). Besides those, the first downstream signaling molecule to be discovered was PKCγ, for which KO mice lacking the kinase have no LTP (Abeliovich et al., 1993). Next is PKA, which can phosphorylate GluR1 subunits at serine 845. Overexpression of mutant forms of GluR1 that cannot be phosporylated (S845A) blocks the maintenance, but not induction, of LTP (Esteban et al., 2003). Finally, PKMζ has been hypothesized to be the sustainer of synaptic plasticity, as reversible inhibitors of PKMζ reversibly decrease LTP (Ling et al., 2002).

1.7 Structural Plasticity

Spines are the basic compartment for excitatory synapses (Yuste and Denk, 1995). For over forty years people have studied how learning and experience can

change spine number (Globus and Scheibel, 1967; Yuste and Bonhoeffer, 2001). More recently, spine morphogenesis has been observed using in vivo imaging to track the number of spines in the same animal during learning (Engert and Bonhoeffer, 1999), and these new spines have been shown to form synapses (Trachtenberg et al., 2002).

Besides an increase in the number of spines during learning, existing spines also change their structure, a phenomenon called structural plasticity. This phenomenon was originally observed in the hippocampus by using EM to study spine size in the DG following stimulation of the perforant path (Fifkova and Van Harreveld, 1977). A series of EM studies over the next decade further showed structural plasticity following LTP in the hippocampus (Lee et al., 1980; Ostroff et al., 2002) and aplysia (Bailey and Chen, 1983). Structural plasticity was finally observed on the population level in real time using two-photon imaging (Maletic-Savatic et al., 1999). The most advanced experiments to date have shown that stimulation of a single spine causes an increase in spine volume, concomitant with an increase in stimulated currents (Matsuzaki et al., 2004).

The increase in spine size following LTP is in accord with the finding that in the basal state spine size is highly correlated with synaptic strength. EM studies have shown that spine head volume is correlated with PSD size, the number of presynaptic vesicles (Harris and Stevens, 1989) and presynaptic active zone size (Schikorski and Stevens, 1997). In turn, immunogold EM has shown that the PSD length is correlated with the number of AMPAR in the PSD, but not the number of NMDAR (Kharazia and Weinberg, 1999; Takumi et al., 1999). Interestingly, these labs found that sufficiently small spines lacked AMPAR altogether, perhaps indicating silent synapses (Nusser et al., 1998; Takumi et al., 1999). Functionally, uncaging evoked currents from spines are

correlated with spine volume (Matsuzaki et al., 2001). Given the strong correlation between spine size and synaptic strength in CA1 pyramidal neurons, for the rest of this work, we will use spine size and structural plasticity as proxies for synaptic strength and synaptic plasticity, respectively.

The timecourse of structural plasticity differs depending on the stimulus protocol used. Focal release of glutamate on spines (by two photon uncaging) without depolarizing the target cell yields a rapid, transient increase in spine volume followed by a plateau (Fig. 4, (Harvey and Svoboda, 2007; Harvey et al., 2008; Lee et al., 2009; Matsuzaki et al., 2004). However, pairing uncaging with depolarization leads to a stepwise increase in synaptic strength, without decay (Harvey and Svoboda, 2007; Lee et al., 2009; Tanaka et al., 2008). Theta-burst protocols similarly cause a rapid, stepwise increase in structural plasticity with no decay (Yang et al., 2008b). The role of this transient phase of structural plasticity is currently unknown.

The signaling pathways involved in structural plasticity are much the same as the pathways for LTP. Structural plasticity can be separated into an early, transient phase and a late phase (>30 min.) Some drugs can block both phases of structural plasticity by preventing the induction of LTP, like NMDAR (CPP) antagonists (Harvey et al., 2008). More typically, drugs reduce late-phase structural plasticity without affecting the early phase. Examples of these include botulinum toxin, a peptide that blocks exocytosis; (Yang et al., 2008b), PKI (PKA) (Yang et al., 2008b), anisomycin (protein synthesis) (Tanaka et al., 2008; Yang et al., 2008b), latrunculin A (actin) (Matsuzaki et al., 2004), KN62 (CaMKII) (Harvey et al., 2008; Lee et al., 2009; Matsuzaki et al., 2004) and U0126 (MEK) (Harvey et al., 2008). Using genetic techniques to reducie CaMKII

autophosphorylation (Lee et al., 2009), and dominant negative Ras (Harvey et al., 2008) both reduce sustained structural plasticity without affecting the transient phase. Note that all of these pathways have also been implicated in LTP. There are no known ways to block the transient phase without effecting the sustained phase.

1.8 Focuses of this dissertation

This dissertation will attempt to address open questions about AMPAR, their trafficking, and the signaling pathways involved in LTP.

What are the relative contributions of surface and endosomal AMPAR during LTP?

AMPAR, for the purposes of this work, exist in two pools: at the cell surface and in endosomes. In the basal condition, 25-66% of the total AMPAR are at the surface (Ehlers, 2000; Passafaro et al., 2001; Shi et al., 1999) where they are concentrated in spines (Kopec et al., 2006). Upon stimulation, the number of AMPAR in the spine increases, drawing from the surface pool of AMPAR, as well as newly exocytosed AMPAR (Kopec et al., 2006; Kopec et al., 2007). A recent paper from the Malinow lab has found that both surface receptors, as well as newly exocytosed receptors reach the spine (Makino and Malinow, 2009). Knowing the source of AMPAR will inform our understanding of the role of exocytosis in synaptic plasticity. If a majority of AMPAR that reach the synapse were already at the surface, it raises questions as to how important exocytosis is.

In section 2.4 we address this issue by stimulating single spines, and manipulating the size of the surface and exocytosed pools of receptors (by bleaching them or inhibiting exocytosis, respectively; Fig. 3, question 1). We found that a majority of the receptors that enter the spine were already at the surface.

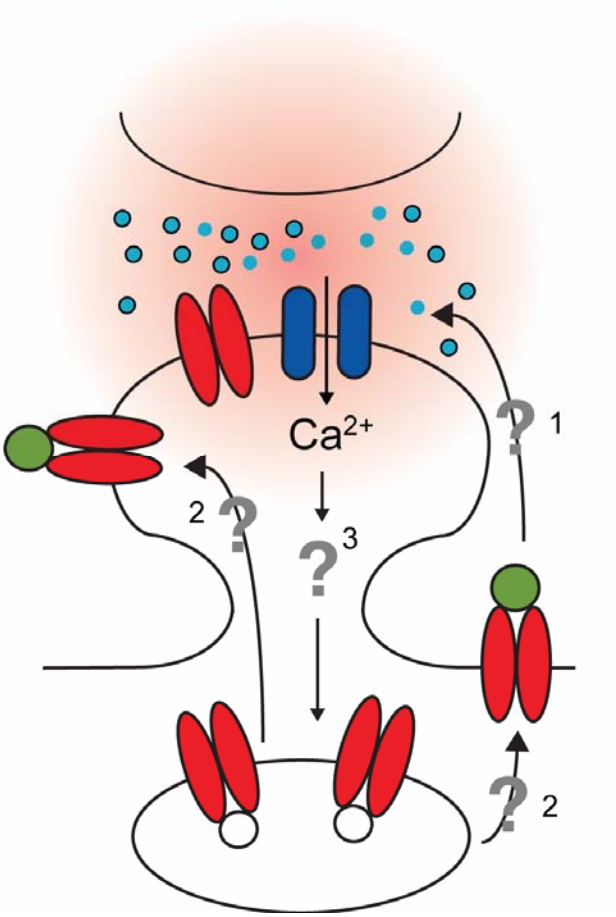

Figure 3: Questions of this dissertation
This dissertation will address the questions: 1. What proportion of AMPAR that reach the synapse during LTP come from an already existing surface population versus newly exocytosed from endosomes? While exocytosis is important for LTP, whether the essential role of exocytosis is to provide AMPAR remains unclear. 2. Where and when AMPAR are exocytosed during synaptic plasticity? The location and timing of exocytosis will determine how quickly AMPAR can reach the synapse. 3. Which signaling pathways signal exocytosis? There is a laundry list of signaling proteins known to be involved in LTP, but which functional outputs they are connected to remains unclear.

When and where are AMPAR exocytosed during synaptic plasticity?

The location of activity-dependent AMPAR exocytosis is under debate. Imaging of AMPAR exocytosis has shown that a large majority of basal exocytosis occurs in the

dendrite (Lin et al., 2009; Yudowski et al., 2007). Furthermore, following synaptic plasticity, there is an increase in dendritic AMPAR current (Andrasfalvy and Magee, 2004). However, the Ehlers lab has imaged transferrin receptor exocytosis following chemical LTP, and has seen exocytosis in spine.

Besides its location, the kinetics of activity-dependent exocytosis have not been explored. Most experimental protocols investigating exocytosis have used widespread chemical LTP, wherein the experimenters cannot determine which synapses are stimulated, and when. It remains unclear how much time elapses before AMPAR are exocytosed, and for how long the exocytosis rate remains elevated. The location and timing of exocytosis have implications for how quickly AMPAR can reach the synapse: the more closely and quickly they are exocytosed, the faster the synapse can potentiate, and different forms of memory can be encoded by this process.

In order to identify the location and timing of exocytosis, in section 2.5 we directly image AMPAR exocytosis events following focal stimulation of single spines (Fig. 3, question 2). We found that AMPAR are exocytosed in both the spine and dendrite shortly after the beginning of stimulation, and for a limited duration (~1 minute).

What signaling pathways lead to AMPAR exocytosis?

A large number of signaling pathways have been identified as important for LTP (see section 1.6), and structural plasticity (section 1.7). However, what specific functions these pathways signal (e.g. anchoring, exocytosis) remains unclear, due to a paucity of methods to directly measure these outputs (Fig. 3, question 3). Given the lack of direct connections, it remains difficult to deduce whether certain signaling pathways are

necessary for LTP, or for more general processes like regulating actin dynamics or ion balance. To truly understand the processes of plasticity and memory, we need to deconstruct the actual roles of each signaling pathway. After developing a system in which to image AMPAR exocytosis, we have applied pharmacological antagonists and genetic perturbations to two signaling pathways - CaMKII and Ras-ERK - and found that the Ras-ERK pathway regulates activity dependent AMPAR exocytosis (the role of CaMKII remains unclear).

What are the characteristics of plasticity at single spines?

The classic properties of LTP in neurons – associativity, cooperativity, and input specificity – were identified relatively quickly following LTP's discovery (see section 1.2). However, the properties of LTP at single synapses are unknown. Two labs have used minimal stimulation techniques to monitor single synapses, which have revealed that plasticity at single synapses occurs in a step-wise fashion (Bagal et al., 2005; Petersen et al., 1998). Other basic properties, such as the threshold for LTP at a single spine, whether plasticity is digital or analog, and whether a single synapse can be repeatedly potentiated, are unknown. We chose to explore the simplest question, whether a single synapse can be repeatedly potentiated, by uncaging on the same spine twice. We found that a second stimulation induced no structural plasticity beyond the initial induction, implying that the synapse is saturated.

Chapter II: Timing and Location of AMPAR Trafficking

In the introduction, I described how AMPAR trafficking is essential for LTP, but that the spatiotemporal kinetics of the process need to be elucidated. In this section, we will address two of the questions posed in the introduction. First, we will investigate the relative contributions of diffusion and exocytosis to increases in synaptic receptor content. We will differentiate between them by comparing AMPAR trafficking in naïve and bleached conditions. Second, we will address the timing and location of AMPAR exocytosis by imaging AMPAR exocytosis in real-time, and look at how activity modifies AMPAR exocytosis by stimulating single spines using glutamate uncaging.

The use of two-photon glutamate uncaging can provide unique insights into these processes due to its temporal and spatial precision. In previous studies of AMPAR trafficking, experimenters would stimulate the entire Schaffer Collateral, or induce chemical LTP (for example (Kopec et al., 2006; Shi et al., 1999) among many others). These protocols stimulate a large number of unidentified synapses such that the analyses inevitably includes both stimulated and naive synapses. Furthermore, these protocols have generally imprecise temporal control such that the timecourses of trafficking must be course. In contrast to these older protocols, glutamate uncaging stimulates individual spines, such that we can restrict the analysis to spines that are being stimulated. It is also more temporally precise, taking approximately one minute, so that we can more accurately measure the timing of trafficking.

2.1 Materials and Methods

Constructs

In order to observe AMPAR trafficking we imaged GFP tagged GluR1, which consists of EGFP tagged to the extracellular n-terminus of GluR1, after the predicted signal peptide cleavage site, where it does not interfere with trafficking or signaling (Shi et al., 1999). To monitor surface AMPAR, we tagged AMPAR with super ecliptic phluorin (SEP), a pH sensitive fluorophore that is fluorescent only at pHs above 7. The fluid in the extracellular matrix has a pH of ~7, while the recycling endosomes of cells have a pH of 5-6.5, depending on their location in secretory pathway. Thus, SEP-GluR1 will be fluorescent at the cell surface, and dim when in endosomes. To label cell volume, we used mCherry. To test that SEP-GluR1 actually labels surface receptors, we applied pH 5.5 ACSF, and saw a decrease in fluorescence (Fig. 4). Then we applied NH_4Cl, which de-acidifies endosomes, and saw an increase in fluorescence (Fig. 4).

The SEP-GluR1 plasmid was generously provided by Scott Soderling (Duke University), the mCherry-IRES-tetanus toxin (mCh-IRES-TeTX) plasmid by Matt Kennedy and Michael Ehlers (Duke University), and the dominant negative Ras (dnRas), H-Ras with N17S mutation, by Linda van Aelst (Cold Spring Harbor Laboratory).

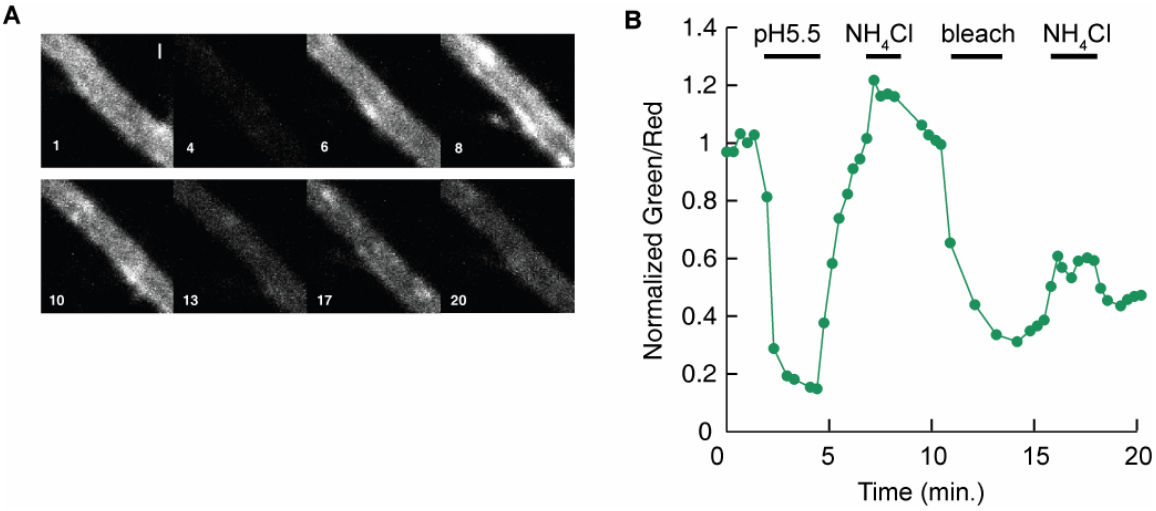

Figure 4: SEP-GluR1 labels surface AMPAR.
A. Images of SEP-GluR1 fluorescence from a primary dendrite during a bleaching protocol. Time shown in minutes, with matching conditions shown at right. Note that after bleaching in ACSF containing NH_4Cl, GluR1-containing endosomes can be visualized as puncta. Scalebar 1µm. **B.** Time course of fluorescence of whole dendrite, expressed as ratio of SEP-GluR1/mCherry (green / red). The fluorescence increase under NH_4Cl is similar before and after bleaching. Similar results were reproduced in 3 cells. Scale bar 1 µm.

Slice Preparation

Hippocampal slice cultures were prepared from postnatal day 6 or 7 rats, in accordance with the animal care and use guidelines of the Duke University Medical Center (Stoppini et al., 1991). Pups were anesthetized under isofluorane, and then their hippocampuses were removed, and placed in chilled dissection media. The hippocampuses were then transferred to a tissue chopper, and sliced into 300µm slices. Next, slices were transferred to a Millipore membrane with 0.2µm pore size filter, and left to incubate in tissue media at 32° C. After 7-12 days in culture, the slices were biolistically transfected (McAllister, 2000) with 1µm gold beads at a 1:1 molar ratio of

SEP-GluR1:mCherry (ratios for other constructs as follows: for GFP-GluR1:mCh, 1:4; for YFP-CD8:mCh, 1:1; for SEP-GluR1:mCh-IRES-TeTX, 1:1; for SEP-GluR1:mCh:dnRas, 3:3:2). Experiments were performed 3-4 days later to allow for full, bright expression of both SEP-GluR1 and mCherry, and to allow TeTX and dnRas to be effective

Imaging and Glutamate Uncaging

We used a custom-built two-photon microscope with two Ti:sapphire lasers (Spectra-physics). One laser was tuned to 920 nm to excite both SEP-GluR1 for AMPAR trafficking, and mCherry for morphology. The second laser was tuned to 720 nm for glutamate uncaging. Each lasers' intensity was controlled independently using electro-optical modulators (Pockels cells, Conoptics). The beams were combined using a beam-splitting cube, and passed through the same set of scan mirrors and objective (60x, 0.9 NA, Olympus). SEP and mCherry fluorescence were separated using a dichroic mirror (565 nm) and bandpass filters (510/70, 635/90; Chroma). Fluorescence signals from PMTs (R3896, Hamamatsu) were acquired by ScanImage using a data acquisition board (PCI-6110, National Instruments) (Pologruto et al., 2003).

All experiments were performed at room temperature (~25° C) in standard artificial cerebral spinal fluid (ACSF) (4 mM $CaCl_2$, 0 mM $MgCl_2$, 1 µM TTX, and 2.5 mM MNI-caged-L-glutamate aerated, 95% O2 and 5% CO_2). Two-photon glutamate uncaging was performed in ACSF lacking Mg^{2+}, in the presence of MNI-caged-L-glutamate (2.5 mM) and TTX (1 µM). The Mg^{2+} free solution allowed the uncaged glutamate to activate NMDAR. In ACSF without Mg^{2+}, regular synaptic activity is

stronger than normal, and can cause the slice to become epileptic. The TTX added to the bath prevents this.

For uncaging, 6-8 mW laser pulses (720 nm) were delivered to the back focal aperture of the objective for 6 ms. The uncaging beam was parked at a manually selected location ~0.5 μm from the tip of the spine head, away from the parent dendrite. Only spines well separated from the parent dendrite and nearby spines were selected for experiments. Typically, 15-30 pulses were applied, saturating structural plasticity.

All images are 128 x 128 pixels (10 μm x 10 μm). For long-term imaging, images were taken as a stack of five slices with 1 μm separation, averaging six frames each for each slice. Typically three stacks of images were taken before uncaging to provide a baseline for normalization. When imaging while uncaging, images were acquired in a single plane every 4-8s, averaging six frames per image. For the exocytosis imaging (section 2.5), frames were acquired in a single plane at 4 Hz for 50s, yielding 200 frames.

For bleaching experiments, we used two methods of bleaching. First, we turned the power of the 920 laser to its maximum to bleach all SEP-GluR1 in the field being imaged, typically at 25x. SEP is a highly sensitive fluorophore, thus 60-120s of bleaching was enough to bleach more than 90% of fluorescence. In contrast, mCh fluorescence was bleached less than 10%, and recovered quickly due to mCh's high diffusion rate. To verify that we were selectively bleaching only surface receptors, and not bleaching internal receptors, we applied NH_4Cl to de-acidify internal stores, raising their pH, and allowing internal receptors to be excited. Both before and after bleaching,

applying NH_4Cl caused fluorescence increases of ~15% of the original fluorescence (Fig. 4), suggesting that our bleaching protocol does not bleach internal stores.

While two-photon bleaching is simple to implement, it has the limitation that the bleaching area is typically restricted (10μm x 10μm area at 25x), and only bleaches in the imaging plane. For a subset of experiments, we also used a lamp bleaching protocol wherein we reduced the aperture of our mercury lamp to its minimum, and turned on the lamp for 60-120s. This bleached a larger area (>20μm radius) of SEP-GluR1, in all planes. It also did not significantly bleach mCherry fluorescence.

Data Analysis

To identify exocytosis events from movies of SEP-GluR1 fluorescence, we filtered movies using a Gaussian spatial filter of 3 pixels (0.75 μm) and a temporal filter of 5 frames (1.25s). Background fluorescence was corrected by simple subtraction of surrounding fluorescence. Spines and dendrites were typically well bleached, and exocytosis events were identified in filtered timecourses as increases above the noise level (Fig. 8C). In the dendrite, exocytosis events were semi-automatically identified by: filtering movies; drawing a kymograph along the dendrite; identifying points with rapid increases (< 1 s) in fluorescence (threshold ~ 30%); then playing movies to verify they were not artifacts due to endosomes moving along the dendrite (when all surface fluorescence is bleached, the small fluorescence from receptors in endosomes is higher than the background, and moving endosomes can appear as rapid fluorescence increase). The identified exocytosis events in spines and dendrites were further verified

for a rapid (< 0.5 s) fluorescence increase lasting more than ~1 s by looking at the unfiltered fluorescence time-course by eye.

2.2 Long-term imaging of AMPAR trafficking

We began our investigation of AMPAR trafficking by overexpressing GFP-GluR1 in area CA1 of the hippocampus. This labeled both internalized AMPAR in endosomes as well as surface AMPAR. GFP-GluR1 (and SEP-GluR1) was expressed throughout the cell body and dendrites of neurons (Kessels et al., 2009). We also expressed mCherry as a cell fill to measure spine volume. To induce plasticity, we uncaged glutamate on single spines, and observed that the volume of the spine increased rapidly to a peak of +260±75% (all numbers in this section are percent change over initial fluorescence) before returning to a plateau of +120±30% that lasted for over thirty minutes (Fig. 5B). The extent and time-course of structural plasticity observed here was similar to that previously reported (e.g. (Harvey et al., 2008; Matsuzaki et al., 2004), confirming that overexpression of GluR1 does not effect plasticity (Fig. 5A-C; (Hayashi et al., 2000; Shi et al., 2001)). Concomitant with the volume increase, the GFP-GluR1 fluorescence also transiently increased by +200±60%, before relaxing to a plateau of +110±12%, which shows that GluR1 was recruited to the spine.

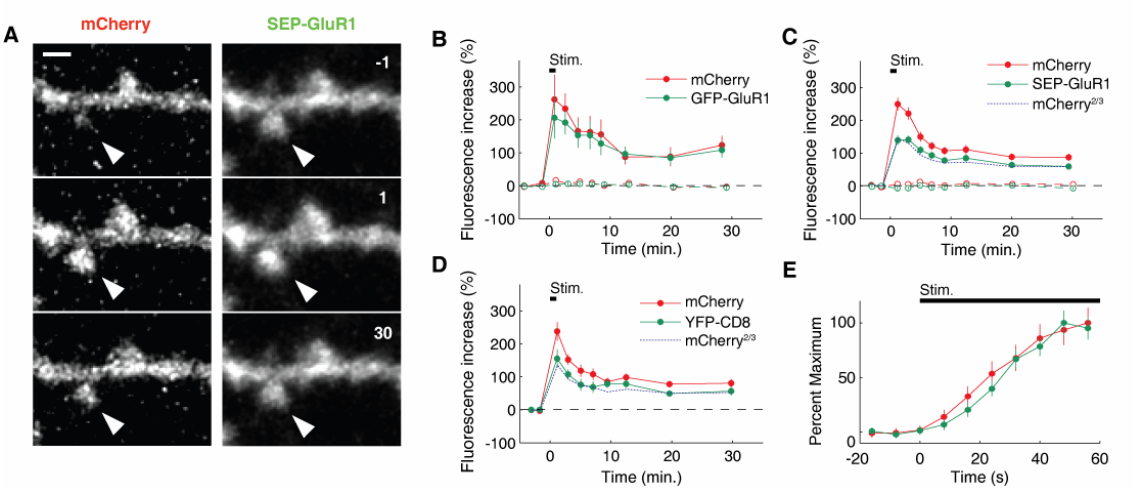

Figure 5: Uncaging causes long-term spine growth and the recruitment of AMPAR **A**. Images of a dendritic segment of a neuron transfected with mCherry (left) and SEP-GluR1 (right) before, immediately following, and 30 minutes following single spine stimulation (from top to bottom). Scale bar 1 µm. **B.** Timecourse of mCherry (red) and GFP-GluR1 (green) fluorescence increase following single spine stimulation. Stimulated spines (closed circles) increase in size transiently before plateauing. Adjacent spines do not grow (open circles). Fluorescence is normalized to three reference images before uncaging. *n* = 8 for stimulated spines, 5 adjacent spines, 3 cells. **C.** Timecourse of mCherry and SEP-GluR1 fluorescence following single spine stimulation. (Red fluorescence)$_{2/3}$ shown as blue dotted line. *n* = 34 for stimulated spines, 16 adjacent spines, 21 cells. **D.** Timecourse of mCherry and membrane tagged YFP-CD8 fluorescence following single spine stimulation. (Red fluorescence)$^{2/3}$ shown as blue dotted line. *n* = 13 spines, 4 cells. **E.** Timecourse of fluorescence (red is mCh, green is SEP-GluR1) increase during uncaging. Magnitudes normalized to peak fluorescence.

The above experiment shows that AMPAR are recruited to the spine, but may include internal AMPAR moving into the spine inside endosomes. To specifically image surface receptors, we transfected neurons with SEP-GluR1, and uncaged on their spines. SEP-GluR1 fluorescence followed a similar time course (Fig. 5C), showing that surface GluR1 also increased in the spine (Kopec et al., 2006; Kopec et al., 2007; Makino and Malinow, 2009). The increase in SEP-GluR1 fluorescence (peak 140±12%, sustained 60±7%) was smaller than the increase in the volume, which may reflect that there are indeed GluR1-containing endosomes that move into the spine, but do not fuse.

Notably, the SEP-GluR1 fluorescence increase was smaller than the mCherry increase at all time points, and may reflect the difference in the geometries labeled: mCherry labels the cell volume, which depends on r^3, while SEP-GluR1 labels a surface, which depends on r^2. Thus, one might naively expect that if SEP-GluR1 was freely diffusible, its fluorescence would increase with the 2/3rds power of the volume. Indeed, when we apply this function to the volume increase, we find that the calculated surface area matches the SEP-GluR1 fluorescence (Fig. 5C). To further verify this, we transfected neurons with YFP-CD8, a general marker for the cell surface, and found that its fluorescence was less than the volume increase, and matched the 2/3rds power rule (Fig. 5D). This indicates that simply overexpressing GluR1 may overwhelm its binding partners, and make it a general label for the cell surface.

This preparation also allows us to answer the question of how rapidly AMPAR enter the spine following stimulation. Increasing the temporal resolution to look at the increase during stimulation shows that both the mCh and SEP-GluR1 fluorescence increase at the same time. This make sense if one considers SEP-GluR1 a freely diffusible protein, and shows that freely diffusible AMPAR can enter spines shortly after stimulation.

2.3 Monitoring AMPAR anchoring using FRAP

AMPAR on the plasma membrane exist in two pools, those that are freely diffusible, and those that are anchored at the synapse. A majority of overexpressed form homomers, which may overwhelm GluR1 binding partners, and let the receptors freely diffuse. Despite this, some fraction of AMPAR are also anchored in the synapse,

and the number of anchored receptors may change following uncaging. In order to test whether more receptors are anchored following uncaging, we used a fluorescence recovery after photobleaching (FRAP) protocol. In this protocol, we bleach SEP-GluR1 in a target spine, and measure the speed of fluorescence recovery (i.e., the half-time, τ), and the extent of recovery (i.e., the mobile fraction; Fig. 6). We performed these experiments on naïve spines, as well as on spines in which we had induced plasticity. In unstimulated spines, the average τ was 0.99±0.28 min, and the mobile fraction was 0.81±0.07. Thirty minutes following uncaging, the average time constant was 1.3±0.35 min., with a mobile fraction of 0.74±0.04 (both changes not significantly different).

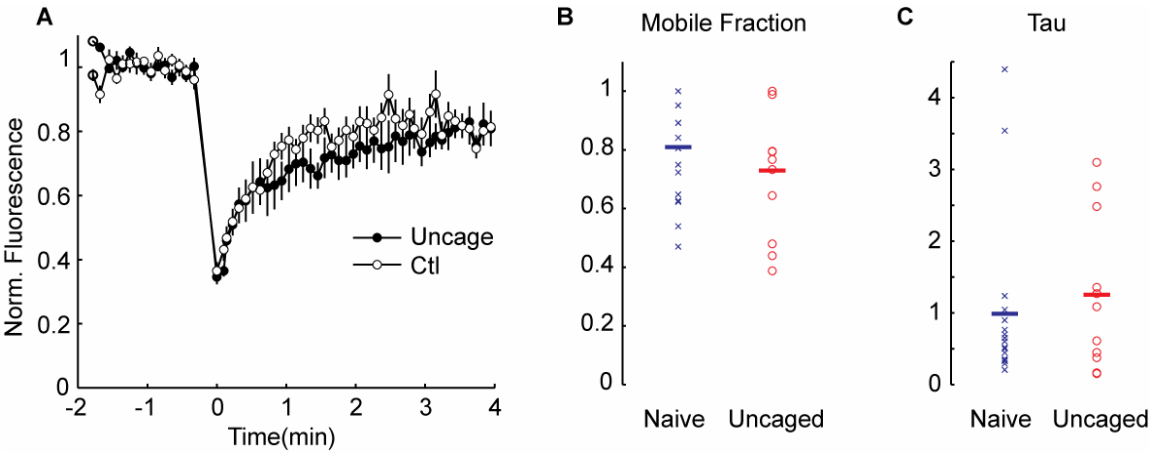

Figure 6: Uncaging decreases mobile fraction, and decreases speed of recovery, as measured by FRAP
A. Average timecourse of FRAP in single spines before and after uncaging. Time constant was 0.99±0.28 min. before uncaging and 1.3±0.35 min. after uncaging. Immobile fraction was 0.19±0.07 before uncaging and 0.26±0.04 after uncaging. *n* = 17 spines before uncaging, and 10 spines after uncaging. **B.** Scatterplot of individual mobile fractions. Average 0.81±0.04 on naïve spines, 0.73±0.07 after uncaging **C.** Scatterplot of individual time constants. Average 0.99±0.28 minutes on naïve spines, 1.25±0.32 minutes after uncaging.

2.4 Results from a wide area bleaching protocol to measure contributions of surface and exocytosis, as well as rapidity of anchoring

Because SEP-GluR1 fluorescence intensity follows the surface area increase during LTP (Fig. 5C), the increase in spine SEP-GluR1 fluorescence may be due to the passive diffusion of pre-existing surface AMPARs into spines from the dendritic shaft. Furthermore, since these receptors are already at the surface, imaging them yields no insight into the role of exocytosis. In order to determine the contribution of newly exocytosed receptors to the increase in spine GluR1 content, we used two-photon imaging to pre-bleach ~85% of surface SEP-GluR1 fluorescence within an ~8 μm radius of a select spine before inducing LTP, so that most fluorescence comes from newly exocytosed receptors (Fig. 7A). mCherry was bleached little by this protocol (<10%), and thus was used to monitor spine structural plasticity (Fig. 7A). Following bleaching, the SEP-GluR1 fluorescence recovery in the spine was slow and small (from 16±2 % to 26±3%; Fig. 7B), presumably due to activity-independent exocytosis or diffusion of non-bleached SEP-GluR1. Similarly, the dendritic area immediately below the spine, or neighboring spines during stimulation had similar recoveries (from 16±2 % to 26±3% for dendrite; from 16±2 % to 23±2% for adjacent spines; Fig. 7B).

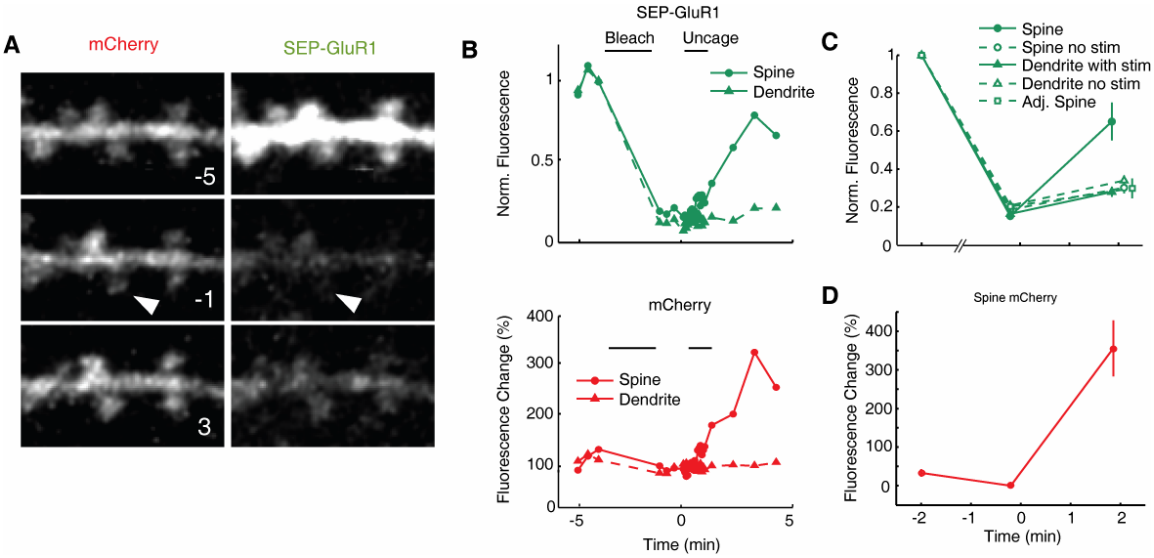

Figure 7: SEP-GluR1 is selectively accumulated in the spine following bleaching and uncaging.
A. Images of mCherry (left) and SEP-GluR1 (right) fluorescence before bleaching, after bleaching, and after uncaging (from top to bottom). **B.** Fluorescence timecourse of SEP-GluR1 (top) and mCherry (bottom) for spine and dendrite shown in **A**. **C.** Population data of SEP-GluR1 fluorescence for bleaching protocol. SEP normalized to pre-bleach fluorescence. **D.** mCh fluorescence following bleaching. Structural plasticity is normal. *n* = 18 spines, 16 neurons for stimulated spines without drugs; 18 spines, 14 cells for no stimulation controls.

Following bleaching, uncaging on a spine caused the volume to increase similarly to unbleached spines (360±60%, Fig 5B), showing that the bleaching protocol is not damaging the cell. At the same time, SEP fluorescence in the stimulated spine increased from 13±2% to 63±9% of the original SEP fluorescence (Fig. 7B). The increase in SEP-GluR1 fluorescence implies that there is exocytosis of AMPAR near enough to the stimulated spine that they can enter the spine rapidly. Furthermore, the selective increase in spine fluorescence versus dendritic fluorescence implies that AMPAR are trapped in the spine following stimulation, but may diffuse away in the dendrite. One might be concerned that the area of dendrite bleached is small enough

that AMPAR can diffuse from unbleached regions within the time frame of the experiment, and the increase in spine fluorescence is due simply to accumulation of unbleached AMPAR. We performed two control experiments to verify that it is indeed exocytosed AMPAR that are responsible for the spine fluorescence increase. First, we employed a lamp bleaching protocol that bleaches over a 20μm radius, making it impossible for unbleached AMPAR to diffuse to the spine during our recordings. Using this protocol, we found that spines selectively had fluorescence increase (Δ0.13+0.04), while the dendrite did not (Fig. 8). The decrease in fluorescence increase magnitude may reflect differences in bleaching protocol, and a reduction of diffusing receptors. Furthermore, we repeated the bleaching protocol in cells expressing TeTX, which blocks exocytosis, and found that these cells did not collect AMPAR in the stimulated spine (Δ0.03±0.03; Fig. 8).

Using the two-photon bleaching data, the contribution from stimulation-dependent exocytosis is the SEP fluorescence increase in the stimulated spine, ~50%, minus the background recovery, ~10%, or roughly ~40%. Dividing this value by the increase of SEP fluorescence without bleaching (40% vs 140%, Fig. 5C), suggests that about 30% of the total GluR1 increase during LTP induction is from newly exocytosed SEP-GluR1, and the rest is due to diffusion of receptors from the parent dendrite. The rapid accumulation of AMPAR in the stimulated spine also shows that AMPAR begin to be anchored there shortly after LTP has been initiated.

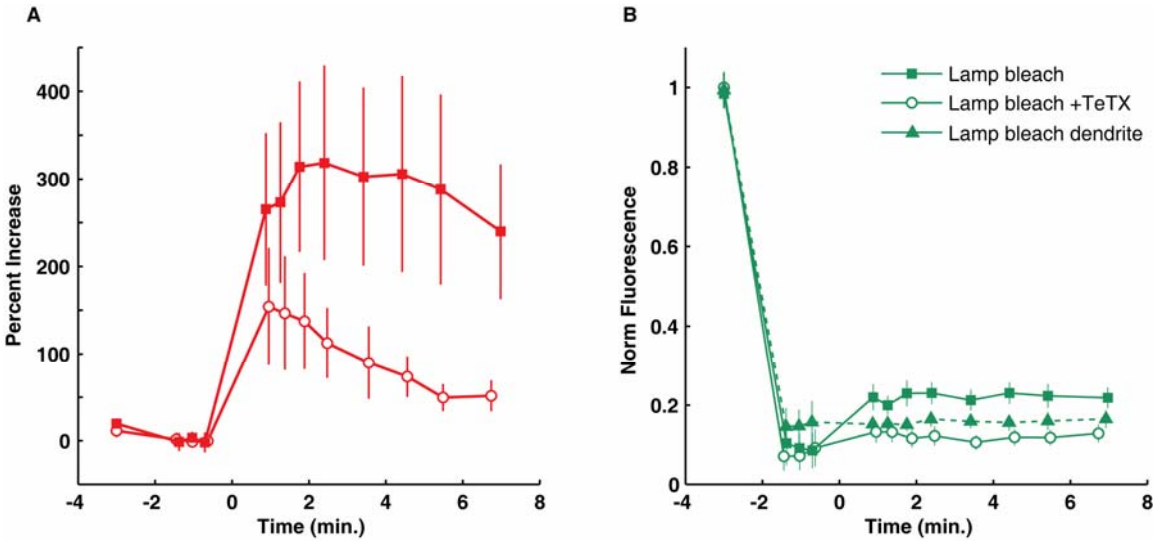

Figure 8: Lamp bleaching and TeTX
A. Timecourse of volume. Fluorescence was bleached in a 20µm area around a spine before performing a normal uncaging protocol on the spine. Under control conditions there was robust spine growth (filled squares). In neurons transfected with TeTX (open circles), there was a partial block of structural plasticity. **B.** Timecourse of SEP-GluR1 fluorescence. n = 11 spines, 6 neurons for control, 7 spines, 3 neurons for TeTX. The dendrite did not recover (filled triangles).

2.5 Direct observation of location and timing of AMPAR exocytosis

The above experiments shed some light on to the source of AMPAR during LTP, and how rapidly they are recruited, but they do not address the questions of when and where AMPAR are exocytosed during LTP. In order to determine the location and timing of individual AMPAR exocytosis events, we imaged while continuously photobleaching all surface receptors on a ~10 μm stretch of dendrite to prevent fluorescence recovery (bleaching τ = 9.1±0.7 s for dendrite 8.4±0.85 s for spine, Fig. 9). Under this condition, we observed fast fluorescence increases in spines and dendrites, presumably reporting single exocytosis events (Lin et al., 2009; Yudowski et al., 2007) (Fig. 9-10). Most exocytosis events had a $\Delta F/F$ of 50-100%, although a small subset were much larger (Fig. 10). When not stimulated, the fluorescence increase in spines quickly returns to baseline within a few seconds (Fig. 11). Because the decay is faster than bleaching and diffusion of AMPARs out of spine (Fig. 9), some component of the decay is presumably due to re-internalization of exocytosed AMPARs.

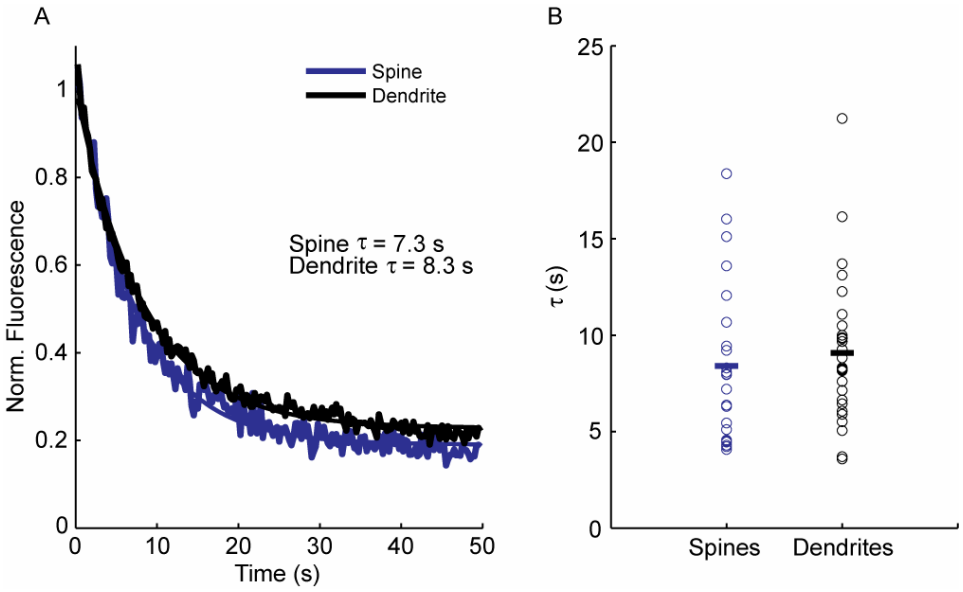

Figure 9: SEP-GluR1 bleaching during exocytosis movies
A. Average bleaching time-course for spines and dendrites (thick lines) during the initial bleaching to remove the pre-existing surface receptors before imaging individual exocytosis events (Fig. 3, 4). Thin lines are exponential fits. The measurement was done
B. Time constant of exponential fits to each bleaching time course. τ = 9.1±0.7 s for dendrite 8.4±0.85 s for spine. *n* = 28 for dendrites, 23 for spine.

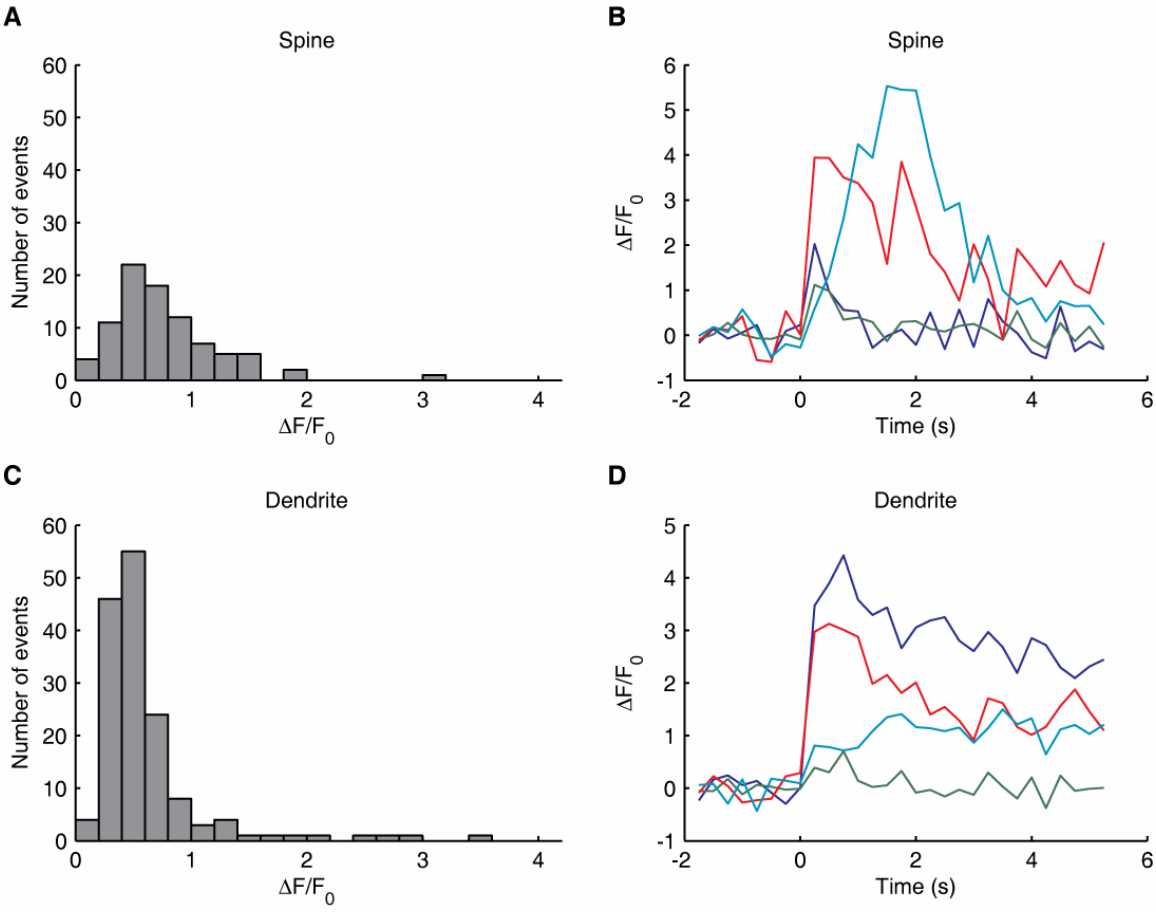

Figure 10: Distribution of exocytosis event size
A. Histrogram of spine exocytosis sizes, from all conditions. The average of the 5 frames following exocytosis is shown. Most events are quite small, but there are a few small events. **B.** Example of small, medium, and large spine exocytosis events. **C.** Histrogram of dendrite exocytosis sizes. **D.** Example of small, medium, and large dendrite exocytosis events. n = 160 events in spines, 293 events in dendrite.

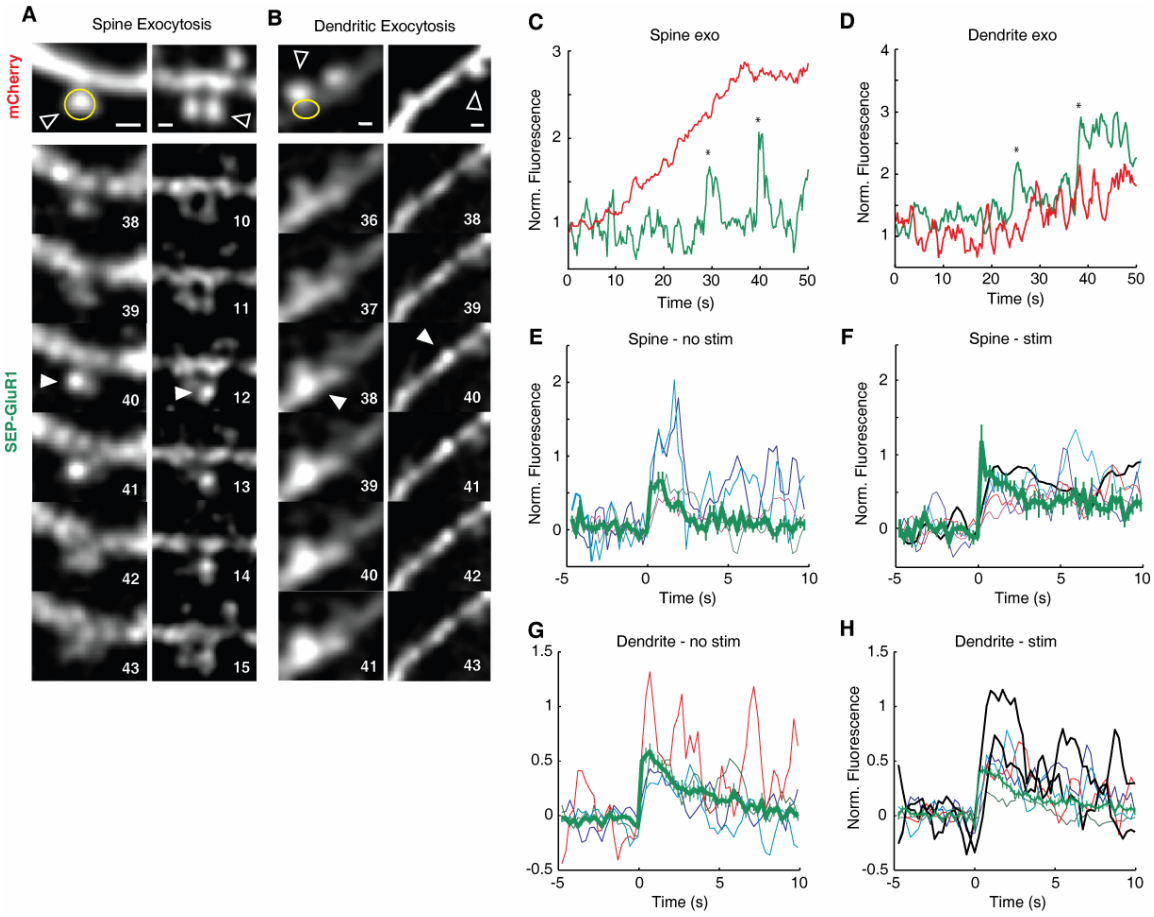

Figure 11: Examples and timecourse of exocytosis events in spine and dendrite
A. mCherry (top image) and SEP-GluR1 images (bottom time series) of spines undergoing stimulation. Filtered spatially (0.75 µm) and temporally (1.25 s). Exocytosis is measured as a sharp increase in spine fluorescence. Stimulated spine shown by open arrowhead. Exocytosis shown by closed arrowhead. Left example is of transient spine exocytosis, right of sustained spine exocytosis. Scale bar 1 µm. The numbers indicate the time after starting uncaging (s). **B.** mCherry and SEP-GluR1 fluorescence during dendritic exocytosis. Left example is in dendrite immediately beneath spine, which shows movement of fluorescence into the stimulated spine (40–41 s), and right example is 2 µm away. **C.** Fluorescence timecourse for region of interest (ROI) shown as yellow circle in **A** (filtered with 1.25 s window). **D.** Fluorescence timecourse for ROI shown in **B**. **E.** Average of all unstimulated spine exocytosis events (thick green line), and four example exocytosis events (thin lines). *n* = 25 events. Average was taken of unfiltered data, while individual traces have been filtered (1.25 s). **F.** Average of all stimulated exocytosis events (thick green line), trace examples in **A** (black lines), and four other example exocytosis timecourses. *n* = 46 events. **G.** Average fluorescence timecourse for unstimulated dendritic exocytosis (thick green), and four individual examples timecourses. **H**. Average timecourse of stimulated dendritic exocytosis events (thick green line), examples from **B** (black lines), and three other example timecourses. *n* = 134 events.

During stimulation, the fluorescence is sustained more than ~10 s in the stimulated spine (Fig. 11F), suggesting that during spine growth AMPARs exocytosed in the stimulated spine are trapped there. This sustained exocytosis is exhausted within 1 min of the cessation of stimulation. We further segregated stimulated exocytosis in spines into transient and sustained types, using a threshold of 30% increase at 4 s after exocytosis, and found that exocytosis events with sustained GluR1 fluorescence are associated with increases in spine volume (Fig. 12). In contrast to the spine exocytosis, the decay time of dendritic exocytosis was independent of stimulation (~10 s) (Fig. 11G-H). We occasionally observed that AMPARs exocytosed into dendrites move into the stimulated spine (Fig. 11B, left column).

The exocytosis rate before stimulation was 0.11±0.05 events/min in the spine (Fig. 13A) and 0.034±0.01 events/min/μm in the dendrite (Fig. 13B). The rate increased by ~5 fold within 15 s of the first stimulus, and remained elevated for the duration of the stimulus protocol to ~0.61±0.1 events/min in the spine (Fig. 13A), and ~0.18±0.04 events/min/μm within 2.5 μm of the spine, in the dendrite (Fig. 13B). After the stimulus ended, the exocytosis rate in both the spine and dendrite quickly returned to baseline within ~1 min (Fig. 13). The increase in exocytosis rate in dendrites during stimulation was highest in the area beneath the stimulated spine, and decayed with distance from the stimulated spine with a length constant of ~3 μm (Fig. 13C). Co-transfection of SEP-GluR1 with tetanus toxin light chain (TeTX), which cleaves vesicle-associated membrane protein (VAMP) specifically (Harms et al., 2005) abolished the activity

dependent increase of AMPAR exocytosis, suggesting that these observed events are VAMP-dependent exocytosis (Fig. 13A-B).

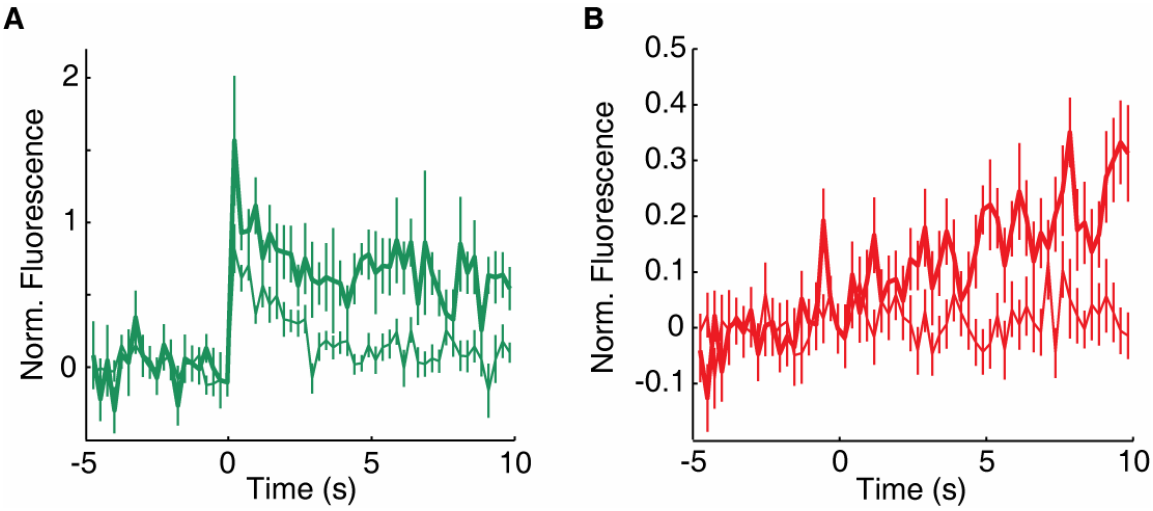

Figure 12: Sustained exocytosis events are correlated with increases in spine size **A.** Fluorescence timecourse of transient (thin line) and sustained (thick line) exocytosis events. **B.** Structural plasticity during sustained and transient events. Sustained exocytosis events are correlated with increases in spine size.

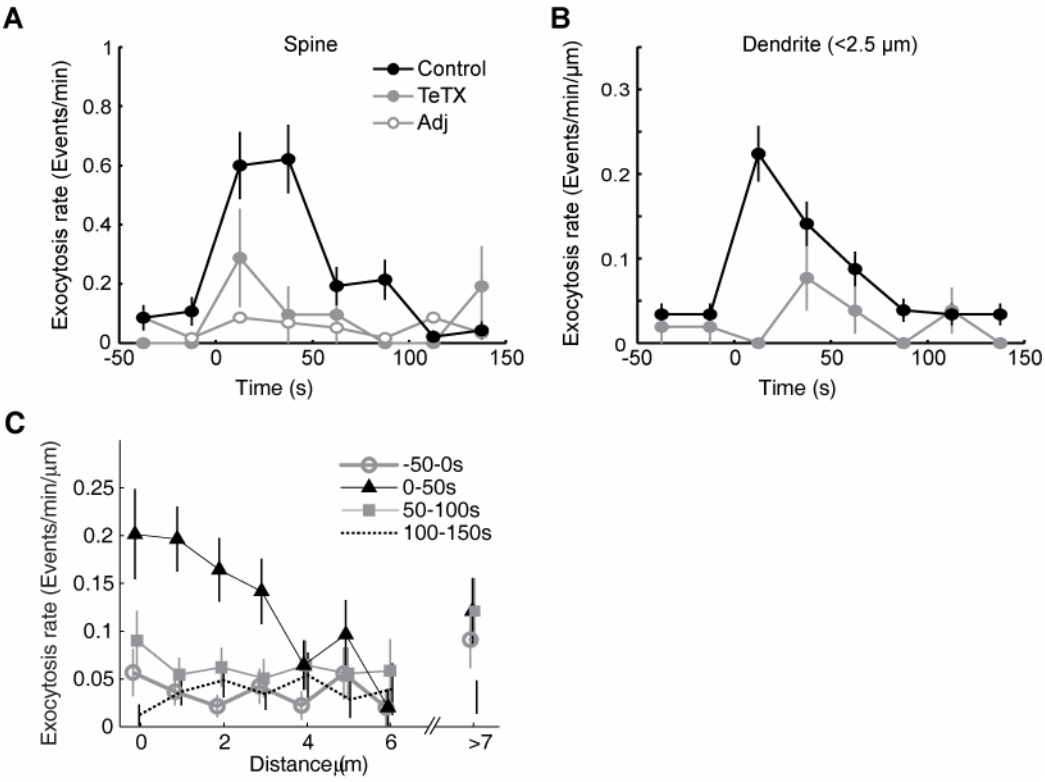

Figure 13: Exocytosis rate increases in spine, and in dendrite within 2.5 µm of the spine Timecourse of exocytosis rate in spines (**A**), dendrites (0–2.5 µm of the stimulated spine) (**B**) and adjacent spines (**A**, open circles), and stimulated spines/dendrites under TeTX (gray circles). **C.** Distance from stimulated spine exocytosis occurred before (gray circles), during (black triangles), and after (gray squares, black diamonds) stimulation. *n* = 112 spines/dendrites from 31 cells for control; 139 spines, 12 cells for adjacent spines; *n* = 25 spines/dendrites, 6 cells for TeTX.

2.6 Discussion

AMPAR reach the synapse by both exocytosis and diffusion

After being trafficked out of the ER and Golgi, AMPAR reside both at the cell surface and in endosomes, with 25-66% of the total AMPAR at the surface (Ehlers, 2000; Passafaro et al., 2001; Shi et al., 1999). Following plasticity, synapses increase their AMPAR content, which prompts the question: do these receptors come from the surface pool or endosomes? The idea that the surface pool of receptors is sufficient is appealing, since dendritic AMPAR are freely diffusible (Borgdorff and Choquet, 2002) While the spine neck is a diffusion barrier (Ashby et al., 2006), it cannot prevent AMPAR from entering the spine. However, the distribution of surface receptors is highly biased towards synaptic localization: immunostaining studies for AMPAR show punctate spine localization ranging from mild for GluR1 to strong for GluR2 (Kopec et al., 2006; Passafaro et al., 2001; Shi et al., 1999). The lower concentration of AMPAR in the dendrite reduces the number of freely diffusible AMPAR that can explore a spine, especially on the time scale of seconds to minutes that matter for plasticity.

In contrast to diffusible surface AMPAR which are uniformly distributed, AMPAR-containing endosomes can be found directly in the spine, and in the dendrite beneath the spine (Ashby et al., 2004; Park et al., 2004). Upon stimulation, these endosomes move into the spines and fuse (Park et al., 2006; Wang et al., 2008). This local exocytosis, while perhaps smaller in size than the total surface pool, has more direct access to the spine.

To determine the source of AMPAR, we induced plasticity in individual spines where we had bleached away all surface fluorescence. We found that the AMPAR signal in the spine still increased, presumably due to the incorporation of newly exocytosed receptors (section 2.4). Comparing the increase following bleaching (20-40% increase) (Fig. 7-8) to the unbleached condition increase (140%, Fig. 5), we estimate that 15-30% of the AMPAR that reach the spine soon after uncaging are from internal stores. This estimate may be low, as overexpressing GluR1 increases the dendritic surface AMPAR complement, which would bias the source of AMPAR towards diffusion. Whatever the exact ratio of surface to exocytosed receptors is, we conclude that a combination of preexisting surface receptors, and newly exocytosed receptors are recruited to stimulated spines.

It is important to note that these experiments do not mean that AMPAR are exocytosed directly into the synapse, or even the spine. Given the timecourse of our imaging (ranging from tens of seconds to minutes), there is time for AMPAR exocytosed in the dendrite to diffuse into the spine. In fact, recent experiments using glutamate reuptake inhibitors have shown that following LTP, the perisynaptic currents increase prior to the synaptic currents (Yang et al., 2008a). Even exocytosed receptors must diffuse into the synapse.

A recent paper from the Malinow lab using similar methods claims that almost all receptors during LTP come from the existing surface pool (Makino and Malinow, 2009). In the most comparable experiment, they found that following FRAP, the immobile fraction increased following uncaging; this is in contrast to our findings that the tau may increase slightly. Unfortunately, there is the confounding factor that spine size increases

following FRAP, which would subsequently change the taus and immobile fraction, which they did not measure. In another set of experiments, they performed wide field bleaching, as we did, and measured fluorescence recovery. They then induced chemical LTP, and found no difference in recovery compared to unstimulated neurons. However, given their chemical LTP protocol, the spines they measured would have a mixed population of stimulated and unstimulated receptors, diluting their signal, and preventing a direct comparison.

Besides searching for the source of AMPAR during plasticity, we also were able to image the relative timing of the induction of structural plasticity and AMPAR trafficking. Previous studies using chemical LTP had found that structural plasticity precedes AMPAR recruitment, but in these imaging was performed 1 and 3 minutes following stimulation (Kopec et al., 2006). Using uncaging, thereby restricting our analysis to spines we know are being stimulated, and imaging more rapidly (every 4s), we found that during the induction of plasticity, both structural plasticity and SEP-GluR1 fluorescence increased at the same time. Given that overexpressed GluR1 forms homomers, and may saturate binding partners, we found that SEP-GluR1 acts as a general marker for surface area, thus making the timecourse of SEP-GluR1 fluorescence the same as mCherry. For anyone interested in using this construct in the future, we would suggest always manipulating the receptor somehow (e.g. via bleaching), or coexpressing with GluR2 to prevent homomers.

During stimulation, the AMPAR exocytosis rate increases only briefly, both in the spine and the nearby dendrite

While exocytosis is known to be essential for LTP, the spatial and temporal kinetics of this process during plasticity remains unclear. Imaging of AMPAR exocytosis has shown that under basal conditions, exocytosis occurs exclusively in the dendrite (Leonoudakis et al., 2008; Lin et al., 2009; Yudowski et al., 2007). Our results confirm that there is more total exocytosis in the dendrite than the spine. The basal exocytosis rate in the spine was 0.1 events/min versus ~0.035 events/min/μm in the denrite. Given dendrites' much higher surface area, more exocytosis occurs in the dendrite. (Fig. 13).

Why has no one else been able to image spine exocytosis? We observed two types of exocytosis events, small and large (Fig. 10). Other experimenters bleached less than we have (Yudowski et. al.: 70-80%; Makino et. al. unspecified) or not at all (Lin et al., 2009). Furthermore, two of these groups (Lin et al., 2009; Yudowski et al., 2007) have reported two different types of exocytosis events: small, transient events with time constants of fluorescence decay < 2s, and longer lasting, sustained events with fluorescence decays of >5s. These groups primarily reported and quantified the larger, events, while we are reporting both. Our higher bleach levels may allow us to visualize smaller fluorescence changes, perhaps from smaller endosomes, and may explain why we see spine exocytosis. (The Makino results are especially suspect for two reasons. While Yudowski et. al., Lin et. al., and ourselves all imaged at frame rates >1Hz, Makino imaged at 0.5Hz. While most AMPAR-containing endosomes are dim, some endosomes are quite bright, either due to high AMPAR content or high pH, and these endosomes are easily visible against a bleached background. These endosomes also move relatively quickly, at ~1μm/s. When imaging at frame rates <1Hz, bright spots of

fluorescence that appear between frames may in fact be moving endosomes. Second, some of the spots reported by Makino have lifetimes of >1 min., much longer than those reported by anyone else. These two technical issues, and the delayed nature of their "exocytosis" make me suspect that they are not imaging AMPAR exocytosis, but simply bright endosomes moving around.)

The rapidity of fluorescence decay requires some explanation. We observed decay in less than 3s, which was faster than the bleaching time constant (τ = 8s) or diffusion as measured by FRAP (τ = 60s). When the signals following exocytosis decay, they are not accompanied by increases in fluorescence at adjacent membrane. A third explanation is that receptors are rapidly re-internalized. This would be in accord with the mounting evidence for "kiss-and-run" exocytosis at axon terminals (He and Wu, 2007). The best way to verify this would be to use antagonists to re-acidification of endosomes, and measure the effect on the character of exocytosis.

Given the increase in exocytosis rate both in the spine and in the dendrite, does the location of exocytosis matter? One might naively assume that a large portion of the AMPAR exocytosed in the dendrite near a spine eventually explore the spine, and can be anchored in the synapse. However, simulations have shown that the chances of an AMPAR entering a given spine decrease exponentially with distance; even being on the opposite side of the dendritic shaft from the spine may be distant enough to make encountering the spine unlikely (Bressloff et al., 2008; Holcman and Triller, 2006). Thus, if AMPAR are to enter the spine within the tens of seconds that are necessary to get LTP, they must be exocytosed as locally as possible.

In the temporal domain, upon stimulation, we observed the exocytosis rate increase both in the spine and the dendrite (Fig. 13). This exocytosis rate was not sustained, returning to baseline immediately after uncaging finished. The transient nature of the increase in exocytosis rate may have a few causes. First, it is possible that exocytosis occurs while one is stimulating, and the duration we see is due to the duration of our stimulating protocol. In order to test this hypothesis, one could vary the duration of the uncaging protocol, and see how this influences the duration of increased exocytosis rate. A second explanation is that only one bout of delivered molecules is necessary to induce plasticity. Other exocytosis-independent processes like protein synthesis may be important for the maintenance of plasticity. One possible explanation for the short burst of exocytosis is that there may be a "readily releasable" pool of AMPAR waiting for plasticity. Once plasticity is induced, this pool may be depleted, and there may be a refractory period for further plasticity. This idea will be further explored by experiments in Chapter IV.

Besides the increase in exocytosis rate, we also noticed a change in the character of spine exocytosis. The timecourse of fluorescence loss for unstimulated spine exocytosis was quite short (<5s), but was sustained more than 10s during uncaging. This sustained increase was despite the effects of bleaching, although there could be secondary, unmeasured exocytosis. Furthermore, we found that these sustained exocytosis events were associated with increases in spine volume within the next 10s. The difference in character could reflect a transition from kiss-and-run exocytosis to full fusion, as well as anchoring of AMPAR in the synapse.

The Ehlers lab has suggested that when endosomes fuse with the plasma membrane, they provide not only signaling molecules, but membrane as well, which could enhance the process of spine expansion (Park et al., 2006). The increase in spine volume immediately following these large, sustained exocytosis events supports this hypothesis. In the volume signal, we occasionally measured step-wise increases in the volume, but these step-wise increases were layered on top of the already increasing mCherry fluorescence, making it difficult to verify that they were in fact step-wise increases. Furthermore, they were rarely correlated with measured exocytosis. A more direct way to test this hypothesis would be to measure a surface area marker simultaneously with exocytosis, rather than the volume. It is unclear whether the increase in membrane from endosomes is a functional effect, or simply a byproduct of delivering molecules. Ultimately, higher resolution techniques will be needed to answer whether this membrane delivery occurs, and what its significance is.

Chapter III: The role of Ras-ERK signaling in AMPAR trafficking

Here we will address the question, what are the functional outputs of specific signaling pathways related to synaptic plasticity? A wide variety of signaling molecules have been identified in synaptic plasticity, including calmodulin, CaM kinases, Ras, PI3K, ERK, etc. We will use pharmacological and genetic tools to downregulate two of these pathways, CaMKII and ERK, and see how that effects structural plasticity and AMPAR exocytosis.

3.1 Materials and Methods

For pharmacology and genetic perturbations, all experiments were performed in pair-wise fashion. For long-term plasticity experiments (Fig. 14), we uncaged on two spines from an identified neuron, then incubated with drugs for ~30 min., then uncaged 2-3 more times on the same neuron. For exocytosis experiments, we pre-incubated all slices with drugs for 1h before imaging, while performing control experiments on other slices prepared on the same day. A different pairing was used here, as exocytosis movies must be taken from spines in a planar dendrite in order to correctly visualize the distance of exocytosis, and planar dendrites are uncommon.

For experiments using genetic manipulations (TeTX and dnRas), we waited 3-4 days post-transfection to ensure that the proteins were adequately expressed. For pairing, we recorded exocytosis movies from slices prepared on the same day as controls.

3.2 Signaling pathways involved in long-term structural plasticity and AMPAR anchoring

The CaMKII and Ras-extracellular signal-regulated kinase (ERK) pathways have been reported to be required for the induction of LTP and associated spine enlargements (Harvey et al., 2008; Hayashi et al., 2000; Lee et al., 2009; Matsuzaki et al., 2004; Zhu et al., 2002). In order to determine whether these signaling pathways play a selective role in AMPAR recruitment, we performed uncaging experiments in the presence of blockers of ERK phosphorylation (U0126) and CaMKII activation (KN62) (Fig. 14A). We found that both of these blockers partially but significantly ($p < 0.05$; paired t-test) blocked structural plasticity as well as long term AMPAR increases (Harvey et al., 2008; Lee et al., 2009; Matsuzaki et al., 2004).

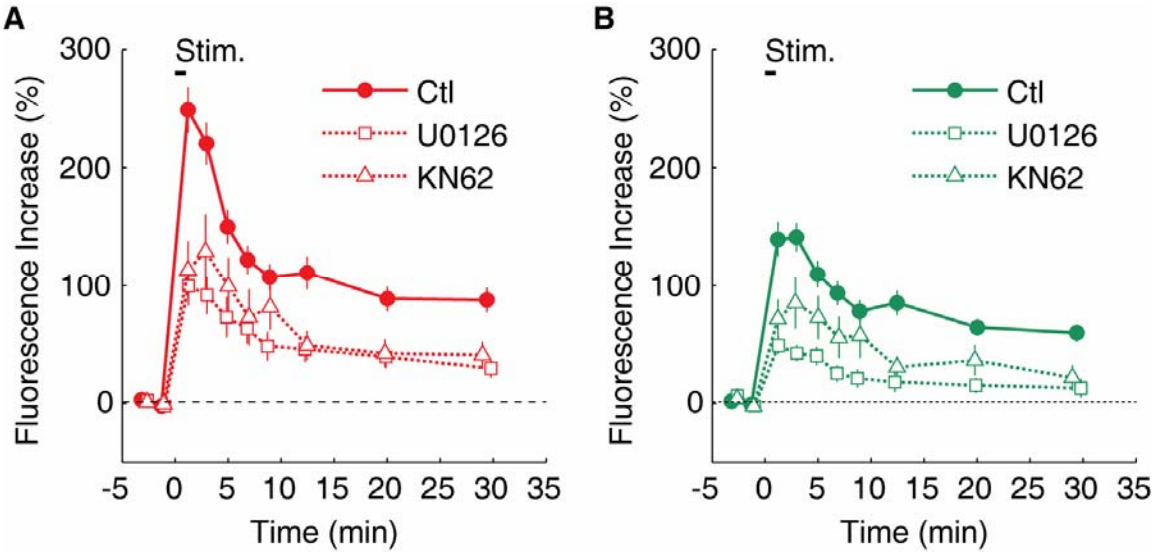

Figure 14: CaMKII and ERK antagonists partially block structural plasticity and AMPAR recruitment
A. Timecourse of mCherry fluorescence under control, MEK inhibitor U0126 (open circles, *n* = 18 spines, 7 cells), and CaM kinase inhibitor KN62 (open triangles, *n* = 17 spines, 7 cells) conditions. **B.** Timecourse of SEP-GluR1 fluorescence under drug conditions.

Given the problems interpreting long-term imaging data without bleaching, we repeated the experiments using our wide field bleaching protocol (Fig. 7). Briefly, we bleached all fluorescence within a 10μm radius of the spine, and then uncaged on the spine. Doing so in the presence of KN62 or U0126 both partially blocked the mCherry fluorescence increase, as well as the SEP-GluR1 fluorescence increase (Fig. 15), suggesting that both CaMKII and ERK signaling are required for insertion of exocytosed AMPARs into the stimulated spine ($p < 0.05$; paired t-test).

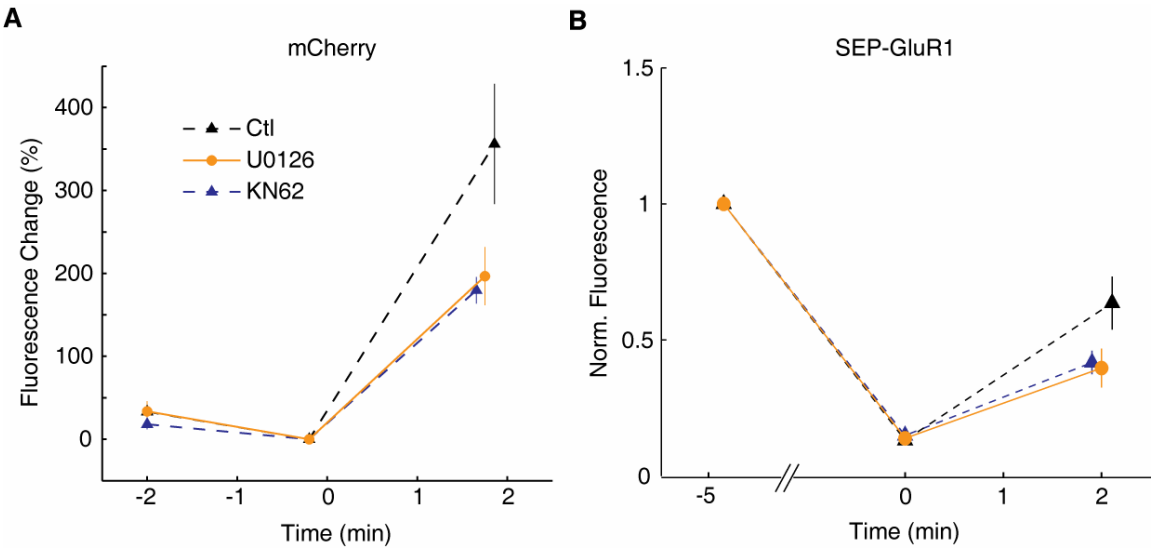

Figure 15: SEP-GluR1 recruitment partially inhibited during bleaching protocol
A. Structural plasticity and the degree of inhibition by KN62 or U0126 under bleaching condition were similar to those under normal condition. **B.** SEP fluorescence under drug conditions. n=10 spines, 6 cells for U0126; and 15 spines, 5 cells for KN62.

3.3 Activity induced AMPAR exocytosis is signaled by the Ras-ERK pathway

In order to determine whether the partial inhibition during the bleaching protocol was due to impaired exocytosis, we repeated our exocytosis experiments (see Chapter II for details) in the presence of antagonists for both CaMKII and Ras-ERK. Neither KN62 nor U0126 effected the basal exocytosis rate, which remained low in their presence (Fig. 16A-B). During uncaging in the presence of KN62, neither the spine nor dendritic exocytosis rates were changed. Furthermore, the spatial localization of exocytosis in the dendrite remained the same, within approximately 2-3μm of the stimulated spine (Fig. 16D). We also tested whether the drugs might modify the character of exocytosis events, and found that the decay time, and sustained portion were the same under KN62 (Fig. 16C).

In contrast to KN62, bath application of U0126 partially inhibited both spine and dendritic activity dependent exocytosis (Fig. 16A,B,D). When we analyzed the spatial profile of this inhibition, we found that it primarily inhibited exocytosis within 2-3μm of the stimulated spine, the area we had identified contained activity dependent exocytosis. To confirm that the Ras pathway is involved in exocytosis, we also antagonized it genetically, using dominant negative Ras (dnRas; Fig. 16A,B,D). Three to four days after transfection, neurons expressing dnRas had significantly reduced spine and dendritic exocytosis. It is possible that dnRas's more strong phenotype is due to more complete blockade of Ras signaling, or due to crosstalk with other Ras-family GTPases.

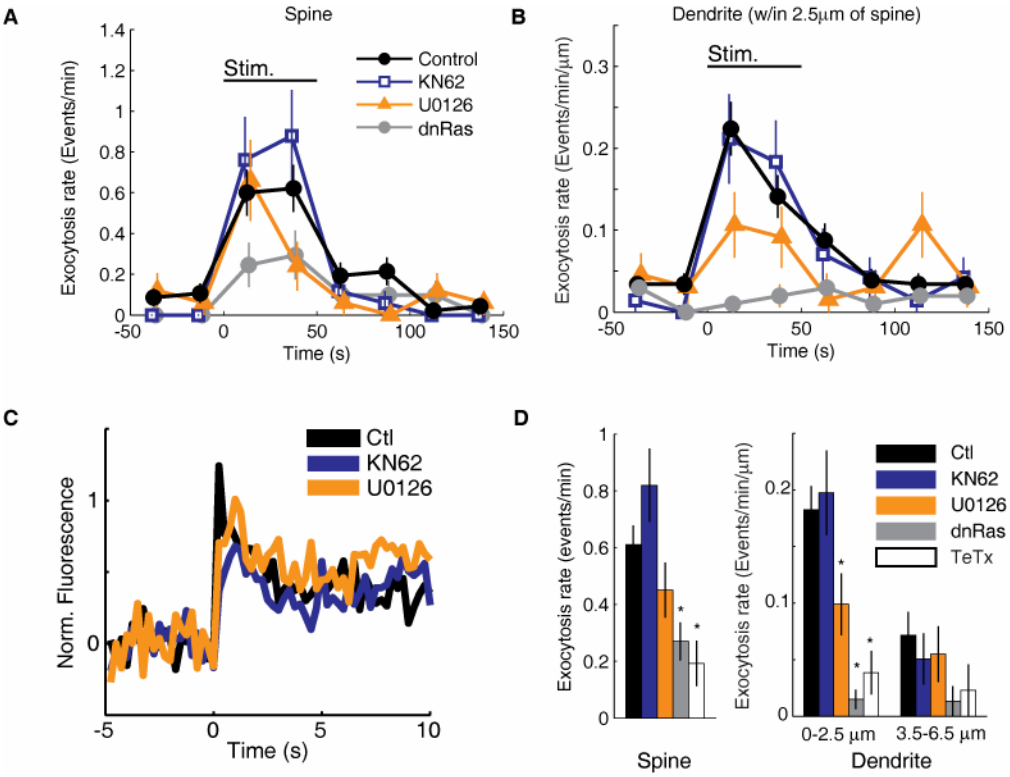

Figure 16: Ras is necessary for activity-dependent exocytosis
A. Timecourse of exocytosis in spine in the presence of antagonists for CaMKII (KN62), Ras-ERK (U0126), and dnRas. **B.** Timecourse of dendritic exocytosis within 2.5 μm of stimulated spine. **C.** Average of stimulated spine exocytosis fluorescence timecourse for three drug conditions. *n* = 46 events for control, 13 for KN62 and, 15 for U0126. **D.** (left) Exocytosis rate in spine during stimulation (0 – 50 s). Same color scheme as **A**. Stars (*) denote significant differences from control rate (ANOVA $p<0.05$). (right) Exocytosis rate in the dendrite, near (0–2.5 μm) and away from (3.5–6.5μm) the stimulated spine during stimulation (0 – 50 s). *n* = 112 spines/dendrites from 31 cells for control; 39 spines, 7 cells for U0126; 41 spines, 9 cells for KN62; 25 spines, 6 cells for tetanus toxin (TeTX); 49 spines, 12 cells for dominant negative Ras (dnRas).

3.4 Discussion

One of the great remaining challenges in studying the cellular basis of memory is tying known signaling pathways to functional outputs. A large number of signaling pathways have been identified as important for memory and plasticity, as well as their downstream effectors, but integrating this knowledge has proved troublesome. For example, it is known that PKA is necessary for LTP (Blitzer et al., 1995); that it phosphorylates AMPAR at S845 (Banke et al., 2000), which increases the peak open probability; and is essential for the synaptic retention of AMPAR (Esteban et al., 2003; Lee et al., 2003). However, the mechanisms by which PKA changes AMPAR open probability, or how PKA influences AMPAR retention remain unclear.

The advent of new imaging technologies has created opportunities to both monitor signaling pathways, and visualize the results of plasticity. Here, we have developed a technique to image AMPAR exocytosis, an epiphenomena of LTP, and manipulated signaling pathways to see which was involved in AMPAR exocytosis. We found that pharmacological blockade of CaMKII or ERK both caused a partial block of structural plasticity, as well as the long term retainment of AMPAR (Fig. 14). Using a bleaching protocol, we similarly found that both CaMKII and ERK antagonists blocked the initial anchoring of AMPAR in the spine (Fig. 15). Finally, using a combination of pharmacological and genetic techniques we found that Ras, but not CaMKII, is necessary for activity-dependent exocytosis following synaptic plasticity (Fig. 16).

Before interpreting these results, it would be helpful to review what is known about CaMKII and Ras-ERK signaling. Calcium-calmodulin kinase II (CaMKII), as its

name implies, is activated by calmodulin following NMDAR receptor activation, early in the signaling pathway. Peptide inhibitors of CaMKII block LTP (Otmakhov et al., 1997), while overexpression of truncated (constitutively active) CaMKII causes an increase in synaptic currents (Hayashi et al., 2000). CaMKII can directly phosphorylate GluR1 at S831 and does so during LTP (Barria et al., 1997b). A recent study using a CaMKII FRET sensor showed that CaMKII is activated only briefly in the spine, with highly restricted localization (Lee et al., 2009).

Like CaMKII, Ras activation is activated by Ca^{2+} (Kennedy et al., 2005; Thomas and Huganir, 2004). As a small GTPase, Ras is activated by guanine nucleotide exchange factors (GEFs), which promote the unbinding of GDP; and inactivated by GTPase activating proteins (GAPs), which increase Ras's GTPase activity. Two Ras GEFs, CalDAG-GEF2 and RasGRF1, are present in the synapse and activated by Ca^{2+} and calmodulin respectively (Sheng and Kim, 2002). Also present in the synapse is SynGAP, which inactivates Ras. In competition with Ras is the GTPase Rap, and it is thought the ratio of Ras to Rap activation can modulate LTP versus LTD (Zhu et al., 2002).

Active Ras phosphorylates Raf-1 and B-Raf, which both can activate MEK (Stork, 2003). Ras also is involved in a positive feedback loop with PI3K (Qin et al., 2005). Active MEK in turn phosphorylates MAPK/ERK. Genetic and pharmacological interference with Ras signaling has been shown to inhibit AMPAR insertion during LTP, while activation of this pathway also can induce insertion in an ERK dependent manner (Zhu et al., 2002). Downstream of Ras, inhibition of MAPKs impairs LTP (English and Sweatt, 1997).

There are a number of functions one can hypothesize for signaling molecules during LTP. First, these signaling molecules could be acting presynaptically, and modify vesicle release from axon terminals (Ninan and Arancio, 2004; Stanton and Gage, 1996). On the postsynaptic side, both CaMKII and Ras are likely second messengers whose effectors perform actions, so we must enumerate these potential actions. They could be involved in actin dynamics, which are the likely driver of increases in spine size (Honkura et al., 2008); the moving of AMPAR-containing endosomes towards or into the spine, as is caused by myosins (Correia et al., 2008; Wang et al., 2008); priming endosomes for fusion; fusion of AMPAR containing endosomes (Park et al., 2004; Park et al., 2006); modification of diffusion of AMPAR (by modifying binding partners) (Bats et al., 2007); or more specifically regulating the anchoring of AMPAR, either by modifying the AMPAR themselves or their binding partners.

We found inhibiting CaMKII caused a partial block of structural plasticity (Fig. 14) and the early recruitment of AMPAR following uncaging (Fig. 15), but did not find a phenotype wherein CaMKII blocked exocytosis. If we were using traditional chemical LTP or tetanus stimuli, one might hypothesize these effects were due to modifying presynaptic release. Since we are directly stimulating the post-synapse via uncaging, bypassing the terminal, the effect of KN62 is likely post-synaptic (although we cannot with complete confidence rule out glutamate activating the presynapse, or retrograde signaling). Thus, we hypothesize that CaMKII is not involved in any AMPAR exocytosis process, but rather in the anchoring of AMPAR in the synapse.

There are a few lines of evidence for this. CaMKII can bind directly to NR2B, letting it sense synaptic Ca^{2+}, and allowing it easy access to other synaptic proteins

(Barria and Malinow, 2005). Second, during plasticity, CaMKII is activated only in the stimulated spine (Lee et al., 2009), in contrast to diffuse exocytosis. Third, CaMKII directly phosphorylates GluR1 at S831, which has been shown to drive AMPAR into synapses. My hypothesis is that CaMKII sits near the synapse, and when activated, phosphorylates all nearby AMPAR, driving them into the synapse. Under normal conditions, this causes a large increase in phosphorylated AMPAR, and some portion of them are retained in the spine. When we uncaged on spines in the presence of KN62, exocytosis still increased the number AMPAR around the spine, but as these could not be anchored, most diffused away within five minutes. We interpret our bleaching results similarly. During our exocytosis imaging, we did not see a change in the character of activity dependent exocytosis, but this could be due to differences in time scale (seconds for exocytosis imaging, versus minutes for anchoring). As a final note, KN62 is a “dirty” drug, which blocks multiple CaM-kinases, and the effects we see may be due to other pathways as well.

When we inhibited the Ras-ERK pathway we saw a partial block of structural plasticity, long-term AMPAR retainment, and short-term AMPAR recruitment as measured by a bleaching protocol. We also found that both pharmacological and genetic blockade of Ras-ERK signaling blocked activity dependent exocytosis in the spine and dendrite. Thus we would conclude that the Ras-ERK pathway signals AMPAR exocytosis. The inhibition of exocytosis, and the resultant decrease in surface AMPAR, would explain the partial block of structural plasticity.

Ras could regulate exocytosis in a few ways. It could bring AMPAR-containing endosomes closer to the spine, priming endosomes for exocytosis, or fusion of

endosomes with the plasma membrane. We occasionally observed high pH endosomes move along the dendrite, but did not quantify the direction or number, and how it may have changed during plasticity. Given that other GTPases, like the Rab family, are involved in trafficking endosomes (Park et al., 2004), we would hypothesize that Ras is involved in the fusion process itself.

The two methods we used to block Ras-ERK trafficking each have their unique downsides. The Ras-Raf-MEK-ERK signaling pathway has four nodes, and each of these are points of convergent and divergent signaling. The antagonist U0126 blocks MEK-ERK signaling, which does not necessarily mean that the upstream signaling is via Ras. The use of dominant negative Ras, in turn, has the usual problems of genetic manipulations. Due to the heavy crosstalk in the Ras-family of small GTPases, it is possible that other GTPases are effected. Second, the chronic expression of dnRas may also allow for compensatory changes in signaling. In an ideal world, it would be possible to genetically manipulate all of the nodes in this pathway in real time, avoiding the pitfalls of each method.

The length constant of dendritic exocytosis was ~3 μm, which is similar to that of Ras activity during LTP induction in single spines, as measured by FLIM imaging (Yasuda et al., 2006). Although it has been suggested that Ras-ERK signaling invades adjacent spines, we did not observe an increase in the exocytosis rate in adjacent spines. Synaptic crosstalk experiments indicate that the initiation of plasticity at a spine can lower the threshold for plasticity in nearby spines in an ERK-dependent manner (Harvey et al., 2008). Our exocytosis results provide one possible mechanism for this crosstalk: AMPARs are exocytosed in a dendritic area around a stimulated spine, and

are available to adjacent spines. Thus, the spreading of Ras-ERK activity is likely important for signaling to recruit AMPARs to the stimulated spine during LTP, as well as for signaling on the micrometer length scale, such as the facilitation of LTP.

Chapter IV: Potential for Synapses to repeatedly potentiate

4.1 Introduction

Since the first studies of LTP, the standard experimental protocol has been to record the local field potential in the area of interest, and then induce plasticity using electrical stimulation of a large number of axons. While these protocols have yielded insight into the characteristics of plasticity on the cellular level – e.g. its associativity and input specificity – they fundamentally cannot describe plasticity on the level of single synapses. There remain a number of unanswered, critical questions: what stimuli (number and type of stimuli) can induce plasticity? What is the calcium threshold? Does plasticity occur gradually or in a step-wise fashion? If plasticity is graded, can it be saturated? Can a synapse be potentiated twice, and if so, how long must one wait before stimulating again?

One lab tried to address these questions electrophysiologically using minimal stimulation techniques to potentiate single synapses. In the first set of experiments, they found that a weak pairing protocol could initiate step-wise plasticity, which could not be further increased using a stronger protocol (Petersen et al., 1998), showing that plasticity is digital and saturable (these experiments were later duplicated (O'Connor et al., 2005)). The authors noted however, that they could not report whether a “given” synapse has these properties. Another lab used focal photolysis of caged glutamate, and found that a single, paired 1ms pulse could induce plasticity, and did so in a step-wise fashion at variable latency (Bagal et al., 2005).

Two-photon uncaging has enabled scientists to answer many of these questions. One can stimulate known synapses, and have far greater control over stimulus parameters like the number and timing of stimulation. The ability to induce plasticity without patching also offers the opportunity to observe plasticity over longer timecourses. We have chosen to answer two simple questions in an exploratory fashion: what happens when you stimulate the same synapse twice? And how does inducing full plasticity at a given synapse influence plasticity at neighboring synapses? These experiments will allow us to answer theoretical questions such as whether plasticity is saturable, and whether synapses can the capacity to be potentiated multiple times, and thus store more information.

All materials and methods are the same as previous chapters.

4.2 Structural plasticity is saturable at single synapses

In our first protocol, we stimulated the same spine twice (30 stimuli at 0.5 Hz) at an interval of fifteen minutes. Ideally, our first stimulation protocol would fully saturate LTP (in test experiments, only fifteen stimuli are sufficient to induce some form of plasticity, although one cannot be absolutely certain this is full plasticity). The second stimulation would then test whether further plasticity was possible in the synapse.

Using our protocol, the first stimuli initiated a transient volume increase of 310±38% and a sustained change of 92±12% at fifteen minutes (Fig. 17A; we are comparing plasticity at fifteen minutes, before the expression of late-phase plasticity, as it is the last available timepoint). The second stimuli caused a transient volume increase

of 360±65% (not significant, $p>0.05$), and a change of 135±22% at fifteen minutes (normalized to the volume before the first stimuli), which was statistically significant ($p<0.05$). For SEP-GluR1 fluorescence, the initial plasticity induced a peak change of 150±14%, and a fifteen minute increase of 56±8%; the second stimulation induced a peak fluorescence increase of 140±25%, and a fifteen minute increase of 72±9, neither of which were significant. In a subset of these experiments, we had paired spines which we stimulated only once, allowing us to compare later phases of plasticity. Comparing the plasticity between singly and doubly stimulated spines showed no difference (Fig. 17B).

To test whether plasticity would recover on a longer time scale, we repeated the protocol with a sixty minute interval. Here, the first peak structural plasticity was 460±130%, with a thirty minute increase of 195±24% (Fig. 17C; we used a thirty minute comparison here because we measured fluorescence for thirty minutes after the second stimuli); the second transient structural plasticity was 420±80%, with a thirty minute increase of 190%±27%, neither of which were statistically different. For the SEP-GluR1 fluorescence, the first peak was 130±40%, with a thirty minute increase of 50±5%; the second peak was 115±25%, with a thirty minute change of 52±18%.

Of the many measurements and comparisons possible, only one was statistically significant, the increase in structural plasticity at fifteen minutes following repeated uncaging protocols at fifteen minute intervals, which we will consider further in the discussion. In general, though, it appears that on the time scale of one hour, plasticity can only be induced in the same spine once.

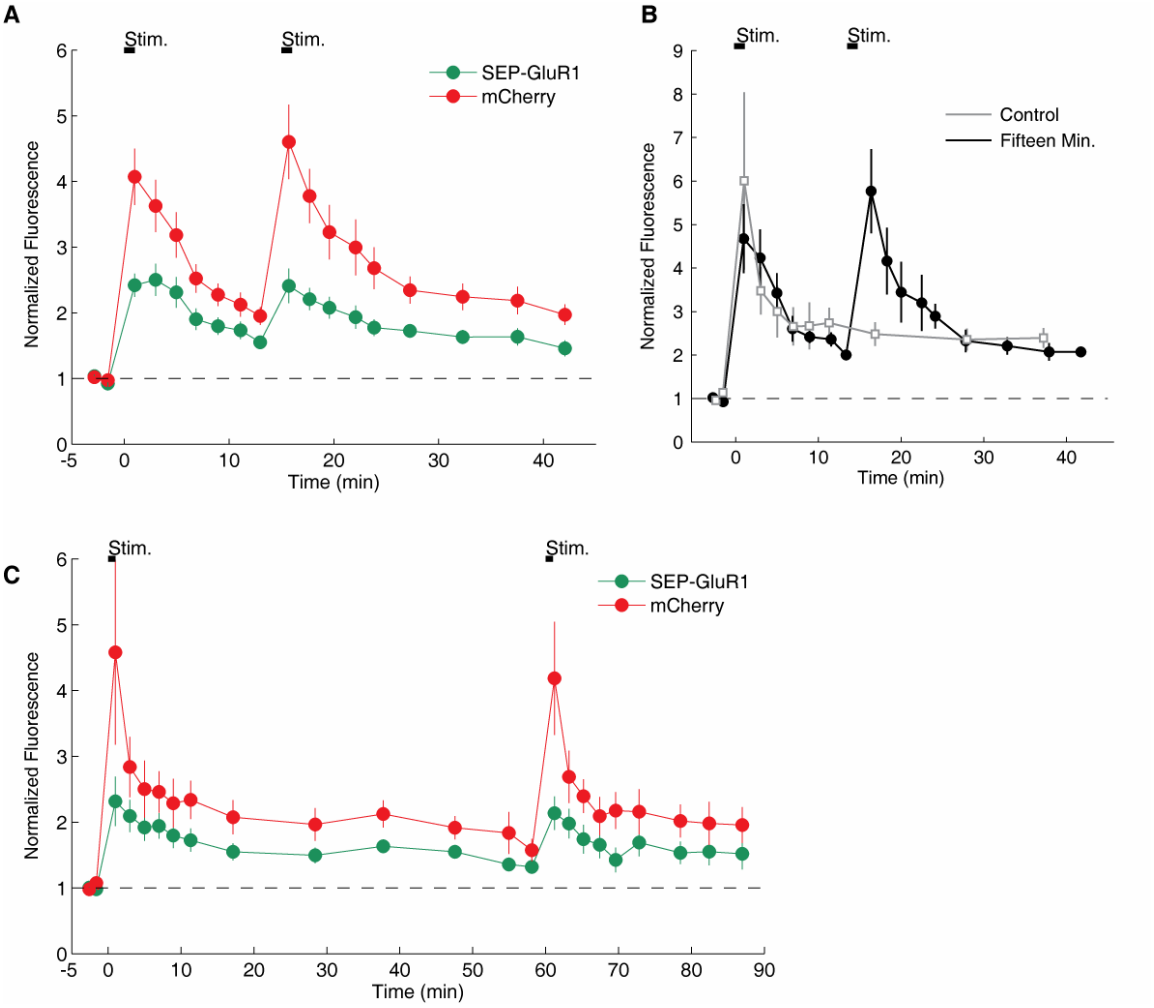

Figure 17: Repeatedly stimulating the same synapse does not yield further plasticity **A.** A standard uncaging protocol was performed on the same spine twice, at fifteen minute separation. The peak and long-term structural plasticity (red) were the same during the first and second stimulation. The same holds true for AMPAR recruitment (green). n = 11 spines, 10 cells. **B.** For a subset of experiments in A, we had paired experiments without a second stimulation. n = 5 spines, 5 cells. **C.** Same experimental protocol as **A**, but at sixty minute interval. The second stimulation does not induce further plasticity. n = 8 spines, 7 cells.

4.3 Potentiation of a synapse inhibits neighboring synapses

Having noticed that inducing plasticity in a spine prevented further plasticity, we also began to wonder if stimulated spines might influence neighbouring spines. Excitatory synaptic crosstalk, wherein stimulation reduces the threshold for plasticity at neighboring synapses, has been observed using similar techniques (Harvey and Svoboda, 2007). On a larger scale, it has been observed that reducing synaptic strength in a subset of synapses increases the strength of others, normalizing the general excitability of a cell (Turrigiano et al., 1998); this process is called homeostatic plasticity.

To investigate the level of crosstalk between synapses, we stimulated a given spine, and then induced plasticity on a neighbouring spine fifteen minutes later, the same time interval used in Fig. 17. Once again, we uncaged 30 times at 0.5 Hz. In this set of experiments, we only measured structural plasticity. All pairs of spines were within 3μm of each other.

Following uncaging, the first spine had a peak volume change of 280±60%, and a sustained volume change of 100±30% (Fig. 18B). When we uncaged on the neighbouring spine, the transient volume increase was 170±27%, with a sustained volume increase of 35±6%. We would conclude from this that inducing plasticity in a spine impairs plasticity at nearby spines within the next tens of minutes.

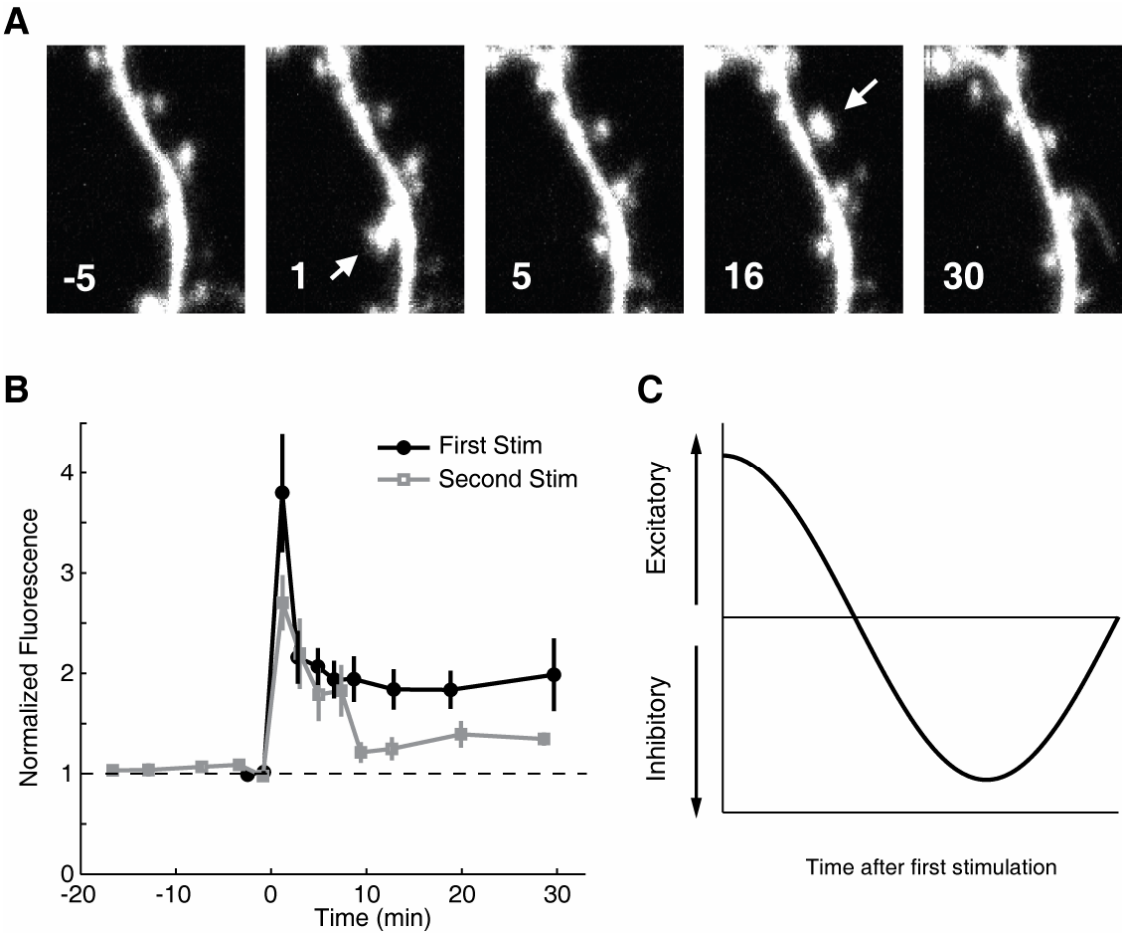

Figure 18: Plasticity at neighbouring spines was inhibited after fifteen minutes
A. Example images from crosstalk uncaging protocol. The standard uncaging protocol was performed on a spine, yielding normal structural plasticity (lower arrow). The same protocol was repeated on a nearby (within 3 μm) spine 15 min. later (upper arrow). **B.** Quantification of plasticity during crosstalk experiment. The second stimulation had partially inhibited plasiticity. n=9 pairs of spines, 7 cells. **C.** Potential timecourse of crosstalk. Initially, crosstalk may be excitatory (Harvey and Svoboda, 2007), then transition to an inhibitory phase, before finally dissipating.

4.4 Discussion

The development of two-photon uncaging on spines now enables scientists to study the fundamental characteristics of memory storage in single spines. Here, we performed two exploratory experiments, stimulating the same spine twice, and stimulating neighbouring spines to see how they interact.

When we stimulated the same spine twice, we found that at a fifteen minute interval, the second stimulation induced structural plasticity slightly larger than the first stimulus; and at a sixty minute interval, the second stimulation induced plasticity identical to the first. The weak plasticity at fifteen minutes is difficult to interpret due to the inability to compare more late-phase measurements (i.e. at thirty minutes). It is possible that at fifteen minutes post-induction, the spine was still in an early phase of LTP, and the second stimulation was superimposed over that. Alternatively, the first and second stimulation may have had different time constants for transitioning from the peak to the late phase (note the peaks are not significantly different). To test these hypotheses, we looked at a subset of experiments where we had doubly stimulated spines paired with singly stimulated spines. Comparing these spines at 45 minutes, we found no difference, and thus we would conclude that the increased signal at fifteen minutes is not further long-term plasticity, but summation of short term plasticity.

The number of states or strengths a synapse can have is important for determining how information is stored in the brain, and how much information can be stored. The minimal number of strengths a synapse might have are zero strength (silent synapses), and high strength, with LTP and LTD transitioning between the states. Alternatively, one might envision multiple high strength states, with transitions between

each of them. At the extreme, synapses may be able to regulate the exact number of AMPAR in the synapse, and the conductance of each of them, making the state of the synapse practically analog. Using our double stimulation protocol (and using structural plasticity as a proxy for synaptic strength), we induced transitions from a low state to a high state, but were not able to induce higher states. Given we were only able to observe two states, we infer that synapses are not analog, and have a small number of states. There is the important caveat, however, that we used a saturating uncaging protocol. Using a smaller number of stimuli may induce intermediate increases in spine size. Testing whether there are intermediate states requires being confident of being able to measure them (i.e., one must be confident that a late phase increase of 10% is indeed an increase, and not noise).

The number of states a synapse can have also has important implications for modeling learning. For binary synapses, this means the information storage of the brain is quite low, and decays quickly (exponentially in some models) (Fusi et al., 2005). If synapses have relatively few states, then the brain will have a limited capacity per synapse, and must rely on other ways to store information like synaptogenesis. When we, as people, learn new things, we might not be modifying the synapses that store information we already know, but creating out new pathways (assuming, of course, we are not forgetting old information in order to learn new stuff).

One of the problems biological storage devices face is storing information for long times despite the inherent instability of biology. Digital storage may offer a solution to these problems (Petersen et al., 1998). In an analog system, trying to maintain a specific value, e.g. 0.5, is difficult due to the turnover of proteins and other factors, and

the value may drift over time. In contrast, trying to maintain a digital state, e.g. 1, is much simpler. If the stored value drifts away from 1, corrective mechanisms can restore the value to 1. Thus, digital storage of information in cells provides inherent error checking, and reliability.

The number of times a spine can be potentiated also has indirect implications for spine size. Spine size varies throughout the brain, and even in the same region, generally ranging from 0.02-0.3 μm^3 (Kasai et al., 2010; Yasumatsu et al., 2008). The largest spines are thought to be formed by the repeated potentiation of small spines, gradually increasing their size. If, however, spines can only be potentiated once, it raises the question of how these different size spines are formed.

It should be noted that our experiments do not explicitly preclude the existence of multiple states for synaptic strength, but merely show there is a refractory period for plasticity, wherein no further plasticity can be induced. It would be useful to repeat these experiments with 6 or 24 hour intervals to see if the ability for plasticity recovers. The difficulty in executing these experiments will be maintaining slice and neuron health in between imaging sessions.

What is the cause of the refractory period? Given the raw nature of our observations, we are left mostly to conjecture. One possibility is that the endosomes containing the essential proteins for plasticity (viz. AMPAR) need time to recover, and restock proteins. Indeed, during our exocytosis imaging, we found the increase in exocytosis rate brief, which may be indicative of a small “readily releasable pool,” to borrow terminology from synaptic vesicle trafficking. Antibody feeding experiments have

measured the time constant of whole cell AMPAR endocytosis as 10 minutes, roughly the same time scale we have observed for the refractory period (Ehlers, 2000).

Having observed a paucity of plasticity from stimulating the same spine twice, we began to wonder whether the mechanisms that prevent the second stimulation from working also influence neighbouring spines. To see if this happens, we induced full plasticity on a given spine, then fifteen minutes later induced plasticity on a neighbouring spine (<3 μm away). When we did so, we observed a partial block of plasticity on the neighbouring spine, which we generally term inhibitory crosstalk.

Previous experiments have identified excitatory crosstalk between spines (Harvey et al., 2008). In those experiments, induction of plasticity reduced the threshold for induction at nearby spines. This phenomena was spatially restricted to within 5 μm, temporally restricted within ten minutes, and Ras-dependent. In contrast to these results, we observe inhibitory crosstalk. As we have not yet fully explored the spatiotemporal aspects of this phenomena, it is possible that our results do not conflict due to differing time scales. Stimulation of a spine may locally increase the potential for plasticity surrounding it on small time and space scales, before inhibiting plasticity later (Fig. 18C). Testing for crosstalk at multiple stimulus intervals and distances apart will be essential towards answering these questions.

What is the mechanism of inhibitory crosstalk? (Note that the mechanisms of crosstalk – suppression and exhaustion – may overlap with those preventing repeated spine plasticity) We see two possibilities. First, it may be due to the spread of active signals that suppress plasticity. Following stimulation of a spine, multiple signaling molecules like Ras and Rho are activated and spread into the dendrite and neighbouring

spines (Harvey et al., 2008). While some of these, like Ras, may be excitatory, others may be inhibitory, and the precise coordination between them will determine whether neighbouring spines are sensitized or inhibited. The second possibility is that groups of neighboring spines share resources, and that the induction of plasticity in a spine exhausts those resources such that other spines cannot use them. Given that AMPAR are exocytosed in a small region of the dendrite, endosomes in that entire region may be "exhausted," causing impaired plasticity.

If we were to continue this line of experiments, we would start by defining the time window of inhibition, performing paired stimulation at time intervals of one and thirty minutes. We would then sample in between these windows if there was an interesting progression. Once we established the time scale of inhibitory crosstalk, we would then look to find the length scale of the effect by performing the experiments at the optimal time for inhibition, and varying the distance between paired spines. Determining the length scale may give insight into the mechanisms of the process. If the length scale is small (<5μm), the crosstalk may be due to exhaustion, or local signaling by molecules like Ras. If, however, the length scale was longer, the crosstalk would be more likely to involve secondary process like protein synthesis or trafficking.

Chapter V: Discussion

In this work, we have performed experiments to elucidate the role of AMPAR trafficking in synaptic plasticity. Using two-photon uncaging, we found that AMPAR are recruited to stimulated spines at the same time the spine is growing in size. Employing a bleaching protocol, we found that these AMPAR come from both internal endosomes, and surface pools of receptors. We imaged AMPAR exocytosis in real time, and found that the exocytosis rate increased transiently, and occurred in both the spine and dendrite. This exocytosis depended on the Ras-ERK signaling pathway. Finally, we investigated the characteristics of plasticity in single spines, and found that spines have a limited capacity for structural plasticity on the timescale of hours. Given these results, it may be interesting to consider their importance in a wider context.

5.1 Importance of exocytosis

One aim of this research was to understand the relative contributions to plasticity of existing surface receptors, and the exocytosis of new receptors. In chapter II, we found that a majority of AMPAR that enter the spine following stimulation were from the surface (with the caveat that we are looking at overexpressed GluR1 receptors, which may change the subunit composition distribution of AMPAR). If surface receptors are playing such a large role, what is the role exocytosis?

First, the exocytosis of proteins other AMPAR may be critical. There are multiple pools of recycling endosomes with differing contents, and some may not contain AMPAR (Gruenberg, 2001). When these endosomes fuse with the plasma membrane, other (probably membrane associated) plasticity machinery may be exocytosed. In fact, the first imaging of activity-dependent exocytosis used transferrin (TfR) receptors (Park et al.,

2006). In preliminary experiments, we transfected neurons with SEP-TfR, and saw frequent exocytosis in the primary dendrite, in comparison to the low exocytosis rates for AMPAR (data not shown). We can only speculate on the identity of these other proteins, but we would venture they include PSD anchoring proteins.

The slot hypothesis may explain how anchoring proteins are important (Barry and Ziff, 2002; Lisman and Raghavachari, 2006). The slot hypothesis states that the PSD has anchoring proteins that act as slots for receptors. As receptors diffuse into and out of the synapse, some of them will be sequestered by slots, and be present to receive synaptic input. When LTP happens, then, the number of post-synaptic slots is increased (mechanism unknown), and as a byproduct the AMPAR content of the PSD increases (while we have considered anchoring before, centering the hypothesis on the anchors rather than the receptors gives new perspective). Evidence for the slot hypothesis is that there is an exchange of GluR1-containing AMPAR for GluR2/3 heteromers, while the synaptic strength remains the same, implying another factor is maintaining synaptic strength (McCormack et al., 2006; Plant et al., 2006). "Slots," whatever complex of proteins they may be, may be exocytosed following stimulation.

Concerning ourselves specifically with AMPAR exocytosis, we furthermore must consider the subunit composition of exocytosed AMPAR. Both GluR1 and GluR2 subunits interact with proteins that regulate their exocytosis: 4.1N (Lin et al., 2009) and NSF (Lee et al., 2002), respectively. Given that AMPAR often form GluR1/2 heteromers, these receptors would have multiple pathways regulating their exocytosis. It is possible that the GluR2/NSF pathway regulates the constitutive trafficking of AMPAR, while the GluR1/4.1N pathway regulates the activity-dependent trafficking. One study used a

GluR2-KO background, and found that synaptic levels of AMPAR could be restored by GluR2 subunits lacking their c-tail, calling into question the necessity of GluR2 for exocytosis (Panicker et al., 2008). Alternatively, both GluR1 and GluR2 pathways could be required for exocytosis, and our imaging of homomers would alter the natural exocytosis process. Also, since the majority of AMPAR that enter the synapse following LTP are not exocytosed, basal trafficking is critical. Interference with AMPAR exocytosis leads to a degradation of synaptic strength, as AMPAR are endocytosed and not replaced (Park et al., 2004). Further work must be performed to confirm the roles of receptor subtypes in AMPAR exocytosis.

5.2 Implications of location of exocytosis

While the location of exocytosis may seem of particular interest to molecular neurobiologists, there are wider implications. The dendrite, while less than 1μm away from the PSD of spines in the spatial dimension, it is meaningfully further away in the time domain. AMPAR have a diffusion constant of ~0.1μm^2/s. AMPAR exocytosed in the dendrite would take 10s longer to diffuse the 1μm from the dendrite to the PSD than AMPAR exocytosed in the spine. The fact that it takes tens of seconds for AMPAR to reach the spine may determine what types of memory are encoded by this phenomena. Working memory lasts on the order of seconds, too fast to be coded this way (Unsworth and Engle, 2007). Short term memory, however, takes seconds to develop, and would be more suited to this process. When someone interrupts you while you are thinking, whether you can remember what you were thinking about may be determined on

whether AMPAR reach the synapse. And that may be determined on far they have to travel to get there.

Besides influencing the timing of integration, the location of exocytosis has implications for our models of how neurons integrate information, and the plasticity of this integration. While the spine is thought to be the fundamental unit of memory, individual spines are incapable of driving a neuron to fire action potentials; rather, sets of spines must be activated (near) simultaneously (Gasparini et al., 2004; Otmakhov et al., 1993). The location of spines on a dendrite matter as well, as short segments of dendrites form functional units, and the excitability of these segments is plastic (Losonczy et al., 2008; Magee and Johnston, 2005). Given our finding that exocytosis occurs within 2-3μm of a stimulated spine, this provides an alternative mechanism for short segments of dendrites to form functional units. This local signaling could enhance plasticity at nearby synapses, as the Svoboda lab has shown (Harvey and Svoboda, 2007), or inhibit them, as we have found.

On a cell biological level, the diffusion of exocytosis may change how people think about compartmentalization. Previously, it had been thought that spines act as both electrical and chemical compartments (Ashby et al., 2006; Bloodgood and Sabatini, 2005; Koch and Zador, 1993; Lee et al., 2009; Muller and Connor, 1991; Yasuda et al., 2004), and that this compartmentalization was important for spine function. Recently, however, it was shown that this is not always true for signaling, as Ras can diffuse from the spine (Harvey et al., 2008; Yasuda et al., 2006). Our findings show that this can also be untrue functionally, as exocytosis escapes the spine. As we discover more of which types of signaling are compartmentalized versus diffuse, we will need to make sense of

why each pathway has a specific character. There may be metabolic and complexity costs for each type of signaling.

5.3 Structural plasticity, memory, and forgetting

In section 1.7, I laid out the long history of structural plasticity, and showed that, on some level, structural plasticity is related with memory. Spines can vary greatly in size, ranging from 0.02-0.3μm^3. In vivo imaging has shown that there is a small, but constant turnover of spines, and that this turnover increases when animals learn (Trachtenberg et al., 2002; Xu et al., 2007). Besides changes in spine number, extant spines are constantly adjusting their spine size as well (Yasumatsu et al., 2008). In addition to these fluctuations, inducing plasticity in spines can cause an increase in spine size. The Kasai lab has proposed a model of learning in spines wherein spine size acts as a measure of the "history" of the spine, showing how many (net) times that synapse has been potentiated (Kasai et al., 2010). In this model, the constant turnover of spines and fluctuations in spine size are constantly wiping clean the memories of neurons, and allowing new memories to be formed.

As we refine our understanding of how spine morphology is involved in memory, we will need to connect characteristics of memory with specific neuronal correlates. One obvious trait of memory is that people can continue to learn (and forget) over their entire lives. Given our finite brains, this process will require reusing the same neurons and synapses in multiple memories. In chapter IV, we tested the capacity of a single spine to be potentiated multiple times, and primitive form of reusing the same spine to learn again. We found that it is difficult to induce structural plasticity in the same spine twice,

at least within one hour. Since large spines do exist, and presumably are not large de novo, we infer that spines need a recovery period before being capable of potentiation again. This refractory period for plasticity, and the finite number of neurons in the brain may set hard limits on people's learning rates. Indeed, psychological studies have found that we are more likely to retain a set of information if we have learned it over a spread out period of time than if we cram (Schmidt and Bjork, 1992). The idea that a refractory period for plasticity is a limiting factor in learning also may explain some differences in intelligence. People with shorter refractory periods may have higher learning rates. On the medicinal side, identifying drugs which can speed the recovery process would be able to enhance human intelligence.

References

Abeliovich, A., Chen, C., Goda, Y., Silva, A.J., Stevens, C.F., and Tonegawa, S. (1993). Modified hippocampal long-term potentiation in PKC gamma-mutant mice. Cell *75*, 1253-1262.

Abraham, W.C., Logan, B., Greenwood, J.M., and Dragunow, M. (2002). Induction and Experience-Dependent Consolidation of Stable Long-Term Potentiation Lasting Months in the Hippocampus. J Neurosci *22*, 9626-9634.

Adesnik, H., and Nicoll, R.A. (2007). Conservation of Glutamate Receptor 2-Containing AMPA Receptors during Long-Term Potentiation. J Neurosci *27*, 4598-4602.

Adesnik, H., Nicoll, R.A., and England, P.M. (2005). Photoinactivation of Native AMPA Receptors Reveals Their Real-Time Trafficking. Neuron *48*, 977-985.

Andersen, P., Sundberg, S.H., Sveen, O., and Wigstrom, H. (1977). Specific long-lasting potentiation of synaptic transmission in hippocampal slices. Nature *266*, 736-737.

Andrasfalvy, B.K., and Magee, J.C. (2001). Distance-Dependent Increase in AMPA Receptor Number in the Dendrites of Adult Hippocampal CA1 Pyramidal Neurons. J Neurosci *21*, 9151-9159.

Andrasfalvy, B.K., and Magee, J.C. (2004). Changes in AMPA receptor currents following LTP induction on rat CA1 pyramidal neurones. J Neuroscience *559*, 543-554.

Arendt, K.L., Royo, M., Fernandez-Monreal, M., Knafo, S., Petrok, C.N., Martens, J.R., and Esteban, J.A. (2009). PIP3 controls synaptic function by maintaining AMPA receptor clustering at the postsynaptic membrane. Nat Neurosci *13*, 36-44.

Armstrong, N., Jasti, J., Beich-Frandsen, M., and Gouaux, E. (2006). Measurement of Conformational Changes accompanying Desensitization in an Ionotropic Glutamate Receptor. Cell *127*, 85-97.

Ashby, M.C., De La Rue, S.A., Ralph, G.S., Uney, J., Collingridge, G.L., and Henley, J.M. (2004). Removal of AMPA Receptors (AMPARs) from Synapses Is Preceded by Transient Endocytosis of Extrasynaptic AMPARs. J Neuroscience *24*, 5172-5176.

Ashby, M.C., Maier, S.R., Nishimune, A., and Henley, J.M. (2006). Lateral Diffusion Drives Constitutive Exchange of AMPA Receptors at Dendritic Spines and Is Regulated by Spine Morphology. J Neuroscience *26*, 7046-7055.

Axelrod, D., Koppel, D.E., Schlessinger, J., Elson, E., and Webb, W.W. (1976). Mobility measurement by analysis of fluorescence photobleaching recovery kinetics. Biophysical J *16*, 1055-1069.

Bagal, A.A., Kao, J.P.Y., Tang, C.-M., and Thompson, S.M. (2005). Long-term potentiation of exogenous glutamate responses at single dendritic spines. PNAS *102*, 14434-14439.

Bailey, C.H., and Chen, M. (1983). Morphological basis of long-term habituation and sensitization in Aplysia. Science *220*, 91-93.

Banke, T.G., Bowie, D., Lee, H.K., Huganir, R.L., Schousboe, A., and Traynelis, S.F. (2000). Control of GluR1 AMPA Receptor Function by cAMP-Dependent Protein Kinase. J Neurosci *20*, 89-102.

Barria, A., Derkach, V., and Soderling, T. (1997a). Identification of the Ca2+/Calmodulin-dependent Protein Kinase II Regulatory Phosphorylation Site in the alpha - Amino-3-hydroxyl-5-methyl4-isoxazole-propionate-type Glutamate Receptor. Science *272*, 32727-32730.

Barria, A., and Malinow, R. (2005). NMDA Receptor Subunit Composition Controls Synaptic Plasticity by Regulating Binding to CaMKII. Neuron *48*, 289-301.

Barria, A., Muller, D., Derkach, V., Griffith, L.C., and Soderling, T.R. (1997b). Regulatory Phosphorylation of AMPA-Type Glutamate Receptors by CaM-KII During Long-Term Potentiation. Science *276*, 2042-2045.

Barry, M.F., and Ziff, E.B. (2002). Receptor trafficking and the plasticity of excitatory synapses. Current Opinion in Neurobiology *12*, 279-286.

Bats, C., Groc, L., and Choquet, D. (2007). The Interaction between Stargazin and PSD-95 Regulates AMPA Receptor Surface Trafficking. Neuron *53*, 719-734.

Baude, A., Nusser, Z., Molnar, E., McIlhinney, R.A.J., and Somogyi, P. (1995). High-resolution immunogold localization of AMPA type glutamate receptor subunits at synaptic and non-synaptic sites in rat hippocampus. Neuroscience *69*, 1031-1055.

Bekkers, J.M., and Stevens, C.F. (1990). Presynaptic mechanism for long-term potentiation in the hippocampus. Nature *346*, 724-729.

Bi, G.-q., and Poo, M.-m. (1998). Synaptic Modifications in Cultured Hippocampal Neurons: Dependence on Spike Timing, Synaptic Strength, and Postsynaptic Cell Type. J Neurosci *18*, 10464-10472.

Blanpied, T.A., Scott, D.B., and Ehlers, M.D. (2002). Dynamics and Regulation of Clathrin Coats at Specialized Endocytic Zones of Dendrites and Spines. Neuron *36*, 435-449.

Bliss, T.V.P., and Lomo, T. (1973). Long-lasting potentiation of synaptic transmission in the dentate area of the anaesthetized rabbit following stimulation of the perforant path. J Physiol *232*, 331-356.

Blitzer, R.D., Wong, T., Nouranifar, R., Iyengar, R., and Landau, E.M. (1995). Postsynaptic cAMP pathway gates early LTP in hippocampal CA1 region. Neuron *15*, 1403-1414.

Bloodgood, B.L., and Sabatini, B.L. (2005). Neuronal Activity Regulates Diffusion Across the Neck of Dendritic Spines. Science *310*, 866-869.

Borgdorff, A.J., and Choquet, D. (2002). Regulation of AMPA receptor lateral movements. Nature *417*, 649-653.

Boulter, J., Hollmann, M., O'Shea-Greenfield, A., Hartley, M., Deneris, E., Maron, C., and Heinemann, S. (1990). Molecular cloning and functional expression of glutamate receptor subunit genes. Science *249*, 1033-1037.

Braithwaite, S.P., Xia, H., and Malenka, R.C. (2002). Differential roles for NSF and GRIP/ABP in AMPA receptor cycling. PNAS *99*, 7096-7101.

Bressloff, P.C., Earnshaw, B.A., and Ward, M.J. (2008). Diffusion of Protein Receptors on a Cylindrical Dendritic Membrane with Partially Absorbing Traps. SIAM Journal on Applied Mathematics *68*, 1223-1246.

Cai, C., Coleman, S.K., Niemi, K., and Keinanen, K. (2002). Selective binding of synapse-associated protein 97 to GluR-A alpha-amino-5-hydroxy-3-methyl-4-isoxazole propionate receptor subunit is determined by a novel sequence motif. J Biol Chem *277*, 31484-31490.

Chung, H.J., Steinberg, J.P., Huganir, R.L., and Linden, D.J. (2003). Requirement of AMPA Receptor GluR2 Phosphorylation for Cerebellar Long-Term Depression. Science *300*, 1751-1755.

Chung, H.J., Xia, J., Scannevin, R.H., Zhang, X., and Huganir, R.L. (2000). Phosphorylation of the AMPA Receptor Subunit GluR2 Differentially Regulates Its Interaction with PDZ Domain-Containing Proteins. J Neurosci *20*, 7258-7267.

Coleman, S.K., Cai, C., Mottershead, D.G., Haapalahti, J.-P., and Keinanen, K. (2003). Surface Expression of GluR-D AMPA Receptor Is Dependent on an Interaction between Its C-Terminal Domain and a 4.1 Protein. J Neurosci *23*, 798-806.

Colledge, M., Dean, R.A., Scott, G.K., Langeberg, L.K., Huganir, R.L., and Scott, J.D. (2000). Targeting of PKA to glutamate receptors through a MAGUK-AKAP complex. Neuron *27*, 107-119.

Collingridge, G.L., Isaac, J.T., and Wang, Y.T. (2004). Receptor trafficking and synaptic plasticity. Nat Rev Neurosci *5*, 952-962.

Correia, S.S., Bassani, S., Brown, T.C., Lise, M.-F., Backos, D.S., El-Husseini, A., Passafaro, M., and Esteban, J.A. (2008). Motor protein-dependent transport of AMPA receptors into spines during long-term potentiation. Nat Neurosci *advanced online publication*.

Dakoji, S., Tomita, S., Karimzadegan, S., Nicoll, R.A., and Bredt, D.S. (2003). Interaction of transmembrane AMPA receptor regulatory proteins with multiple membrane associated guanylate kinases. Neuropharmacology *45*, 849-856.

Davies, J., Francis, A.A., Jones, A.W., and Watkins, J.C. (1981). 2-Amino-5-phosphonovalerate (2APV), a potent and selective antagonist of amino acid-induced and synaptic excitation. Neuroscience Letters *21*, 77-81.

Delgado, J.Y., Coba, M., Anderson, C.N.G., Thompson, K.R., Gray, E.E., Heusner, C.L., Martin, K.C., Grant, S.G.N., and O'Dell, T.J. (2007). NMDA Receptor Activation Dephosphorylates AMPA Receptor Glutamate Receptor 1 Subunits at Threonine 840. J Neurosci *27*, 13210-13221.

Derkach, V., Barria, A., and Soderling, T.R. (1999). Ca2+/calmodulin-kinase II enhances channel conductance of alpha-amino-3-hydroxy-5-methyl-4-isoxazolepropionate type glutamate receptors. PNAS *96*, 3269-3274.

Derkach, V.A., Oh, M.C., Guire, E.S., and Soderling, T.R. (2007). Regulatory mechanisms of AMPA receptors in synaptic plasticity. Nat Rev Neurosci *8*, 101-113.

Dingledine, R., Borges, K., Bowie, D., and Traynelis, S.F. (1999). The Glutamate Receptor Ion Channels. Pharmacological Review *51*, 7-62.

Dong, H., O'Brien, R.J., Fung, E.T., Lanahan, A.A., Worley, P.F., and Huganir, R.L. (1997). GRIP: a synaptic PDZ domain-containing protein that interacts with AMPA receptors. Nature *386*, 279-284.

Douglas, R.M., and Goddard, G.V. (1975). Long-term potentiation of the perforant path-granule cell synapse in the rat hippocampus. Brain Research *86*, 205-215.

Doyle, D.A., Lee, A., Lewis, J., Kim, E., Sheng, M., and MacKinnon, R. (1996). Crystal Structures of a Complexed and Peptide-Free Membrane Protein Binding Domain: Molecular Basis of Peptide Recognition by PDZ. Cell *85*, 1067-1076.

Ehlers, M.D. (2000). Reinsertion or Degradation of AMPA Receptors Determined by Activity-Dependent Endocytic Sorting. Neuron *28*, 511-525.

Ehlers, M.D., Heine, M., Groc, L., Lee, M.-C., and Choquet, D. (2007). Diffusional Trapping of GluR1 AMPA Receptors by Input-Specific Synaptic Activity. Neuron *54*, 447-460.

Ehrlich, I., Klein, M., Rumpel, S., and Malinow, R. (2007). PSD-95 is required for activity-driven synapse stabilization. PNAS *104*, 4176-4181.

Elias, G.M., Funke, L., Stein, V., Grant, S.G., Bredt, D.S., and Nicoll, R.A. (2006). Synapse-Specific and Developmentally Regulated Targeting of AMPA Receptors by a Family of MAGUK Scaffolding Proteins. Neuron *52*, 307-320.

Engert, F., and Bonhoeffer, T. (1999). Dendritic spine changes associated with hippocampal long-term synaptic plasticity. Nature *399*, 66-70.

English, J.D., and Sweatt, J.D. (1997). A Requirement for the Mitogen-activated Protein Kinase Cascade in Hippocampal Long Term Potentiation. JBC *272*, 19103-19106.

Enoki, R., Hu, Y.-l., Hamilton, D., and Fine, A. (2009). Expression of Long-Term Plasticity at Individual Synapses in Hippocampus Is Graded, Bidirectional, and Mainly Presynaptic: Optical Quantal Analysis. Neuron *62*, 242-253.

Esteban, J.A., Shi, S.-H., Wilson, C., Nuriya, M., Huganir, R.L., and Malinow, R. (2003). PKA phosphorylation of AMPA receptor subunits controls synaptic trafficking underlying plasticity. Nat Neurosci *6*, 136-143.

Feng, W., and Zhang, M. (2009). Organization and dynamics of PDZ-domain-related supramodules in the postsynaptic density. Nat Rev Neurosci *10*, 87-99.

Fifkova, E., and Van Harreveld, A. (1977). Long-lasting morphological changes in dendritic spines of dentate granular cells following stimulation of the entorhinal area. J Neurocytol *6*, 211-230.

Fusi, S., Drew, P.J., and Abbott, L.F. (2005). Cascade Models of Synaptically Stored Memories. Neuron *45*, 599-611.

Garner, C.C., Nash, J., and Huganir, R.L. (2000). PDZ domains in synapse assembly and signalling. Trends in Cell Biology *10*, 274-280.

Gasparini, S., Migliore, M., and Magee, J.C. (2004). On the Initiation and Propagation of Dendritic Spikes in CA1 Pyramidal Neurons. J Neurosci *24*, 11046-11056.

Gerges, N.Z., Backos, D.S., Rupasinghe, C.N., Spaller, M.R., and Esteban, J.A. (2006). Dual role of the exocyst in AMPA receptor targeting and insertion into the postsynaptic membrane. Embo J *25*, 1623-1634.

Globus, A., and Scheibel, A.B. (1967). The effect of visual deprivation on cortical neurons: a Golgi study. Exp Neurol *19*, 331-345.

Greger, I.H., Ziff, E.B., and Penn, A.C. (2007). Molecular determinants of AMPA receptor subunit assembly. Trends in Neurosciences *30*, 407-416.

Gruenberg, J. (2001). The endocytic pathway: a mosaic of domains. Nat Rev Mol Cell Biol *2*, 721-730.

Grunditz, A., Holbro, N., Tian, L., Zuo, Y., and Oertner, T.G. (2008). Spine Neck Plasticity Controls Postsynaptic Calcium Signals through Electrical Compartmentalization. J Neurosci *28*, 13457-13466.

Hanley, J.G., and Henley, J.M. (2005). PICK1 is a calcium-sensor for NMDA-induced AMPA receptor trafficking. Embo J *24*, 3266-3278.

Hansen, K.B., Yuan, H., and Traynelis, S.F. (2007). Structural aspects of AMPA receptor activation, desensitization and deactivation. Current Opinion in Neurobiology *17*, 281-288.

Harms, K.J., Tovar, K.R., and Craig, A.M. (2005). Synapse-Specific Regulation of AMPA Receptor Subunit Composition by Activity. J Neurosci *25*, 6379-6388.

Harris, K.M., and Stevens, J.K. (1989). Dendritic spines of CA 1 pyramidal cells in the rat hippocampus: serial electron microscopy with reference to their biophysical characteristics. J Neurosci *9*, 2982-2997.

Harvey, C.D., and Svoboda, K. (2007). Locally dynamic synaptic learning rules in pyramidal neuron dendrites. Nature *450*, 1195-1200.

Harvey, C.D., Yasuda, R., Zhong, H., and Svoboda, K. (2008). The Spread of Ras Activity Triggered by Activation of a Single Dendritic Spine. Science *321*, 136-140.

Hayashi, Y., Shi, S.-H., Esteban, J., eacute, A., Piccini, A., Poncer, J.-C., and Malinow, R. (2000). Driving AMPA Receptors into Synapses by LTP and CaMKII: Requirement for GluR1 and PDZ Domain Interaction. Science *287*, 2262-2267.

He, L., and Wu, L.-G. (2007). The debate on the kiss-and-run fusion at synapses. Trends in Neurosciences *30*, 447-455.

Heine, M., Groc, L., Frischknecht, R., Beique, J.-C., Lounis, B., Rumbaugh, G., Huganir, R.L., Cognet, L., and Choquet, D. (2008). Surface Mobility of Postsynaptic AMPARs Tunes Synaptic Transmission. Science *320*, 201-205.

Hoffman, D.A., Sprengel, R., and Sakmann, B. (2002). Molecular dissection of hippocampal theta-burst pairing potentiation. PNAS *99*, 7740-7745.

Holcman, D., and Triller, A. (2006). Modeling Synaptic Dynamics Driven by Receptor Lateral Diffusion. Biophysics Journal *91*, 2405-2415.

Hollmann, M., and Heinemann, S. (1994). Cloned Glutamate Receptors. Annual Review of Neuroscience *17*, 31-108.

Honkura, N., Matsuzaki, M., Noguchi, J., Ellis-Davies, G.C.R., and Kasai, H. (2008). The Subspine Organization of Actin Fibers Regulates the Structure and Plasticity of Dendritic Spines. Neuron *57*, 719-729.

Hume, R.I., Dingledine, R., and Heinemann, S.F. (1991). Identification of a site in glutamate receptor subunits that controls calcium permeability. Science *253*, 1028-1031.

Hung, A.Y., and Sheng, M. (2002). PDZ Domains: Structural Modules for Protein Complex Assembly. JBC *277*, 5699-5702.

Isaac, J.T., Nicoll, R.A., and Malenka, R.C. (1995). Evidence for silent synapses: implications for the expression of LTP. Neuron *15*, 427-434.

Kasai, H., Fukuda, M., Watanabe, S., Hayashi-Takagi, A., and Noguchi, J. (2010). Structural dynamics of dendritic spines in memory and cognition. Trends in Neurosciences *33*, 121-129.

Kauer, J.A., Malenka, R.C., and Nicoll, R.A. (1988). A persistent postsynaptic modification mediates long-term potentiation in the hippocampus. Neuron *1*, 911-917.

Kelso, S.R., Ganong, A.H., and Brown, T.H. (1986). Hebbian synapses in hippocampus. Proc Natl Acad Sci U S A *83*, 5326-5330.

Kennedy, M.B., Beale, H.C., Carlisle, H.J., and Washburn, L.R. (2005). Integration of Biochemical Signalling in Spines. Nature Reviews Neuroscience *6*, 423-434.

Kennedy, M.J., and Ehlers, M.D. (2006). Organelles and trafficking machinery for postsynaptic plasticity. Annu Rev Neurosci *29*, 325-362.

Kessels, H.W., Kopec, C.D., Klein, M.E., and Malinow, R. (2009). Roles of stargazin and phosphorylation in the control of AMPA receptor subcellular distribution. Nat Neurosci *12*, 888-896.

Kharazia, V.N., and Weinberg, R.J. (1999). Immunogold localization of AMPA and NMDA receptors in somatic sensory cortex of albino rat. J Comp Neurology *412*, 292-302.

Kleschevnikov, A.M., Sokolov, M.V., Kuhnt, U., Dawe, G.S., Stephenson, J.D., and Voronin, L.L. (1996). Changes in paired-pulse facilitation correlate with induction

of long-term potentiation in area CA1 of rat hippocampal slices. Neuroscience *76*, 829-843.

Koch, C., and Zador, A. (1993). The function of dendritic spines: devices subserving biochemical rather than electrical compartmentalization. J Neurosci *13*, 413-422.

Kohler, M., Kornau, H.C., and Seeburg, P.H. (1994). The organization of the gene for the functionally dominant alpha-amino-3-hydroxy-5-methylisoxazole-4-propionic acid receptor subunit GluR-B. JBC *269*, 17367-17370.

Kopec, C.D., Li, B., Wei, W., Boehm, J., and Malinow, R. (2006). Glutamate Receptor Exocytosis and Spine Enlargement during Chemically Induced Long-Term Potentiation. J Neuroscience *26*, 2000-2009.

Kopec, C.D., Real, E., Kessels, H.W., and Malinow, R. (2007). GluR1 Links Structural and Functional Plasticity at Excitatory Synapses. J Neurosci *27*, 13706-13718.

Kott, S., Werner, M., Korber, C., and Hollmann, M. (2007). Electrophysiological Properties of AMPA Receptors Are Differentially Modulated Depending on the Associated Member of the TARP Family. J Neurosci *27*, 3780-3789.

Kulangara, K., Kropf, M., Glauser, L., Magnin, S., Alberi, S., Yersin, A., and Hirling, H. (2007). Phosphorylation of Glutamate Receptor Interacting Protein 1 Regulates Surface Expression of Glutamate Receptors. J Biol Chem *282*, 2395-2404.

Lee, H.-K., Takamiya, K., Han, J.-S., Man, H., Kim, C.-H., Rumbaugh, G., Yu, S., Ding, L., He, C., Petralia, R.S.*, et al.* (2003). Phosphorylation of the AMPA Receptor GluR1 Subunit Is Required for Synaptic Plasticity and Retention of Spatial Memory. Cell *112*, 631-643.

Lee, H.-K., Takamiya, K., Kameyama, K., He, K., Yu, S., Rossetti, L., Wilen, D., and Huganir, R.L. (2007). Identification and characterization of a novel phosphorylation site on the GluR1 subunit of AMPA receptors. Molecular and Cellular Neuroscience *In Press, Corrected Proof*.

Lee, K.S., Schottler, F., Oliver, M., and Lynch, G. (1980). Brief bursts of high-frequency stimulation produce two types of structural change in rat hippocampus. J Neurophysiol *44*, 247-258.

Lee, S.-J.R., Escobedo-Lozoya, Y., Szatmari, E.M., and Yasuda, R. (2009). Activation of CaMKII in single dendritic spines during long-term potentiation. Nature *458*, 299-304.

Lee, S.H., Liu, L., Wang, Y.T., and Sheng, M. (2002). Clathrin Adaptor AP2 and NSF Interact with Overlapping Sites of GluR2 and Play Distinct Roles in AMPA Receptor Trafficking and Hippocampal LTD. Neuron *36*, 661-674.

Lee, S.H., Simonetta, A., and Sheng, M. (2004). Subunit rules governing the sorting of internalized AMPA receptors in hippocampal neurons. Neuron *43*, 221-236.

Leonard, A.S., Davare, M.A., Horne, M.C., Garner, C.C., and Hell, J.W. (1998). SAP97 Is Associated with the alpha -Amino-3-hydroxy-5-methylisoxazole-4-propionic Acid Receptor GluR1 Subunit. J Biol Chem *273*, 19518-19524.

Leonoudakis, D., Zhao, P., and Beattie, E.C. (2008). Rapid Tumor Necrosis Factor {alpha}-Induced Exocytosis of Glutamate Receptor 2-Lacking AMPA Receptors to Extrasynaptic Plasma Membrane Potentiates Excitotoxicity. J Neurosci *28*, 2119-2130.

Liao, D., Hessler, N.A., and Malinow, R. (1995). Activation of postsynaptically silent synapses during pairing-induced LTP in CA1 region of hippocampal slice. Nature *375*, 400-404.

Lin, D.-T., and Huganir, R.L. (2007). PICK1 and Phosphorylation of the Glutamate Receptor 2 (GluR2) AMPA Receptor Subunit Regulates GluR2 Recycling after NMDA Receptor-Induced Internalization. J Neurosci *27*, 13903-13908.

Lin, D.-T., Makino, Y., Sharma, K., Hayashi, T., Neve, R., Takamiya, K., and Huganir, R.L. (2009). Regulation of AMPA receptor extrasynaptic insertion by 4.1N, phosphorylation and palmitoylation. Nat Neurosci *12*, 879-887.

Ling, D.S., Benardo, L.S., Serrano, P.A., Blace, N., Kelly, M.T., Crary, J.F., and Sacktor, T.C. (2002). Protein kinase Mzeta is necessary and sufficient for LTP maintenance. Nat Neurosci *5*, 295-296.

Lisman, J., and Raghavachari, S. (2006). A Unified Model of the Presynaptic and Postsynaptic Changes During LTP at CA1 Synapses. STKE *2006*, re11-.

Lisman, J.E., Raghavachari, S., and Tsien, R.W. (2007). The sequence of events that underlie quantal transmission at central glutamatergic synapses. Nat Rev Neurosci *8*, 597-609.

Lomeli, H., Mosbacher, J., Melcher, T., Hoger, T., Geiger, J.R., Kuner, T., Monyer, H., Higuchi, M., Bach, A., and Seeburg, P.H. (1994). Control of kinetic properties of AMPA receptor channels by nuclear RNA editing. Science *266*, 1709-1713.

Losonczy, A., Makara, J.K., and Magee, J.C. (2008). Compartmentalized dendritic plasticity and input feature storage in neurons. Nature *452*, 436-441.

Lu, J., Helton, T.D., Blanpied, T.A., Racz, B., Newpher, T.M., Weinberg, R.J., and Ehlers, M.D. (2007). Postsynaptic Positioning of Endocytic Zones and AMPA Receptor Cycling by Physical Coupling of Dynamin-3 to Homer. Neuron *55*, 874-889.

Lu, W.-Y., Man, H.-Y., Ju, W., Trimble, W.S., MacDonald, J.F., and Wang, Y.T. (2001). Activation of Synaptic NMDA Receptors Induces Membrane Insertion of New AMPA Receptors and LTP in Cultured Hippocampal Neurons. Neuron *29*, 243-254.

Lu, W., Shi, Y., Jackson, A.C., Bjorgan, K., During, M.J., Sprengel, R., Seeburg, P.H., and Nicoll, R.A. (2009). Subunit Composition of Synaptic AMPA Receptors Revealed by a Single-Cell Genetic Approach. Neuron *62*, 254-268.

Lu, W., and Ziff, E.B. (2005). PICK1 Interacts with ABP/GRIP to Regulate AMPA Receptor Trafficking. Neuron *47*, 407-421.

Luscher, C., Xia, H., Beattie, E.C., Carroll, R.C., von Zastrow, M., Malenka, R.C., and Nicoll, R.A. (1999). Role of AMPA Receptor Cycling in Synaptic Transmission and Plasticity. Neuron *24*, 649-658.

Lynch, G., Larson, J., Kelso, S., Barrionuevo, G., and Schottler, F. (1983). Intracellular injections of EGTA block induction of hippocampal long-term potentiation. Nature *305*, 719-721.

MacDermott, A.B., Mayer, M.L., Westbrook, G.L., Smith, S.J., and Barker, J.L. (1986). NMDA-receptor activation increases cytoplasmic calcium concentration in cultured spinal cord neurones. Nature *321*, 519-522.

Magee, J.C., and Cook, E.P. (2000). Somatic EPSP amplitude is independent of synapse location in hippocampal pyramidal neurons. Nat Neurosci *3*, 895-903.

Magee, J.C., and Johnston, D. (2005). Plasticity of dendritic function. Current Opinion in Neurobiology *15*, 334-342.

Makino, H., and Malinow, R. (2009). AMPA Receptor Incorporation into Synapses during LTP: The Role of Lateral Movement and Exocytosis. Neuron *64*, 381-390.

Malenka, R.C., Kauer, J.A., Perkel, D.J., Mauk, M.D., Kelly, P.T., Nicoll, R.A., and Waxham, M.N. (1989). An essential role for postsynaptic calmodulin and protein kinase activity in long-term potentiation. Nature *340*, 554-557.

Maletic-Savatic, M., Malinow, R., and Svoboda, K. (1999). Rapid Dendritic Morphogenesis in CA1 Hippocampal Dendrites Induced by Synaptic Activity. Science *283*, 1923-1927.

Malinow, R., and Tsien, R.W. (1990). Presynaptic enhancement shown by whole-cell recordings of long-term potentiation in hippocampal slices. Nature *346*, 177-180.

Man, H.-Y., Wang, Q., Lu, W.-Y., Ju, W., Ahmadian, G., Liu, L., D'Souza, S., Wong, T.P., Taghibiglou, C., Lu, J.*, et al.* (2003). Activation of PI3-Kinase Is Required for

AMPA Receptor Insertion during LTP of mEPSCs in Cultured Hippocampal Neurons. Neuron *38*, 611-624.

Manabe, T., Wyllie, D.J., Perkel, D.J., and Nicoll, R.A. (1993). Modulation of synaptic transmission and long-term potentiation: effects on paired pulse facilitation and EPSC variance in the CA1 region of the hippocampus. J Neurophys *70*, 1451-1459.

Markram, H., Lubke, J., Frotscher, M., and Sakmann, B. (1997). Regulation of Synaptic Efficacy by Coincidence of Postsynaptic APs and EPSPs. Science *275*, 213-215.

Matsuzaki, M., Ellis-Davies, G.C., Nemoto, T., Miyashita, Y., Iino, M., and Kasai, H. (2001). Dendritic spine geometry is critical for AMPA receptor expression in hippocampal CA1 pyramidal neurons. Nat Neurosci *4*, 1086-1092.

Matsuzaki, M., Honkura, N., Ellis-Davies, G.C.R., and Kasai, H. (2004). Structural basis of long-term potentiation in single dendritic spines. Nature *429*, 761-766.

Mayer, M.L., Westbrook, G.L., and Guthrie, P.B. (1984). Voltage-dependent block by Mg2+ of NMDA responses in spinal cord neurones. Nature *309*, 261-263.

McAllister, A.K. (2000). Biolistic Transfection of Neurons. STKE *2000*, pl1.

McCormack, S.G., Stornetta, R.L., and Zhu, J.J. (2006). Synaptic AMPA Receptor Exchange Maintains Bidirectional Plasticity. Neuron *50*, 75-88.

McNaughton, B.L., Douglas, R.M., and Goddard, G.V. (1978). Synaptic enhancement in fascia dentata: Cooperativity among coactive afferents. Brain Research *157*, 277-293.

Migaud, M., Charlesworth, P., Dempster, M., Webster, L.C., Watabe, A.M., Makhinson, M., He, Y., Ramsay, M.F., Morris, R.G.M., Morrison, J.H.*, et al.* (1998). Enhanced long-term potentiation and impaired learning in mice with mutant postsynaptic density-95 protein. Nature *396*, 433-439.

Morris, R.G., Anderson, E., Lynch, G.S., and Baudry, M. (1986). Selective impairment of learning and blockade of long-term potentiation by an N-methyl-D-aspartate receptor antagonist, AP5. Nature *319*, 774-776.

Muller, D., and Lynch, G. (1988). Long-term potentiation differentially affects two components of synaptic responses in hippocampus. PNAS *85*, 9346-9350.

Muller, W., and Connor, J.A. (1991). Dendritic spines as individual neuronal compartments for synaptic Ca2+ responses. Nature *354*, 73-76.

Nakanishi, N., Shneider, N.A., and Axel, R. (1990). A family of glutamate receptor genes: evidence for the formation of heteromultimeric receptors with distinct channel properties. Neuron *5*, 569-581.

Ninan, I., and Arancio, O. (2004). Presynaptic CaMKII Is Necessary for Synaptic Plasticity in Cultured Hippocampal Neurons. Neuron *42*, 129-141.

Nishimune, A., Isaac, J.T.R., Molnar, E., Noel, J., Nash, S.R., Tagaya, M., Collingridge, G.L., Nakanishi, S., and Henley, J.M. (1998). NSF Binding to GluR2 Regulates Synaptic Transmission. Neuron *21*, 87-97.

Noel, J., Ralph, G.S., Pickard, L., Williams, J., Molnar, E., Uney, J.B., Collingridge, G.L., and Henley, J.M. (1999). Surface Expression of AMPA Receptors in Hippocampal Neurons Is Regulated by an NSF-Dependent Mechanism. Neuron *23*, 365-376.

Nowak, L., Bregestovski, P., Ascher, P., Herbet, A., and Prochiantz, A. (1984). Magnesium gates glutamate-activated channels in mouse central neurones. Nature *307*, 462-465.

Nusser, Z., Lujan, R., Laube, G., Roberts, J.D.B., Molnar, E., and Somogyi, P. (1998). Cell Type and Pathway Dependence of Synaptic AMPA Receptor Number and Variability in the Hippocampus. Neuron *21*, 545-559.

O'Connor, D.H., Wittenberg, G.M., and Wang, S.S.H. (2005). Graded bidirectional synaptic plasticity is composed of switch-like unitary events. PNAS *102*, 9679-9684.

Osten, P., Srivastava, S., Inman, G.J., Vilim, F.S., Khatri, L., Lee, L.M., States, B.A., Einheber, S., Milner, T.A., Hanson, P.I., and Ziff, E.B. (1998). The AMPA Receptor GluR2 C Terminus Can Mediate a Reversible, ATP-Dependent Interaction with NSF and [alpha]- and [beta]-SNAPs. Neuron *21*, 99-110.

Osterweil, E., Wells, D.G., and Mooseker, M.S. (2005). A role for myosin VI in postsynaptic structure and glutamate receptor endocytosis. J Cell Biol *168*, 329-338.

Ostroff, L.E., Fiala, J.C., Allwardt, B., and Harris, K.M. (2002). Polyribosomes Redistribute from Dendritic Shafts into Spines with Enlarged Synapses during LTP in Developing Rat Hippocampal Slices. Neuron *35*, 535-545.

Otmakhov, N., Griffith, L.C., and Lisman, J.E. (1997). Postsynaptic Inhibitors of Calcium/Calmodulin-Dependent Protein Kinase Type II Block Induction But Not Maintenance of Pairing-Induced Long-Term Potentiation. J Neurosci *17*, 5357-5365.

Otmakhov, N., Shirke, A.M., and Malinow, R. (1993). Measuring the impact of probabilistic transmission on neuronal output. Neuron *10*, 1101-1111.

Palmer, C.L., Lim, W., Hastie, P.G.R., Toward, M., Korolchuk, V.I., Burbidge, S.A., Banting, G., Collingridge, G.L., Isaac, J.T.R., and Henley, J.M. (2005). Hippocalcin Functions as a Calcium Sensor in Hippocampal LTD. Neuron *47*, 487-494.

Panicker, S., Brown, K., and Nicoll, R.A. (2008). Synaptic AMPA receptor subunit trafficking is independent of the C terminus in the GluR2-lacking mouse. PNAS *105*, 1032-1037.

Park, M., Penick, E.C., Edwards, J.G., Kauer, J.A., and Ehlers, M.D. (2004). Recycling Endosomes Supply AMPA Receptors for LTP. Science *305*, 1972-1975.

Park, M., Salgado, J.M., Ostroff, L., Helton, T.D., Robinson, C.G., Harris, K.M., and Ehlers, M.D. (2006). Plasticity-Induced Growth of Dendritic Spines by Exocytic Trafficking from Recycling Endosomes. Neuron *52*, 817-830.

Partin, K.M., Patneau, D.K., Winters, C.A., Mayer, M.L., and Buonanno, A. (1993). Selective modulation of desensitization at AMPA versus kainate receptors by cyclothiazide and concanavalin A. Neuron *11*, 1069-1082.

Passafaro, M., PiÃ«ch, V., and Sheng, M. (2001). Subunit-specific temporal and spatial patterns of AMPA receptor exocytosis in hippocampal neurons. Nat Neurosci *4*, 917-926.

Pellegrini-Giampietro, D.E., Bennett, M.V., and Zukin, R.S. (1991). Differential expression of three glutamate receptor genes in developing rat brain: an in situ hybridization study. Proc Natl Acad Sci U S A *88*, 4157-4161.

Perez, J.L., Khatri, L., Chang, C., Srivastava, S., Osten, P., and Ziff, E.B. (2001). PICK1 Targets Activated Protein Kinase C{alpha} to AMPA Receptor Clusters in Spines of Hippocampal Neurons and Reduces Surface Levels of the AMPA-Type Glutamate Receptor Subunit 2. J Neurosci *21*, 5417-5428.

Petersen, C.C.H., Malenka, R.C., Nicoll, R.A., and Hopfield, J.J. (1998). All-or-none potentiation at CA3-CA1 synapses. PNAS *95*, 4732-4737.

Petralia, R.S., Wang, Y.-X., and Wenthold, R.J. (2003). Internalization at glutamatergic synapses during development. European Journal of Neuroscience *18*, 3207-3217.

Petrini, E.M., Lu, J., Cognet, L., Lounis, B., Ehlers, M.D., and Choquet, D. (2009). Endocytic Trafficking and Recycling Maintain a Pool of Mobile Surface AMPA Receptors Required for Synaptic Potentiation. Neuron *63*, 92-105.

Plant, K., Pelkey, K.A., Bortolotto, Z.A., Morita, D., Terashima, A., McBain, C.J., Collingridge, G.L., and Isaac, J.T.R. (2006). Transient incorporation of native GluR2-lacking AMPA receptors during hippocampal long-term potentiation. Nat Neurosci *9*, 602-604.

Pologruto, T., Sabatini, B., and Svoboda, K. (2003). ScanImage: Flexible software for operating laser scanning microscopes. BioMedical Engineering Online *2*, 13.

Qin, Y., Zhu, Y., Baumgart, J.P., Stornetta, R.L., Seidenman, K., Mack, V., van Aelst, L., and Zhu, J.J. (2005). State-dependent Ras signaling and AMPA receptor trafficking. Genes & Development *19*, 2000-2015.

Racz, B., Blanpied, T.A., Ehlers, M.D., and Weinberg, R.J. (2004). Lateral organization of endocytic machinery in dendritic spines. Nat Neurosci *7*, 917-918.

Raghavachari, S., and Lisman, J.E. (2004). Properties of Quantal Transmission at CA1 Synapses. J Neurophysiol *92*, 2456-2467.

Reisel, D., Bannerman, D.M., Schmitt, W.B., Deacon, R.M.J., Flint, J., Borchardt, T., Seeburg, P.H., and Rawlins, J.N.P. (2002). Spatial memory dissociations in mice lacking GluR1. Nat Neurosci *5*, 868-873.

Robert, A., and Howe, J.R. (2003). How AMPA Receptor Desensitization Depends on Receptor Occupancy. J Neurosci *23*, 847-858.

Roche, K.W., O'Brien, R.J., Mammen, A.L., Bernhardt, J., and Huganir, R.L. (1996). Characterization of Multiple Phosphorylation Sites on the AMPA Receptor GluR1 Subunit. Neuron *16*, 1179-1188.

Rosenmund, C., Stern-Bach, Y., and Stevens, C.F. (1998). The Tetrameric Structure of a Glutamate Receptor Channel. Science *280*, 1596-1599.

Rumbaugh, G., Sia, G.-M., Garner, C.C., and Huganir, R.L. (2003). Synapse-Associated Protein-97 Isoform-Specific Regulation of Surface AMPA Receptors and Synaptic Function in Cultured Neurons. J Neuroscience *23*, 4567-4576.

Sakimura, K., Bujo, H., Kushiya, E., Araki, K., Yamazaki, M., Yamazaki, M., Meguro, H., Warashina, A., Numa, S., and Mishina, M. (1990). Functional expression from cloned cDNAs of glutamate receptor species responsive to kainate and quisqualate. FEBS Lett *272*, 73-80.

Sanderson, D.J., Good, M.A., Skelton, K., Sprengel, R., Seeburg, P.H., Rawlins, J.N., and Bannerman, D.M. (2009). Enhanced long-term and impaired short-term spatial memory in GluA1 AMPA receptor subunit knockout mice: evidence for a dual-process memory model. Learn Mem *16*, 379-386.

Sanhueza, M., McIntyre, C.C., and Lisman, J.E. (2007). Reversal of synaptic memory by Ca2+/calmodulin-dependent protein kinase II inhibitor. J Neurosci *27*, 5190-5199.

Sanna, P.P., Cammalleri, M., Berton, F., Simpson, C., Lutjens, R., Bloom, F.E., and Francesconi, W. (2002). Phosphatidylinositol 3-Kinase Is Required for the Expression But Not for the Induction or the Maintenance of Long-Term Potentiation in the Hippocampal CA1 Region. J Neurosci *22*, 3359-3365.

Sans, N., Racca, C., Petralia, R.S., Wang, Y.-X., McCallum, J., and Wenthold, R.J. (2001). Synapse-Associated Protein 97 Selectively Associates with a Subset of AMPA Receptors Early in their Biosynthetic Pathway. J Neurosci *21*, 7506-7516.

Sastry, B.R., Goh, J.W., and Auyeung, A. (1986). Associative induction of posttetanic and long-term potentiation in CA1 neurons of rat hippocampus. Science *232*, 988-990.

Sato, K., Kiyama, H., and Tohyama, M. (1993). The differential expression patterns of messenger RNAs encoding non-N-methyl-D-aspartate glutamate receptor subunits (GluR1-4) in the rat brain. Neuroscience *52*, 515-539.

Schikorski, T., and Stevens, C.F. (1997). Quantitative Ultrastructural Analysis of Hippocampal Excitatory Synapses. J Neurosci *17*, 5858-5867.

Schmidt, R.A., and Bjork, R.A. (1992). New Conceptualizations of Practice: Common Principles in Three Paradigms Suggest New Concepts for Training. Psychological Science *3*, 207-217.

Schmitt, J.M., Guire, E.S., Saneyoshi, T., and Soderling, T.R. (2005). Calmodulin-Dependent Kinase Kinase/Calmodulin Kinase I Activity Gates Extracellular-Regulated Kinase-Dependent Long-Term Potentiation. J Neurosci *25*, 1281-1290.

Schnell, E., Sizemore, M., Karimzadegan, S., Chen, L., Bredt, D.S., and Nicoll, R.A. (2002). Direct interactions between PSD-95 and stargazin control synaptic AMPA receptor number. PNAS *99*, 13902-13907.

Schulz, P.E., Cook, E.P., and Johnston, D. (1994). Changes in paired-pulse facilitation suggest presynaptic involvement in long-term potentiation. J Neurosci *14*, 5325-5337.

Schwartzkroin, P.A., and Wester, K. (1975). Long-lasting facilitation of a synaptic potential following tetanization in thein vitro hippocampal slice. Brain Research *89*, 107-119.

Schwenk, J., Harmel, N., Zolles, G., Bildl, W., Kulik, A., Heimrich, B., Chisaka, O., Jonas, P., Schulte, U., Fakler, B., and Klocker, N. (2009). Functional Proteomics

Identify Cornichon Proteins as Auxiliary Subunits of AMPA Receptors. Science *323*, 1313-1319.

Serulle, Y., Zhang, S., Ninan, I., Puzzo, D., McCarthy, M., Khatri, L., Arancio, O., and Ziff, E.B. (2007). A GluR1-cGKII Interaction Regulates AMPA Receptor Trafficking. Neuron *56*, 670-688.

Setou, M., Seog, D.-H., Tanaka, Y., Kanai, Y., Takei, Y., Kawagishi, M., and Hirokawa, N. (2002). Glutamate-receptor-interacting protein GRIP1 directly steers kinesin to dendrites. Nature *417*, 83-87.

Sharma, K., Fong, D.K., and Craig, A.M. (2006). Postsynaptic protein mobility in dendritic spines: Long-term regulation by synaptic NMDA receptor activation. Molecular and Cellular Neuroscience *31*, 702-712.

Shen, L., Liang, F., Walensky, L.D., and Huganir, R.L. (2000). Regulation of AMPA Receptor GluR1 Subunit Surface Expression by a 4.1N-Linked Actin Cytoskeletal Association. J Neurosci *20*, 7932-7940.

Sheng, M., and Kim, M.J. (2002). Postsynaptic Signaling and Plasticity Mechanisms. Science *298*, 776-780.

Shi, S.-H., Hayashi, Y., Esteban, J.A., and Malinow, R. (2001). Subunit-Specific Rules Governing AMPA Receptor Trafficking to Synapses in Hippocampal Pyramidal Neurons. Cell *105*, 331-343.

Shi, S.-H., Hayashi, Y., Petralia, R.S., Zaman, S.H., Wenthold, R.J., Svoboda, K., and Malinow, R. (1999). Rapid Spine Delivery and Redistribution of AMPA Receptors After Synaptic NMDA Receptor Activation. Science *284*, 1811-1816.

Smith, M.A., Ellis-Davies, G.C.R., and Magee, J.C. (2003). Mechanism of the distance-dependent scaling of Schaffer collateral synapses in rat CA1 pyramidal neurons. J Physiol *548*, 245-258.

Smith, T.C., and Howe, J.R. (2000). Concentration-dependent substate behavior of native AMPA receptors. Nat Neurosci *3*, 992-997.

Song, I., Kamboj, S., Xia, J., Dong, H., Liao, D., and Huganir, R.L. (1998). Interaction of the N-Ethylmaleimide Sensitive Factor with AMPA Receptors. Neuron *21*, 393-400.

Stanton, P.K., and Gage, A.T. (1996). Distinct synaptic loci of Ca2+/calmodulin-dependent protein kinase II necessary for long-term potentiation and depression. J Neurosci *76*, 2097-2101.

Stoppini, L., Buchs, P.A., and Muller, D. (1991). A simple method for organotypic cultures of nervous tissue. Journal of Neuroscience Methods *37*, 173-182.

Stork, P.J.S. (2003). Does Rap1 deserve a bad Rap? Trends in Biochemical Sciences *28*, 267-275.

Takumi, Y., Ramirez-Leon, V., Laake, P., Rinvik, E., and Ottersen, O.P. (1999). Different modes of expression of AMPA and NMDA receptors in hippocampal synapses. Nat Neurosci *2*, 618-624.

Tanaka, J.-i., Horiike, Y., Matsuzaki, M., Miyazaki, T., Ellis-Davies, G.C.R., and Kasai, H. (2008). Protein Synthesis and Neurotrophin-Dependent Structural Plasticity of Single Dendritic Spines. Science, 1152864.

Tardin, C., Cognet, L., Bats, C., Lounis, B., and Choquet, D. (2003). Direct imaging of lateral movements of AMPA receptors inside synapses. Embo J *22*, 4656-4665.

Terashima, A., Cotton, L., Dev, K.K., Meyer, G., Zaman, S., Duprat, F., Henley, J.M., Collingridge, G.L., and Isaac, J.T.R. (2004). Regulation of Synaptic Strength and AMPA Receptor Subunit Composition by PICK1. J Neurosci *24*, 5381-5390.

Terashima, A., Pelkey, K.A., Rah, J.-C., Suh, Y.H., Roche, K.W., Collingridge, G.L., McBain, C.J., and Isaac, J.T.R. (2008). An Essential Role for PICK1 in NMDA Receptor-Dependent Bidirectional Synaptic Plasticity. Neuron *57*, 872-882.

Thomas, G.M., and Huganir, R.L. (2004). MAPK CASCADE SIGNALLING AND SYNAPTIC PLASTICITY. Nature Reviews Neuroscience *5*, 173-183.

Tomita, S., Byrd, R.K., Rouach, N., Bellone, C., Venegas, A., O'Brien, J.L., Kim, K.S., Olsen, O., Nicoll, R.A., and Bredt, D.S. (2007). AMPA receptors and stargazin-like transmembrane AMPA receptor-regulatory proteins mediate hippocampal kainate neurotoxicity. J Neurosci *104*, 18784-18788.

Tomita, S., Chen, L., Kawasaki, Y., Petralia, R.S., Wenthold, R.J., Nicoll, R.A., and Bredt, D.S. (2003). Functional studies and distribution define a family of transmembrane AMPA receptor regulatory proteins. JCB *161*, 805-816.

Tonegawa, S. “Molecular, cellular and circuit mechanisms for hippocampal learning and memory.” Broad Foundation seminar series on neurobiology and disease, Duke University, Durham, NC. May 13, 2008. http://lectopia.oit.duke.edu/ilectures/ilectures.lasso?ut=302&id=8569

Trachtenberg, J.T., Chen, B.E., Knott, G.W., Feng, G., Sanes, J.R., Welker, E., and Svoboda, K. (2002). Long-term in vivo imaging of experience-dependent synaptic plasticity in adult cortex. Nature *420*, 788-794.

Turrigiano, G.G., Leslie, K.R., Desai, N.S., Rutherford, L.C., and Nelson, S.B. (1998). Activity-dependent scaling of quantal amplitude in neocortical neurons. Nature *391*, 892-896.

Unsworth, N., and Engle, R.W. (2007). On the division of short-term and working memory: an examination of simple and complex span and their relation to higher order abilities. Psychol Bull *133*, 1038-1066.

von Engelhardt, J., Mack, V., Sprengel, R., Kavenstock, N., Li, K.W., Stern-Bach, Y., Smit, A.B., Seeburg, P.H., and Monyer, H. (2010). CKAMP44: A Brain-Specific Protein Attenuating Short-Term Synaptic Plasticity in the Dentate Gyrus. Science *327*, 1518-1522.

Waites, C.L., Specht, C.G., Hartel, K., Leal-Ortiz, S., Genoux, D., Li, D., Drisdel, R.C., Jeyifous, O., Cheyne, J.E., Green, W.N.*, et al.* (2009). Synaptic SAP97 Isoforms Regulate AMPA Receptor Dynamics and Access to Presynaptic Glutamate. J Neurosci *29*, 4332-4345.

Wang, Z., Edwards, J.G., Riley, N., Provance, D.W., Karcher, R., Li, X.-d., Davison, I.G., Ikebe, M., Mercer, J.A., Kauer, J.A., and Ehlers, M.D. (2008). Myosin Vb Mobilizes Recycling Endosomes and AMPA Receptors for Postsynaptic Plasticity. Cell *135*, 535-548.

Wenthold, R.J., Petralia, R.S., Blahos J, II, and Niedzielski, A.S. (1996). Evidence for multiple AMPA receptor complexes in hippocampal CA1/CA2 neurons. J Neuroscience *16*, 1982-1989.

Wu, H., Nash, J.E., Zamorano, P., and Garner, C.C. (2002). Interaction of SAP97 with Minus-end-directed Actin Motor Myosin VI. IMPLICATIONS FOR AMPA RECEPTOR TRAFFICKING. J Biol Chem *277*, 30928-30934.

Wyszynski, M., Kim, E., Dunah, A.W., Passafaro, M., Valtschanoff, J.G., Serra-Pages, C., Streuli, M., Weinberg, R.J., and Sheng, M. (2002). Interaction between GRIP and Liprin-[alpha]/SYD2 Is Required for AMPA Receptor Targeting. Neuron *34*, 39-52.

Xu, H.-T., Pan, F., Yang, G., and Gan, W.-B. (2007). Choice of cranial window type for in vivo imaging affects dendritic spine turnover in the cortex. Nat Neurosci *10*, 549-551.

Yang, Y., Wang, X.-b., Frerking, M., and Zhou, Q. (2008a). Delivery of AMPA receptors to perisynaptic sites precedes the full expression of long-term potentiation. PNAS *105*, 11388-11393.

Yang, Y., Wang, X.-b., Frerking, M., and Zhou, Q. (2008b). Spine Expansion and Stabilization Associated with Long-Term Potentiation. J Neurosci *28*, 5740-5751.

Yasuda, R., Harvey, C.D., Zhong, H., Sobczyk, A., van Aelst, L., and Svoboda, K. (2006). Supersensitive Ras activation in dendrites and spines revealed by two-photon fluorescence lifetime imaging. Nat Neurosci *9*, 283-291.

Yasuda, R., Nimchinsky, E.A., Scheuss, V., Pologruto, T.A., Oertner, T.G., Sabatini, B.L., and Svoboda, K. (2004). Imaging calcium concentration dynamics in small neuronal compartments. Sci STKE *2004*, pl5.

Yasumatsu, N., Matsuzaki, M., Miyazaki, T., Noguchi, J., and Kasai, H. (2008). Principles of Long-Term Dynamics of Dendritic Spines. J Neurosci *28*, 13592-13608.

Yudowski, G.A., Puthenveedu, M.A., Leonoudakis, D., Panicker, S., Thorn, K.S., Beattie, E.C., and von Zastrow, M. (2007). Real-Time Imaging of Discrete Exocytic Events Mediating Surface Delivery of AMPA Receptors. J Neurosci *27*, 11112-11121.

Yuste, R., and Bonhoeffer, T. (2001). MORPHOLOGICAL CHANGES IN DENDRITIC SPINES ASSOCIATED WITH LONG-TERM SYNAPTIC PLASTICITY. Ann Rev Neurosci *24*, 1071-1089.

Yuste, R., and Denk, W. (1995). Dendritic spines as basic functional units of neuronal integration. Nature *375*, 682-684.

Zamanillo, D., Sprengel, R., Hvalby, Oslash, ivind, Jensen, V., Burnashev, N., Rozov, A., Kaiser, K.M., nbsp*, et al.* (1999). Importance of AMPA Receptors for Hippocampal Synaptic Plasticity But Not for Spatial Learning. Science *284*, 1805-1811.

Zhu, J.J., Esteban, J.A., Hayashi, Y., and Malinow, R. (2000). Postnatal synaptic potentiation: Delivery of GluR4-containing AMPA receptors by spontaneous activity. Nat Neurosci *3*, 1098-1106.

Zhu, J.J., Qin, Y., Zhao, M., Van Aelst, L., and Malinow, R. (2002). Ras and Rap Control AMPA Receptor Trafficking during Synaptic Plasticity. Cell *110*, 443-455.

Biography

Birthplace

Cleveland, OH April 21, 1982

Education

BA in Computational Neuroscience, minor in Physics
Case Western Reserve University August 1999 - December 2003
Cleveland, OH
Dean's Approved Major

PhD in Neurobiology
Duke University August 2004 – May 2010
Durham, NC

Publications

MA Patterson, and R Yasuda. (under revision) AMPA Receptors are exocytosed near stimulated spines in a Ras-ERK dependent manner during long-term potentiation. PNAS.

M Patterson, J Sneyd, and DD Friel (2007). Depolarization-induced Calcium Responses in Sympathetic Neurons: Relative Contributions from Ca2+Entry, Extrusion, ER/Mitochondrial Ca2+ Uptake and Release, and Ca2+ Buffering. J Gen Physiol 129: 29-56.

K Wada, JT Howard, P McConnell, O Whitney, T Lints, MV Rivas, H Horita, **MA Patterson**, ... ED Jarvis (2006). A molecular neuroethological approach for identifying and characterizing a cascade of behaviorally regulated genes. PNAS 103(41): 15212-15217.

Awards and Fellowships

Ruth L. Kirschstein National Research Service Award (NIH F31) 2009-2010

Duke University Graduate School Conference Travel Fellowship 2008, 2009